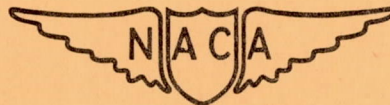# NATIONAL ADVISORY COMMITTEE
FOR AERONAUTICS

TECHNICAL NOTE

No. 1495

ANALYSIS, VERIFICATION, AND APPLICATION OF EQUATIONS

AND PROCEDURES FOR DESIGN OF

EXHAUST-PIPE SHROUDS

By Herman H. Ellerbrock, Jr., Chester R. Wcislo,
and Howard E. Dexter

Langley Memorial Aeronautical Laboratory
Langley Field, Va.

Washington
December 1947

NATIONAL ADVISORY COMMITTEE FOR AERONAUTICS

————————

TECHNICAL NOTE NO. 1495

————————

ANALYSIS, VERIFICATION, AND APPLICATION OF EQUATIONS

AND PROCEDURES FOR DESIGN OF

EXHAUST-PIPE SHROUDS

By Herman H. Ellerbrock, Jr., Chester R. Wcislo,
and Howard E. Dexter

SUMMARY

Results are presented of an investigation to develop simpli-
fied methods for designing exhaust-pipe shrouds to provide desired
or maximum cooling of exhaust installations in which the dynamic
pressure of flight is utilized to force the cooling air through the
shroud. Design equations derived from fundamental laws of heat
transfer and pressure drop are given for parallel- and counter-flow
exhaust-pipe-shroud systems. The only data required for use in the
design equations are the upstream temperatures and flow rates of
the exhaust gas and cooling air and the upstream pressures of the
cooling air. The design equations for the parallel-flow system
were verified within the limits of engineering accuracy for one
shroud to exhaust-pipe diameter ratio by tests of an experimental
exhaust-pipe-shroud setup. The equations have no diameter-ratio
limitations provided that cooling-air flow in the annulus is turbu-
lent. The verification of these equations for one diameter ratio
lends support to the belief that the equations are applicable to
all practical shroud to exhaust-pipe diameter ratios for which the
cooling-air flow is expected to be turbulent. Although no tests of
counter-flow systems were run, the counter-flow equations are believed
to be equally applicable because of their similarity to the parallel-
flow equations.

For simplification of the design equations, constant values
of 0.24 and 0.30 were used for the specific heats of cooling air and
exhaust gas, respectively, and air properties were substituted for
exhaust-gas properties in determining the heat-transfer coefficient
of the exhaust gas. Calculations showed that these substitutions
for the precise terms have a negligible effect on the accuracy of
results obtained with the design equations.

Detailed procedures and charts for the design of shrouds are
presented for both parallel-flow and counter-flow systems. These

procedures permit the determination of the proportions of an exhaust-pipe shroud that will provide desired cooling of the exhaust installation or, if desired cooling cannot be attained, permit the determination of the proportions of the shroud that will provide the maximum cooling and the values of installation temperatures that will exist with that shroud. The design procedures, based on the derived equations, are complete in themselves as regards shroud design. An example of the use of the shroud-design procedures for a four-engine bomber is included.

The equations and methods of shroud design presented are believed to be directly applicable to the design of shrouds for the tail pipes of jet engines provided that the luminosity of the gases in the tail pipe is negligible and the cooling air exits to the atmosphere. For jet-engine installations in which the luminosity of the gases is not negligible, however, the present analysis must be extended to include the heat transfer to the exhaust pipe by gas radiation. If the cooling-air exit pressure is decreased from atmospheric pressure by means of flaps or ejector pumps, the method of application of the pressure-drop relations to shroud design presented must be modified to account for the departure from atmospheric pressure at the cooling-air exit.

INTRODUCTION

Shrouded exhaust-pipe systems are generally used in airplanes to reduce the fire hazard, to cool the exhaust pipe, to reduce the heat radiated to other components of the installation, and to cool the exhaust gas flowing to turbines. An illustration of such a system is shown as figure 1. The systems usually consist of an exhaust pipe surrounded by another pipe, with cooling air passing through the annular space formed by the pipes and reducing the temperatures of the exhaust gas and the pipes.

Although many of the necessary fundamental data have been available, the design of shrouded exhaust-pipe systems has been hampered by the lack of a coordinated rational design procedure. This difficulty has undoubtedly been one of the important reasons that shroud system trouble has been so prevalent.

The present paper is divided into two parts. The purpose of part I is to present (a) an analysis of the heat exchange and the pressure drop in parallel-flow and counter-flow exhaust-pipe shroud systems and (b) an experimental verification of the analysis for the parallel-flow system over a representative range of air- and gas-flow rates. Part II presents detailed procedures to facilitate

application of the analysis to shroud design. A summary of the necessary physical properties of air and exhaust gases, extended where necessary, is given in an appendix.

SYMBOLS

In addition to the following definitions of symbols, a graphical representation is presented in figure 2.

A duct cross-sectional area, square feet

a velocity of sound, feet per second

C constant in equations (26) and (31)

c_p instantaneous specific heat of fluid at constant pressure, Btu/(lb)($^{\circ}$F)

$\bar{c}_p$ mean of instantaneous specific heats of fluid at constant pressure, Btu/(lb)($^{\circ}$F)

D hydraulic diameter of duct, feet $\left(\dfrac{4 \times \text{Cross-sectional area}}{\text{Wetted perimeter}} \right)$

d diameter, feet

F_A shape modulus in radiation equation

F_c factor of compressibility $\left(1 + \dfrac{M^2}{4} + \dfrac{M^4}{40} \cdots \right)$

F_E emissivity modulus in radiation equation

f friction factor $\left(\dfrac{\Delta p_f D}{4 \bar{q} l} \right)$; also used for fuel-air ratio

g ratio of absolute to gravitational unit of mass, pounds per slug, or acceleration due to gravity, feet per second per second

H mean total pressure, pounds per square foot

h heat-transfer coefficient, Btu/(sec)(sq ft)($^{\circ}$F)

J   mechanical equivalent of heat, foot pounds per Btu (778)

k   thermal conductivity of fluid flow, Btu/(sec)(sq ft)($^\circ$F/ft)

l length between stations, feet

M   Mach number

m   mass rate of fluid flow, slugs per second

N   any number to be raised to 0.8 and to 1.8

n   an exponent

p   mean static pressure, pounds per square foot absolute

Q   quantity of heat dissipated, Btu per second

q   mean dynamic pressure, pounds per square foot $\left(\frac{1}{2\rho}\left(\frac{m}{A}\right)^2\right)$

$\bar{q}$ average of upstream and downstream mean dynamic pressures, pounds per square foot

S   surface area of body through which heat is being transferred

T   mixed mean temperature, $^\circ$F absolute

t   mixed mean temperature, $^\circ$F

V   mean fluid velocity, feet per second $\left(\frac{m}{\rho A}\right)$

$\bar{V}$ value of velocity such that $\bar{\rho}\bar{V} = \rho_1 V_1 = \rho_2 V_2$, feet per second

W   weight rate of fluid flow, pounds per second

$Z = \dfrac{\bar{c}_{p_e} W_e}{\bar{c}_{p_a} W_a}$

$\triangle$ denotes difference

ϵ emissivity

θ temperature difference, $^\circ$F

μ absolute viscosity of fluid, slugs per foot-second

ρ mean density of fluid, slugs per cubic foot $(0.000583\ p/T)$

$\bar{\rho}$ average of upstream and downstream mean densities of fluid, slugs per cubic foot

ϕ factor depending on ratio of pipe diameters in heat-transfer equation (See equation (19).)

ϕ' factor depending on ratio of pipe diameters in friction-factor equation (See equation (27).)

$$\psi = \frac{1 - Z}{\overline{c}_{p_e} W_e}\left(\frac{\pi d_p l}{\dfrac{1}{h_a + h_r} + \dfrac{1}{h_e}}\right)$$

$$\omega = \frac{1 + Z}{\overline{c}_{p_e} W_e}\left(\frac{\pi d_p l}{\dfrac{1}{h_a + h_r} + \dfrac{1}{h_e}}\right)$$

R   Reynolds number

Pr   Prandtl number

σ ratio of density to standard sea-level density $(\rho/0.002378)$

Subscripts:

a   cooling air

b   bend

d   diffuser

e   exhaust gas except when used with ΔH when it refers to shroud exit

f   friction pressure drop

h   due to heating of cooling air

i   inlet duct to shroud

m   at manifold

o   free stream

p   exhaust pipe

r   denotes radiation heat transfer

s   shroud

t   total or stagnation conditions

x   refers to any station x feet from shroud entrance

1   station 1

2   station 2

3   station 3

0-1   from free stream to station 1

1-2   from station 1 to 2

1-3   from station 1 to 3

I - ANALYSIS AND VERIFICATION

ANALYSIS OF HEAT EXCHANGE AND PRESSURE DROP

IN EXHAUST-PIPE-SHROUD SYSTEMS

An adequate exhaust-pipe-shroud system is one for which all
parts of the system and the downstream exhaust-gas are below
limiting temperatures and the pressure drop required for forcing
air through the system does not exceed the pressure drop available.
The analysis of such a system, consequently, requires equations for
predicting design temperatures and pressure drop on the cooling-air
side of the system. These equations should be in a form such that
the desired temperatures and pressure losses will be a function of
known conditions. The present analysis derives such equations for
the usual straight annular exhaust-pipe-shroud systems for both the
case of parallel flow and the case of counter flow. The simplifying
assumption of straight flow is made, inasmuch as bends increase the
local heat transfer and cooling-air pressure losses and therefore
should be avoided. In the present analysis cooling air flows in
the annular space around the exhaust pipe, which is the case usually
encountered.

Parallel Flow

Heat-exchange processes in exhaust-pipe-shroud combinations.-
The analysis for parallel flow is for the case of exhaust-gas
mixture and cooling air flowing in the same direction. (See
fig. 2(a).) For a parallel-flow exhaust-pipe-shroud combination
with exhaust gas flowing in the inner pipe and cooling air flowing
in the annular space, the mechanism of heat transfer is as follows:

(a) Heat flows from the exhaust gas to the exhaust pipe by
forced convection

(b) Heat flows from the exhaust gas to the exhaust pipe by
thermal radiation

(c) Heat flows from the exhaust pipe to the cooling air by
forced convection

(d) Heat flows from the exhaust pipe to the shroud by thermal
radiation through the cooling air which is a nonabsorbing medium

(e) Heat is exchanged between the shroud and the cooling air
by forced convection

(f) Heat flows from the shroud to the surrounding atmosphere
by natural convection

The thermal radiation from the exhaust gas to the exhaust pipe
has been neglected in this analysis. By use of the radiation
formulas for nonluminous gases, calculations show that this radia-
tion is small provided that afterburning does not occur. If combus-
tion with a luminous flame does occur, the heat transfer to the pipe
will be greatly increased, and the analysis should be extended to
include this effect. The heat loss from the shroud by natural con-
vection will also be neglected. It is assumed that the heat given
up by the exhaust gas is equal to that picked up by the cooling air.
The fluid temperature differences for use in the convection-heat-
transfer formulas are determined from the true temperatures, although
for preciseness, stagnation temperatures should be used. In well-
designed shrouds, however, the cooling-air velocities are low enough
to make the error introduced by use of true temperatures negligible.

The design temperatures in an exhaust-pipe-shroud system with
parallel flow are the downstream gas temperature t_{e_2} (when a
turbosupercharger is used), the exhaust-pipe temperatures t_p, and
the shroud temperatures t_s. (See fig. 2(a).) In the present paper

equations are given for these design temperatures. Assumptions are made herein, which are thought to be permissible wherever it is advantageous to the simplification of the final results.

Equations for design temperatures.- The heat transfer from a hot gas to a cold gas can be represented by the equation

$$Q = \bar{h}\bar{\theta}S \tag{1}$$

where

$\bar{h}$ mean heat-transfer coefficient

$\bar{\theta}$ mean temperature difference

S surface area of body through which heat is being transferred

For the present case of the parallel-flow exhaust-pipe-shroud system it can be shown by use of information available in standard heat-transfer text books and on the basis of the assumptions given that

$$\bar{h} = \frac{1}{\dfrac{1}{h_e} + \dfrac{1}{h_a + h_r}} \tag{2}$$

where h_e and h_a are convection-heat-transfer coefficients on the gas and air sides, respectively, and h_r is the radiant-heat-transfer coefficient from pipe to shroud, and

$$\bar{\theta} = \frac{\theta_1 - \theta_2}{\log_e \dfrac{\theta_1}{\theta_2}} \tag{3}$$

where

$$\theta_1 = t_{e_1} - t_{a_1} \tag{4}$$

$$\theta_2 = t_{e_2} - t_{a_2} \tag{5}$$

The use of the log mean temperature difference (equation (3)) is based on the postulate that h_e, h_a, and h_r do not vary along the tube length. The area S for the system is assumed to be

$$S = \pi d_p l \tag{6}$$

The small difference in pipe area on gas and air sides is neglected in the theory presented herein and the outer diameter of the pipe is used.

The heat lost by the exhaust gas and gained by the cooling air can be obtained by means of the following equations:

$$Q = \overline{c}_{p_e} W_e \left(t_{e_1} - t_{e_2} \right) \tag{7}$$

$$Q = \overline{c}_{p_a} W_a \left(t_{a_2} - t_{a_1} \right) \tag{8}$$

In these equations $\overline{c}_{p_e}$ and $\overline{c}_{p_a}$ are the integrated mean values of the instantaneous specific heats c_{p_e} and c_{p_a}, respectively, between stations 1 and 2.

By use of equations (1) to (8) the following expression can be obtained:

$$t_{e_2} - t_{a_2} = \frac{t_{e_1} - t_{a_1}}{e^{\omega}} \tag{9}$$

where

$$\omega = \frac{1 + Z}{\overline{c}_{p_e} W_e} \left(\frac{\pi d_p l}{\dfrac{1}{h_a + h_r} + \dfrac{1}{h_e}} \right) \tag{10}$$

$$Z = \frac{\overline{c}_{p_e} W_e}{\overline{c}_{p_a} W_a} \tag{11}$$

If equation (7) is made equal to equation (8), the following expression is obtained for t_{a_2}:

$$t_{a_2} = Z\left(t_{e_1} - t_{e_2}\right) + t_{a_1} \tag{12}$$

Substituting for t_{a_2} in equation (9) the equivalent value given by equation (12) and solving the resulting equation for t_{e_2} gives the following equation for the downstream exhaust-gas temperature:

$$t_{e_2} = \frac{1}{1 + Z}\left(t_{a_1} + Z t_{e_1} + \frac{t_{e_1} - t_{a_1}}{e^{\omega}}\right) \tag{13}$$

The exhaust-pipe temperatures can be obtained with reasonable accuracy from an equation which neglects radiant-heat transfer from the exhaust pipe to the shroud. This equation is obtained by making the heat transferred by convection from the gas to the pipe equal to the heat transferred from the pipe to the cooling air for a differential length dl. (See fig. 2(a).) At any point x the equation for pipe temperature becomes

$$t_{p_x} = \frac{h_e t_{e_x} + h_a t_{a_x}}{h_e + h_a} \tag{14}$$

Equation (14) is applicable to any station if the appropriate gas and air temperatures are used. The downstream pipe temperature t_{p_2} is determined from the downstream air temperature t_{a_2} and gas temperature t_{e_2} which are obtained from equations (12) and (13).

The shroud metal temperature at each station is assumed to be equal to the corresponding cooling-air temperature at that station in order to avoid the necessity for solving complicated analytical equations for the shroud temperatures. This assumption is conservative, for in the normal case the shroud temperature is slightly lower than the adjacent mean cooling-air temperature.

From equations (12) to (14) and the simplifying assumptions given for shroud temperatures, the design temperatures can be determined from the dimensions of the exhaust-pipe-shroud system, the

upstream temperatures, the air and gas flow rates, the specific heats of air and gas, and the heat-transfer coefficients, all of which will be known in a design problem. The equations for the heat-transfer coefficients are given in the following section.

Fundamental laws for heat-transfer coefficients.- The relation between the convection-heat-transfer coefficient, the exhaust-gas factors, and the exhaust-pipe diameter is shown in the following equation based on the law of heat transfer for turbulent flow in pipes as given in reference 1, page 168:

$$\frac{h_e d_p}{k_e} = 0.023 \left(\frac{V_e \rho_e d_p}{\mu_e}\right)^{0.8} \left(\frac{c_{p_e} \mu_e g}{k_e}\right)^{0.4} \tag{15}$$

The gas properties are determined at the bulk temperature of the fluid which to be precise should be the integrated mean temperature from station 1 to station 2. Actually, however, the bulk temperature can be taken as the temperature at the upstream station with little error in h_e because the predominating factor affecting h_e, as shown by equation (15), is the mass flow per unit area. The upstream temperature was used in the present work. If, instead of gas properties at the temperature t_{e_1} being used, air properties determined at the same temperature could be used with little error, the necessity for determining the fuel-air-ratio and the hydrogen-carbon-ratio factors would be avoided and the equations would be somewhat simplified. By substitution of air properties determined at temperature t_{e_1} and the equation

$$V_e \rho_e = \frac{4 W_e}{\pi d_p^2 g} \tag{16}$$

in equation (15) the heat-transfer-coefficient equation for exhaust gas then becomes

$$\frac{h_e d_p}{k_a} = 0.023 \left(\frac{4 W_e}{\pi d_p \mu_a g}\right)^{0.8} \left(\frac{c_{p_a} \mu_a g}{k_a}\right)^{0.4} \tag{17}$$

or

$$h_e = 0.001735 \frac{k_a(Pr_a)^{0.4}}{\mu_a^{0.8} d_p^{1.8}} W_e^{0.8} \tag{18}$$

An equation similar in form to equation (15) can be used to determine the convection-heat-transfer coefficient h_a in the annular space. The diameter d_p, however, must be replaced by the equivalent (or hydraulic) diameter of the annular space $d_s - d_p$. (See reference 1, p. 200, and references 2 to 4.) In addition, according to reference 3, the constant 0.023 must be multiplied by a factor dependent upon the ratio of the diameters of the inner and the outer pipes. This factor is

$$\phi = \frac{2 \log_e \frac{d_s}{d_p} - \left(\frac{d_s}{d_p}\right)^2 + 1}{\frac{d_s}{d_p} - \frac{d_p}{d_s} - 2 \frac{d_s}{d_p} \log_e \frac{d_s}{d_p}} \tag{19}$$

References 1 and 2 make no mention of such a factor, but a general review of the literature on annular spaces shows an increase in heat transfer of annular spaces as compared with that of circular pipes. This factor will therefore be included in the present analysis. The Prandtl number for air $\left(c_{p_a}\mu_a g/k_a\right)$ is about constant and equal to approximately 0.73 over a large range of inlet-air temperature. Also, $10\mu_a$ can be substituted for k_a with little error. With the foregoing assumptions and the fact that $V_a \rho_a g$ equals the weight rate of air flow divided by the cross-sectional area of the annular space, the equation for h_a becomes

$$h_a = 0.01528 \, \phi \, \frac{\mu_a^{0.2}}{\left(d_s + d_p\right)^{0.8} \left(d_s - d_p\right)} W_a^{0.8} \tag{20}$$

The upstream temperature t_{a_1} was used instead of the bulk temperature of the fluid to determine the air property in equation (20)

because the mass flow per unit area is the predominating factor affecting h_a and the error involved is therefore negligible.

The expression for the radiant-heat-transfer coefficient h_r is derived in the following manner: The heat transfer by radiation from the exhaust pipe to the shroud at any point x and for a differential length dl (see fig. 2(a)) can be expressed by the equation (reference 5, p. 50)

$$dQ_r = \frac{0.1728}{3600} F_A F_E \left[\left(\frac{T_{p_x}}{100} \right)^4 - \left(\frac{T_{s_x}}{100} \right)^4 \right] \pi d_p \, dl \qquad (21)$$

The temperatures T_{p_x} and T_{s_x} are the appropriate pipe and shroud temperatures. For the usual shroud-design problem it can be shown by means of an equation in reference 5, page 54, that the emissivity modulus F_E is not much smaller than the pipe emissivity ϵ_p. For the simplification of the present analysis the approximation of ϵ_p for F_E will be used hereinafter. The shape modulus F_A is a factor which allows for the geometrical position of the radiating surfaces and, for the case of an annular space, is equal to unity (reference 5, p. 54). The radiant-heat transfer must be expressed in a form similar to that for convective heat transfer to obtain the coefficient h_r; thus

$$dQ_r = h_r \left(t_{p_x} - t_{a_x} \right) \pi d_p \, dl \qquad (22)$$

By use of equations (21) and (22) and of factors given for F_A and F_E, the following equation for h_r can be derived:

$$h_r = \frac{\frac{0.1728}{3600} \epsilon_p \left[\left(\frac{T_{p_x}}{100} \right)^4 - \left(\frac{T_{s_x}}{100} \right)^4 \right]}{t_{p_x} - t_{a_x}} \qquad (23)$$

The convection-heat-transfer coefficients h_e and h_a have been shown to be little affected by variations of temperatures along the length and consequently were assumed constant along the length. Although the same assumption will cause appreciable inaccuracies in

the coefficient h_r, the fact that h_r is so much smaller than h_a causes variations in h_r to affect the over-all coefficient $\bar{h}$ very little as can be shown by means of equation (2). The assumption has been made that h_r is also constant along the pipe length. Use of the log-mean-temperature difference is based on the postulate of the constancy of the coefficients in accordance with the statement in reference 2 that the use of this temperature difference will be sufficiently accurate for such systems.

With the assumption that the radiant-heat-transfer coefficient is invariant with the length, the temperatures of the pipe, the shroud, and the air at station 1 can be used in equation (23) to determine h_r. The use of cooling-air temperature for the shroud temperature can be made as previously recommended. The pipe temperature t_{p_1} is determined by means of equation (14).

Pressure loss in annular passage.- The pressure loss through an annular passage consists of the friction drop, the loss due to accelerating the fluid, and the loss at the exit; thus

$$\Delta H = \Delta p_f + \Delta H_h + \Delta H_e \tag{24}$$

The friction pressure drop in an annulus (see references 1 and 5) can be expressed as follows:

$$\Delta p_f = 4f \frac{l}{d_s - d_p} \bar{q} \tag{25}$$

The friction factor f for smooth pipe varies with Reynolds number in the following manner:

$$f = \frac{C}{R^n} \tag{26}$$

Over a wide range of Reynolds number in the turbulent region for pipes of both circular and annular cross section the value of n is about 0.2. For pipes of circular cross section, the value of C is almost constant over this range and various results are in agreement as to the value. (For smooth and commercial pipes, the values of C are 0.046 and 0.054, respectively.) There is a wide dissimilarity of results for the value of C for pipes of annular cross

section. In references 1 and 2 the circular-pipe value of C is
used with the Reynolds number based on the equivalent diameter. In
references 3 and 4 a much higher value for C is advocated than
that for circular pipes as well as use of Reynolds number based on
the equivalent diameter. In reference 3, for instance, it was deter-
mined from data that the value for C of circular pipes should be
increased by multiplying by the factor

$$\phi' = \frac{\dfrac{d_s}{d_p} + \phi}{\dfrac{d_s}{d_p} + 1} \tag{27}$$

For hot tests, also, no full agreement is reached as to the tempera-
ture to use in determining the properties of the fluid. Some inves-
tigators use a film temperature and others use the bulk temperature
of the fluid. Finally, for pipes that are not smooth an equation
in the form of equation (26) is not applicable for some ranges of
Reynolds number and, even if it were applicable, the value of C
would depend upon the degree of roughness. Because of the undecided
status of results on annular cross-section pipes and inasmuch as the
steel generally used in the shroud systems has some roughness, the
friction factors in the present tests were determined experimentally
in order to provide data which would be generally applicable to
exhaust-pipe-shroud systems in airplane installations. The Reynolds
numbers used herein were based on the equivalent diameter of the
passage $d_s - d_p$.

If the variation of ~~velocity and~~ density with length in the
annular space is assumed to be linear, the continuity equation
$\left(\rho_{a_1} V_{a_1} = \rho_{a_2} V_{a_2} = \overline{\rho}_a \overline{V}_a \right)$ may be used to show that

$$\overline{q} = \frac{1}{4} \left(\overline{\rho}_a \overline{V}_a \right)^2 \left(\frac{1}{\rho_{a_1}} + \frac{1}{\rho_{a_2}} \right) \tag{28}$$

Now

$$R = \frac{\overline{\rho}_a \overline{V}_a \left(d_s - d_p \right)}{\mu_a} \tag{29}$$

and

$$\bar{\rho}_a \bar{V}_a = \frac{4W_a}{\pi\left(d_s^2 - d_p^2\right)\beta} \tag{30}$$

From equations (25), (26), (28), (29), and (30), therefore,

$$\Delta p_f = \left(\frac{4}{\pi\beta}\right)^{2-n} C \frac{l\mu_a^n W_a^{2-n}}{\left(d_s + d_p\right)^{2-n}\left(d_s - d_p\right)^3}\left(\frac{1}{\rho_{a_1}} + \frac{1}{\rho_{a_2}}\right) \tag{31}$$

As in the heat-transfer equation μ_a can be determined at the temperature t_{a_1} with little error resulting in Δp_f. This procedure is used herein.

The cooling air is heated in passing through the annular passage. This heating of the air causes a pressure drop to occur due to the expansion of the air in addition to the frictional pressure drop. The pressure drop due to the expansion of the air is a large fraction of the total pressure drop in the annular space.

The loss in total pressure due to acceleration of the air from V_{a_1} to V_{a_2} can be derived from equations in reference 1 as follows:

$$\Delta H_h = q_{a_2} - q_{a_1} \tag{32}$$

where

$$q_a = \frac{1}{2}\rho_a V_a^2 \tag{33}$$

In the derivation of equation (30), compressibility factors were neglected because they had very little effect on the differences of dynamic pressures used to determine ΔH_h. Use of the continuity equation and equations (30), (32), and (33) leads to the following expression for ΔH_h:

$$\Delta H_h = \frac{1}{2} \left(\frac{4}{\pi g}\right)^2 \frac{W_a^2}{\left(d_s + d_p\right)^2 \left(d_s - d_p\right)^2} \left(\frac{1}{\rho_{a_2}} - \frac{1}{\rho_{a_1}}\right) \qquad (34)$$

In equation (34) the constant factors reduce to 0.000781.

An exit loss from the shroud to the free-air stream is also present. Inasmuch as the velocities in the shroud are appreciable, it is assumed that all the velocity pressure is lost at the exit. The assumption is also made that p_{a_2} equals the atmospheric pressure which generally is, or is close to, the existing condition. Then

$$\Delta H_e = q_{a_2} = \frac{0.000781 \, W_a^2}{\left(d_s + d_p\right)^2 \left(d_s - d_p\right)^2 \rho_{a_2}} \qquad (35)$$

The sum of the pressure drop due to heating of the air and the pressure drop for the exit loss can be expressed in the following form:

$$\Delta H_h + \Delta H_e = 2q_{a_2} - q_{a_1} \qquad (36)$$

This expression becomes, through use of equations (34) and (35),

$$\Delta H_h + \Delta H_e = \frac{0.3284}{\sigma_{a_1}} \frac{W_a^2}{\left(d_s + d_p\right)^2 \left(d_s - d_p\right)^2} \left(2 \frac{\rho_{a_1}}{\rho_{a_2}} - 1\right) \qquad (37)$$

where

σ_{a_1} ratio of ρ_{a_1} to standard density at sea level

$$\left(\rho_{a_1} \middle/ 0.002378\right)$$

The total pressure loss in the exhaust-pipe-shroud system, exclusive of any losses up to the beginning of the annular passage,

will then be the summation of the losses given by equations (31) and (37) as shown by equation (24).

Counter Flow

Equations for design temperatures.- In the case of counter flow the downstream exhaust-gas temperature t_{e_2} and the temperatures at station 1 of the exhaust pipe and shroud t_{p_1} and t_{s_1}, respectively, (fig. 2(b)) will be the design temperatures for which an adequate system must be obtained. For counter flow, t_{a_1} is the outgoing-air temperature and t_{a_2} is the incoming-air temperature. (See fig. 2(b).)

Equations (9), (12), and (14) are applicable to the case of counter flow with the following exceptions:

(a) Exponent ω is replaced with ψ where

$$\psi = \frac{1 - Z}{\overline{c}_{p_e} W_e} \frac{\pi d_p l}{\dfrac{1}{h_a + h_r} + \dfrac{1}{h_e}} \tag{38}$$

(b) In equation (12), t_{a_1} is interchanged with t_{a_2}. Substitution of the equation for downstream air temperature in equation (9) for counter flow results in the following expression for t_{e_2}:

$$t_{e_2} = \frac{t_{a_2}\left(1 - e^{\psi}\right) - t_{e_1}(1 - Z)}{Z - e^{\psi}} \tag{39}$$

The design temperature t_{p_1} is obtained by use of equation (14), the upstream gas temperature t_{e_1}, and the downstream air temperature t_{a_1}. To determine the shroud temperature t_{s_1} analytically involves complications similar to those in the case of parallel flow. Consequently, the method of designing for air temperature t_{a_1} in place of shroud temperature t_{s_1} used in parallel flow will also be used in the case of counter flow.

As in the case of parallel flow the following assumptions are made for counter flow:

(a) The heat-transfer coefficients are constant along the pipe length. Equations (18) and (20) are, therefore, applicable for evaluating h_e and h_a.

(b) The upstream gas temperature t_{e_1} can be used to evaluate the air properties in equation (18).

(c) The upstream air temperature t_{a_2} can be used to evaluate air viscosity in equation (20).

The radiant-heat-transfer coefficient h_r is evaluated by use of equation (23), the pipe temperature t_{p_2}, and the temperature t_{a_2} for both the air and shroud temperatures. A trial-and-error solution necessitated by the use of t_{e_2} in equation (14) to evaluate t_{p_2} for use in the h_r equation is avoided by the substitution of t_{e_1} in place of t_{e_2}. Since the gas temperature drop is small, this substitution will cause little error in the calculated design temperature t_{e_2}.

Pressure drop.- Equations (24), (31), (34), (35), and (37) are applicable for the determination of pressure drop for the counter-flow case with the following exceptions:

(a) σ_{a_1} is replaced with σ_{a_2}.

(b) $\mu_a^{0.2}$ is evaluated at temperature t_{a_2}.

(c) ρ_{a_1} is interchanged with ρ_{a_2}.

EXPERIMENTAL VERIFICATION OF PARALLEL-FLOW EQUATIONS

Heat-transfer and pressure-drop tests were made with an experimental exhaust-pipe-shroud setup for parallel flow in order to verify the final parallel-flow design equations (12), (13), (14), (31), and (34). A further purpose was to determine the degree of conservativeness of using air temperature for shroud temperature.

Exhaust-Pipe-Shroud Setup

Exhaust-pipe-shroud flow system.- The test equipment consisted
essentially of an experimental exhaust-pipe-shroud test section, an
aircraft engine, and a source of cooling air. A diagrammatic sketch
of the entire system is shown in figure 3.

The test section consisted of two concentric pipes 20 feet long.
The outside pipe or shroud was made of black iron with an 11-inch
inside diameter; the inner or exhaust pipe was made of stainless
steel with a $6\frac{3}{16}$-inch outside diameter. The shroud was covered with
a 3-inch thickness of rock wool, and the entire test section was then
surrounded with a metal shield to protect it from the blast of the
propeller on the engine. The pipes were centered at both ends of
the test section and were spaced at the midpoint by three small steel
fins which were welded radially to the exhaust pipe with enough
clearance to provide for expansion of the exhaust pipe and shroud
at high temperatures.

An Allison V-3420-11 engine was utilized as the exhaust-gas
producer. Expansion between the engine and the test section and
engine vibrations were absorbed by four stainless-steel expansion
joints welded in the exhaust pipe.

The shroud cooling air was supplied by a centrifugal blower
provided with a bell-shaped inlet and a 40-mesh copper screen at the
blower outlet to reduce air-flow pulsations to a minimum. A 12-inch
radial-vaned flow straightener was placed 1 foot downstream of the
discharge as a precaution against whirl in the air flow, and a
venturi 10 diameters below the blower outlet measured the cooling-
air flow. The cooling air had to be conducted around a bend of
about 135° before it entered the test section. In order to reduce
the bend loss, the diameter of the pipe from the venturi to the bend
was gradually increased. A 40-mesh copper screen placed at the end
of the bend and a radial-vaned flow straightener placed in the con-
tracting section were required in order to insure a good distribu-
tion of the cooling-air velocity and total pressure at the entrance
to the test section. The cooling air was discharged at the end of
the test section through a diffuser to decrease the exit loss and
consequently to release a larger quantity of the available blower
pressure for forcing air through the system.

Instrumentation.- The instrumentation installed in each of the
stations is illustrated in figure 4. The three stations were numbered
from the upstream end of the test section and spaced as follows:
9.9 feet from station 1 to station 2 and 10 feet from station 2 to

station 3. The relative location of all the thermocouples and pressure tubes at a typical station is shown in figure 5. All instruments at each station were mounted in one plane perpendicular to the axis of the pipes at 120° intervals.

All temperatures were measured with chromel-alumel thermocouples in conjunction with a Brown self-balancing potentiometer. Exhaust-gas temperatures were measured with two radiation-shielded inconel-covered thermocouples per station which were located near the center of the exhaust pipe. Average exhaust-pipe temperatures were measured at each station with two thermocouples spot welded to the outside of the exhaust pipe. These thermocouples were placed radially in line with the exhaust-gas thermocouples to produce a minimum blocking effect in the annular space. Three thermocouples were spot welded to the outside of the shroud at each station, and one thermocouple was placed midway between the stations for an average station temperature and a representative temperature gradient down the pipe. Cooling-air temperatures were measured with three radiation-shielded-traversing thermocouples per station. All thermocouples were calibrated before and after the tests.

Three rakes were installed radially in the annular space at each station. Each rake consisted of four shielded total-pressure tubes, one unshielded total-pressure tube, and one static-pressure tube; the static-pressure tube was nearest the exhaust pipe. The shield had to be removed from the total-pressure tube nearest the static-pressure tube as the shield was responsible for disturbing the air flow over the static-pressure tube. Three wall static-pressure orifices were also installed at each station.

The flow of the exhaust gas was obtained by measuring the engine charge air with a calibrated venturi and by measuring the fuel flow with a rotameter. The gasoline used in the tests was 100-octane grade 130 aromatic fuel, specification AN-F-28 with a hydrogen-carbon ratio of approximately 0.17.

Tests

Isothermal pressure-drop tests.- One test (test A) was made to determine the pressure drop in the annular space with only air passing through the system. These runs were made to establish the friction formula inasmuch as the measured pressure differences were about equal to the friction losses; the momentum loss due to change in density was negligible with no heat present. The speed of the cooling-air blower was varied so that the range of Reynolds number, based on the equivalent diameter of the annular space, was from about 100,000 to 324,000. Pressure equilibrium was determined for all observations from line plots.

Heat-transfer tests.- Four series of runs were made to include an appreciable range of Reynolds and Prandtl numbers with both cooling air and exhaust gas flowing in the system. A tabulation of approximate values of the variables involved in the isothermal and heat-transfer tests is shown in table 1.

The effect of Prandtl number on the gas and air heat-transfer coefficients was obtained by varying the fuel-air ratio over a range from 0.063 to 0.090 while Reynolds number on the gas and air sides of the exhaust pipe was held constant (test B). This variation of fuel-air ratio gave a large variation in gas temperature.

The effect of exhaust-gas Reynolds number on the heat-transfer coefficient of the exhaust gas was established over a large range of Reynolds number in two tests. While the fuel-air ratio and cooling-air Reynolds number were held constant, the engine power was varied to obtain a variation in exhaust-gas Reynolds number. In one test (test C_1) the exhaust-gas Reynolds number was varied from approximately 120,000 to 220,000 at a constant cooling-air Reynolds number of 170,000. In the other test (test C_2, a continuation of C_1) the exhaust-gas Reynolds number was varied from 215,000 to 360,000 at a constant cooling-air Reynolds number of 250,000.

The effect of the cooling-air Reynolds number on the heat-transfer coefficient of the cooling air was obtained in test D by varying the Reynolds number over a range from 170,000 to 280,000 while the exhaust-gas Reynolds number and the fuel-air ratio were held constant. The cooling-air Reynolds number was varied by varying the air flow by means of the blower.

The cooling-air pressure differences were obtained in each of the four heat-transfer tests to compare these results when an appreciable momentum pressure loss was present with the results of the isothermal tests and to determine the applicability of the friction formula established in the isothermal tests. The extensive range of Reynolds number obtained in test D provided for a large range of pressure drop.

Temperature traverses of the annular space at each station and pressure and temperature equilibrium from line plots were obtained for all observations.

A comparison of exhaust-gas samples upstream and downstream of the test section showed that no afterburning occurred in the exhaust pipe.

Methods

Verification of shroud-design equations.- The method of checking the equations for the design temperatures and pressure drops was to

compare the values measured in the tests with the values calculated
by means of the equations, the measured values of temperatures at
the upstream station, and the flow rates. In the present tests no
exit loss was involved and calculated values of $(\Delta p_f + \Delta H_h)$ were
compared with measured values. The degree of conservatism of the
method of designing for limiting air temperatures rather than for
limiting shroud temperatures was obtained by comparing the measured
air temperatures with the measured shroud temperatures.

The calculated values of temperatures required determination of
the heat-transfer coefficients h_a, h_r, and h_e. Equation (20),
equation (23), and methods outlined in the section entitled "Funda-
mental laws for heat-transfer coefficients" were used to calculate
the convection coefficient on the air side h_a and the radiant-heat-
transfer coefficient h_r.

The emissivity of the exhaust pipe, which was required in
evaluating h_r, and the emissivity of the shroud were obtained from
reference 5. This reference shows values of 0.79 for oxidized steel
and a selected value of 0.70 for stainless steel (8 percent nickel,
18 percent chromium).

For all tests both equations (15) and (18) were used to calcu-
late the convection-heat-transfer coefficient h_e, and tempera-
tures obtained by use of the values calculated from each equation
were compared to determine the effect of using air properties in
place of gas properties. The appropriate temperatures used for
determining the properties were given in the section on "Fundamental
laws for heat-transfer coefficients." The properties were obtained
from the appendix. A check was made for a few tests of the error
involved in the calculated temperatures by use of 0.30 and 0.24
for $\bar{c}_{p_e}$ and $\bar{c}_{p_a}$, respectively, rather than the integrated mean
values of specific heats.

The measured values of air and exhaust-gas temperatures at sta-
tion 1 and the weight-flow rates of air and gas were substituted in
equation (13) in order to calculate the downstream exhaust-gas tem-
peratures. Measured values of air and gas temperatures at station 1
and calculated values of these temperatures at the downstream sta-
tions were used to calculate pipe temperatures by means of equa-
tion (14). The air temperatures at the downstream stations were
calculated from equation (12) and calculated values of downstream-
gas temperature.

The friction factors were obtained first for the data of the
isothermal tests (table 1) by use of equation (25) and were plotted

against Reynolds number. It was determined from this plot whether
the simple exponential variation of equation (26) is valid and, if
such were the case, whether the values of C and n may be used.
Values of the friction factor f or of C and n from the iso-
thermal tests were then available to calculate Δp_f for the heat-
transfer tests with either equation (25) or equation (31). Equa-
tion (34) was used to calculate ΔH_h in the heat-transfer tests.
Values of calculated downstream air temperatures were used to cal-
culate downstream air densities for use in the formulas.

Verification of the design formulas was accomplished by com-
paring the foregoing calculations with the measured values at both
station 2 and station 3; station 1 was used as the upstream station
in both cases. The appropriate pipe length was used in the formulas
in each case.

Integrated mean temperatures and pressures.- As a result of the
large temperature gradient of the cooling air in the annular space
true mean air temperatures and pressures could only be obtained by
integrating the measured pressure- and temperature-distribution
curves across the annulus. The integration of all the data obtained
in the tests would have involved a vast amount of labor and time
which did not seem warranted. Consequently, a method was developed
for correcting arithmetic averages. For test D mean values of the
measured air temperatures were obtained for the three stations on
both an integrated and an arithmetic basis. The arithmetic values
were plotted against the integrated values and the resulting straight-
line curves were used to correct the arithmetic averages of the
measured air temperatures for all of the other tests. In all plots
presented for the comparison of calculated and measured values, the
results are based on these corrected arithmetic-mean measured air
temperatures.

In order to integrate the air temperatures of test D with the
individual measured temperatures weighted according to the local
weight rate of flow, the static and total pressures as well as the
temperatures at each local point must be known. When the pressure
and temperature distributions in the annular space were plotted,
some doubt arose as to the correct profile for the curves from the
tube and thermocouple positions nearest the walls of the pipes to
the walls inasmuch as the nearest pressure and temperature readings
were about $\frac{3}{8}$ inch from the walls of the pipes. As a consequence,
the pressure-distribution curves in the vicinity of the walls of the
annular space for the isothermal tests were obtained by applying
methods available in reference 6 for obtaining velocity profiles in
pipes and by using a uniform temperature gradient across the space.

In the heat-transfer tests the temperatures in the vicinity of the exhaust-pipe and shroud walls which were required to apply the methods of reference 6 were not available. The pressure-distribution curves were therefore faired approximately like those of the isothermal tests.

In order to determine the effect of this fairing on the integrated temperature average, one run of test D was obtained from another fairing in which the pressure-distribution curve was extended much closer to the pipe walls. The temperatures obtained from a survey nearest a pressure rake (see fig. 5) were used in conjunction with the pressures of that rake to obtain the integrated-temperature averages at the pressure-rake location. The error involved in the integrated air temperatures by using such noncoinciding temperatures was also checked by computing one run of test D by use of temperatures obtained from cross plots of the temperature test data at points coinciding with the pressure-tube locations. The temperature-distribution curves for test D from the point of reading nearest the walls to the walls for any survey were determined by a trial-and-error process by use of information from reference 6 and the pressure-distribution curves obtained as previously explained.

Only the temperatures at the center of the exhaust pipe were obtained at each station because of practical difficulties and also because, in turbulent flow in a circular pipe, the mean temperature is very close to the center temperature. The center values were therefore used for the mean values.

The integrated-pressure averages at each station for test D were obtained by weighting the individual pressure and temperature values according to the local weight rate of flow. The required individual pressure and temperature values were obtained from the distribution curves described in the section entitled "Verification of shroud-design equations." For one run of test D the integrated values for each station were obtained for each of the three types of fairing described in the foregoing paragraphs. Pressure losses were then compared by using both the integrated- and arithmetic-measured pressure averages. For tests other than test D, only arithmetic averages of the measured pressures were used to calculate the losses.

Inasmuch as a few thermocouple failures resulted in the loss of some of the temperature data, the missing temperature values were determined by assuming a heat balance between the gas and the cooling air. The prohibitive time element involved in repeating tests until a complete set of temperature data was obtained was considered to be adequate justification for this procedure.

Comparison of Experimental and Calculated Values

The comparisons of temperatures and pressures drops calculated
by using the theoretical equations with measured values will be
given in the following sections. A 45° line is drawn on each part
of each figure presented. When the plotted data fall on these lines,
perfect agreement between the measured and calculated values is indi-
cated. The results of the calculations to determine the effects of
using air properties for gas properties in the equation for gas
convection-heat-transfer coefficient h_e, the constant specific-
heat values, the arithmetic pressure averages to determine pressure
losses, and the three types of fairing of pressure- and temperature-
distribution curves for the annular space are given first inasmuch
as they had a direct bearing on the workup of the remaining results.

Effects of approximations and fairing methods.- The effects of
the different fairing methods and the approximations to simplify the
computations on the calculated design temperatures and pressure
losses can be obtained from table 2. In this table the percent
difference between the approximate values and precise values or
percent difference between the results based on methods of refer-
ence 6 and results based on other fairing methods are given.

Comparison of calculated values of downstream exhaust-gas tem-
peratures, cooling-air temperatures, and exhaust-pipe temperatures
obtained by use of values of h_e based on air properties at tem-
perature t_{e_1} with values of temperatures obtained by use of values
of h_e based on gas properties at temperature t_{e_1} showed negligible
differences in the gas and air temperatures and only small differ-
ences in the pipe temperatures. (See table 2.) The pipe tempera-
tures based on air properties were about 4 percent lower than those
based on gas properties. Consequently, comparisons of calculated
temperatures and measured values presented hereinafter have used a
value of h_e based on air properties to determine the calculated
values.

The calculations to determine the effect of using constant
values of specific heats in place of integrated mean values showed
that no noticeable error was introduced in the values of calculated
design temperatures. (See table 2.) In the following results,
constant values of specific heats were therefore used to calculate
the temperatures.

The integrated station pressure averages obtained from the
three types of fairing differed to some extent, but the resulting
station-to-station pressure losses agreed very well. (See table 2.)
Also, the pressure losses for test D based on the arithmetic averages

of measured pressures were in excellent agreement with losses based on integrated averages of measured pressures. This agreement was considered sufficient justification for the procedure of using the arithmetic averages of the measured pressures to determine the measured pressure losses.

The three types of fairing resulted in slightly different integrated mean air-station temperatures, but these differences and their consequent effect on the results from the design equations (table 2) were not significant enough to warrant basing the integrated mean air temperatures on any other than the original fairing described in the methods. The original fairing method was consequently used to determine the integrated air temperatures for all of the runs of test D.

With regard to the comparison of arithmetic and integrated average temperatures, the following results of test D may be of interest to other investigators:

(a) Measured air temperatures based on arithmetic averages were about 5 percent higher than those based on integrated averages.

(b) Calculated downstream exhaust-gas temperatures based on arithmetic averages were about 1 percent higher than those based on integrated averages.

(c) Calculated downstream air temperatures based on arithmetic averages were about 4 percent higher than those based on integrated averages.

Downstream exhaust-gas temperatures.- A comparison of the calculated downstream exhaust-gas temperatures with the measured temperatures for stations 2 and 3 is given in figure 6. The calculated temperatures are less than $1\frac{1}{2}$ percent lower than the measured values. This small difference probably results either from determining the heat-transfer coefficients for use in equation (13) by the methods outlined or from errors of measurement. A conclusion is drawn that the design equation (13) and the simplified equations for heat-transfer coefficients for determining the downstream exhaust-gas temperature are satisfactorily verified.

Exhaust-pipe temperatures.- The comparison of the calculated exhaust-pipe temperatures with the measured temperatures for the three stations are presented in figure 7. At station 1 the calculated temperatures average about 3 percent lower than the measured values. Corresponding values for stations 2 and 3 are approximately 5 percent and 4 percent lower, respectively. The difference between

the calculated and measured values at station 1 is probably due to
the fact that the pipe-temperature equation was derived by assuming
that the radiation was negligible, which tends to make the calculated
values higher than the measured values. An opposite effect is
created by using the heat-transfer coefficient h_e based on air
properties rather than on gas properties; this substitution has a
tendency to reduce the pipe temperatures. The difference between
the calculated and measured downstream temperatures may be a cumula-
tive effect caused (1) by using calculated exhaust-gas temperatures
which are lower than the measured values, (2) by using calculated
air temperatures which are higher than the measured values, (3) by
neglecting radiation, and (4) by using air properties in the equa-
tion for value of h_e. The first and fourth factors tend to decrease
and the second and third factors tend to increase the calculated
exhaust-pipe temperatures. From figure 7 it is concluded that
exhaust-pipe temperatures, predicted from equations of the type of
equation (14) with air properties used throughout in the heat-
transfer-coefficient formulas, will be from 3 to 5 percent too low.
The verification is still acceptable, however, within the limits of
engineering practicability.

Cooling-air temperatures.- The calculated downstream cooling-
air temperatures deviate about 3 to 4 percent from the measured
values as shown by figure 8. This difference is attributed to the
fact that the calculated exhaust-gas temperatures used in equa-
tion (12) were about $1\frac{1}{2}$ percent lower than the measured values. In
the lower range of temperatures at station 2 the calculated tempera-
tures are higher than the measured values whereas in the higher
range the opposite is true. At station 3 the calculated values are
in general higher than the measured values. The use of gas prop-
erties instead of air properties would not have appreciably changed
the result given in figure 8 because such a substitution had a
negligible effect on the calculated downstream exhaust-gas and air
temperatures. Although the difference between the calculated and
measured air temperatures is rather large, the proposed method
apparently leads to the prediction of conservative values of down-
stream air temperatures. The use of equation (12) and methods given
to predict air temperatures are therefore considered satisfactory
for shroud design purposes.

Relation of measured shroud temperatures to measured cooling-
air temperatures.- Inasmuch as the analysis uses as a design criterion
the cooling-air temperature rather than the shroud temperature, these
two temperatures should be compared. The results of this comparison
are shown in figure 9. The shroud temperature was about 20° F higher
than the corrected arithmetic mean cooling-air temperature at station 1,

about 20° F lower at station 2, and 40° F lower at station 3. The shroud temperature also increased from the upstream station to the downstream stations. Inasmuch as the calculated downstream air temperatures were in general higher than the measured air temperatures, the procedure of using the air temperature as a design criterion will result in a very conservative design for the shroud temperatures.

Determination of constants in friction-pressure-drop equation.- The friction factors for the isothermal tests were plotted against Reynolds number of the cooling air on logarithmic coordinates (fig. 10) and the values of C and n for use in equation (31) were found to be 0.07 and 0.20, respectively. The exponent n is approximately the value obtained for straight pipes but the value of C is high as compared with values obtained for smooth and commercial pipes (0.046 and 0.054, respectively, reference 1). Although in references 3 and 4 higher values of C are advocated for annular spaces than for pipes, the value of C determined for the diameter ratio of the test setup on the basis of equation (27) was calculated to be 0.058, which is still lower than the value of 0.07 determined experimentally. Consequently, it is believed that indeterminate pipe roughness was probably a factor influencing the value of C. Inserting the values of C and n in equation (31) gives the following expression for Δp_f:

$$\Delta p_f = \frac{0.0879}{\sigma_{a_1}} \frac{l \mu_a^{0.2}}{\left(d_s + d_p\right)^{1.8} \left(d_s - d_p\right)^3} \left(1 + \frac{\rho_{a_1}}{\rho_{a_2}}\right) W_a^{1.8} \qquad (40)$$

Cooling-air pressure losses for heat-transfer tests.- The data of figure 11 show the comparison of the calculated and measured cooling-air pressure losses from stations 1 to 2 and stations 1 to 3 for the heat-transfer tests. The isothermal data are also plotted in figure 11 as a check on the calculations. Perfect agreement between the calculated and measured pressure losses is obtained for the isothermal data, as indicated by the plotted points which fall along the 45° lines, because the C and n values used to calculate the friction pressure drops were obtained from the measured pressure drops.

The calculated values of the pressure loss averaged about 10 percent higher than the measured values for the heat-transfer tests. This difference is due partly to a slight overestimation of the heating- and friction-pressure losses from equations (34) and (40)

since these equations are very sensitive to downstream air tempera-
tures, which have previously been shown to have been overestimated
by about 3 or 4 percent. The difference between the calculated and
measured pressure losses for the heat-transfer tests is in the con-
servative direction, as was the calculated cooling-air temperature,
and therefore a design based on the equations will be conservative.

GENERAL DISCUSSION

The cooling-air flow rates and the ratios of the cooling-air
flow rates to exhaust-gas flow rates used in the experiments were
much higher than those usually encountered in flight. These rates
and ratios were used because errors in measurement are reduced when
larger quantities are involved and because the flow rates in flight
are in the turbulent-flow region as were those of the experiments.
Moreover, the laws of heat transfer and pressure loss in pipes
established in a certain range of the turbulent-flow region are
generally applicable with little error to other ranges in the region.
For the latter two reasons and because, in general, the design
formulas for parallel-flow systems were verified in the experiments,
it is believed that the design formulas will be applicable to flight.
In a calculation of a shroud design the fact that the pressure loss
will be overestimated will result in the calculated temperatures
being more nearly equal to the actual temperatures than in the
experimental results.

Since the equations have no diameter-ratio limitation provided
that the cooling-air flow in the annulus is turbulent, the verifica-
tion of the parallel-flow equations for one ratio of shroud diameter
to exhaust-pipe diameter lends support to the belief that these equa-
tions are applicable to all practical values of the ratio of shroud
diameter to exhaust-pipe diameter for which the cooling-air flow is
expected to be turbulent. Although no counter-flow tests were run,
the counter-flow equations are believed to be equally as applicable
to design problems as the parallel-flow equations because of their
similarity. In the analysis the assumption that the downstream
shroud temperature would always be a little less than the downstream
cooling-air temperature was made for the case of parallel flow and
the case of counter flow. The validity of this assumption was
verified for parallel flow by experimental data. In the case of
counter flow, however, the temperatures of the exhaust gas, the
exhaust pipe, and the cooling air are highest at the downstream sta-
tion of the shroud. It may be possible, therefore, because of radia-
tion from the exhaust pipe and because of the small temperature differ-
ential between the cooling air and the shroud that the shroud tempera-
ture may be higher than the cooling-air temperature at the downstream

station. Thorough exploration of this possibility would require either a complex analysis or further testing, both of which were outside the scope of the present investigation.

One problem of immediate importance for which the equations derived in this paper should be applicable is the design of shrouds for the tail pipes of jet engines. The design equations will be applicable without modification if the luminosity of the gases is negligible. If luminosity of the gases is appreciable, the analysis will require extension to account for the heat transfer from the exhaust gas to the exhaust pipe by thermal radiation. If flaps or ejector pumps are used, and the cooling-air exit pressure is thus decreased from atmospheric, the application of the pressure-drop relation to shroud design must include methods for determining this cooling-air exit pressure.

Further research is needed to establish definitely the basic laws of heat transfer and pressure losses in annular spaces, especially with respect to the fluid temperatures and constants that should be used. The principal source of difficulty in the determination of such laws is the temperature gradient of the cooling air. In addition, investigation of pressure losses in annular bends would be a great aid in predicting accurately the pressure drops in specific exhaust-pipe-shroud installations. Finally, the extension of the present work to include tests of shrouded tail pipes for jet-engine installations would be desirable.

SUMMARY OF RESULTS

The design equations for predicting shrouded exhaust-pipe-installation temperatures for parallel-flow systems were verified within the limits of engineering requirements by tests of an experimental exhaust-pipe-shroud setup for one ratio of shroud diameter to exhaust-pipe diameter. A comparison of measured values with values calculated by use of the design equations based on constant values of specific heats of exhaust gas and cooling air, air properties, and corrected mean air temperatures showed that:

(a) The calculated values of downstream exhaust-gas temperatures generally were never more than $1\frac{1}{2}$ percent lower than the measured values.

(b) The calculated values of exhaust-pipe temperatures generally were lower than the measured values by not more than 5 percent.

(c) At the downstream stations the calculated cooling-air temperatures were above the measured shroud temperatures.

(d) Conservative values of cooling-air total-pressure losses were obtained with the pressure-drop equation. The calculated values of total-pressure loss were about 10 percent higher than the measured values.

The use of constant values of 0.24 and 0.30 for the specific heats of cooling air and exhaust gas, respectively, and the substitution of air properties for exhaust-gas properties for determining the heat-transfer coefficient for the exhaust-gas in the design equations resulted in a negligible change in the values of calculated exhaust-gas and cooling-air temperatures and only a slight decrease in the values of calculated exhaust-pipe temperature.

II - PROCEDURES FOR SHROUD DESIGN

GENERAL DESIGN CONSIDERATIONS

The problem of shroud design requires the determination of the diameter of the shroud for which certain design-installation temperatures will not exceed specified limits when the pressure drop available for forcing air through the system is known. In order to provide satisfactory cooling for all operating conditions, the shroud must be designed for the flight condition in which the cooling requirements are the most difficult to meet; generally, this condition will be maximum power (climb) at rated altitude.

An analytical method for determining the shroud diameter with a minimum of pressure loss in order not to exceed a limiting temperature such as that given in detail for the case of intercooler design in reference 7 could theoretically be developed. Such methods are impractical if not almost impossible with the complex equations which were derived in the analysis, and, consequently, graphical solutions were used.

The general procedure for design is, for a given length of shroud, to use the equations to determine the design temperatures and the cooling-air pressure drop. A value of shroud diameter is assumed and calculations are made for several assumed values of cooling-air-flow rate. These calculations are repeated for other assumed values of shroud diameter. Curves of the significant design temperatures are plotted against cooling-air-flow rate for each shroud diameter assumed. From these curves the value of cooling-air flow rate for each shroud diameter giving a temperature equal to one

of the imposed limit temperatures and lower than all the other
limiting values is noted. Each of these combinations of shroud
diameter and cooling-air-flow rate for which choking does not occur
$(M_{a2} < 1.0)$ is then used to calculate the pressure loss in the
shroud. A plot of this pressure loss against shroud diameter is
made and compared with the pressure available for forcing air through
the shroud system. Any shroud diameter for which the pressure loss
required is less than that available will give adequate cooling.
The diameter to choose will be that diameter which will give the
greatest available pressure loss, unless this diameter causes exces-
sive cooling drag. When the latter condition occurs the diameter to
choose is that for which cooling drag is a minimum.

When the pressure drop required is greater than that available
and augmentation methods fail to increase the available pressure
drop sufficiently, the shroud may be divided into shorter segments
so that two or more cooling-air entrances and exits are provided as
diagrammed in figure 12. The shorter-length segments require less
pressure drop than the single-segment design. Due to the complexity
of the duct systems involved, no more than two segments will generally
be used. If the limits imposed on the design installation tempera-
tures cannot be met with a shroud system of practical size or number
of segments for the pressure drop available, some alternatives are
available and will be discussed in a section to follow.

The choice of the size of the inlet duct carrying the cooling
air from the free stream to the shroud inlet is important and is
interrelated with the shroud design, because part of the dynamic
pressure of flight is utilized to overcome the losses in this duct
and thereby a decrease is caused in the pressure drop available for
cooling in the shroud. The choice of size, within practical limits,
is such that no appreciable gain in pressure drop available is
obtained with further increase in the area of the duct.

Detail step-by-step procedures for the design of a shroud are
given for the following systems:

(a) Single-segment system for parallel flow

(b) Single-segment system for counter flow

(c) Multisegment system for parallel or counter flow

In order to expedite use of these procedures methodical calculation
forms for parallel flow and counter flow are given in tables 3 and 4,
respectively. In addition, table 5 and figures 13 to 16 are given
to simplify the calculations. The design procedures are concerned

with step-by-step explanation of how these calculation forms are used to design a shroud for a specific installation. Figure 2 illustrates the symbol notation in the shroud-system sketch.

A typical example has been solved for an installation of a four-engine bomber and results are listed coincidental to the discussion of the procedures. The numerical calculations are included in table 3 and pertinent values are given in the discussion of the procedures. The example uses a straight exhaust-pipe-shroud system for parallel flow with the exhaust gases being delivered to the turbine of the turbosupercharger through a single, straight exhaust pipe. A straight inlet duct of constant cross-sectional area has also been assumed. Temperature limits were specified for all the design installation temperatures for illustrative reasons. In an actual design problem, however, the design installation temperatures for which limits must be specified are peculiar to each installation.

SUPPLEMENTARY THEORETICAL CONSIDERATIONS

Certain derivations, other than those given in the analysis presented, are required in the procedures in order to design a shroud system. The methods of determining the cooling-air weight rate of flow at which choking occurs at the shroud exit (designated herein the choke factor), the cooling drag, and the pressure, temperature, and available pressure drop at the shroud entrance must be considered. The discussion of these factors follows.

Choke factor.- The method in the parallel-flow design procedures for determining the cooling-air weight rate of flow at which choking occurs in the shroud system is dependent on a relation obtained from compressible-flow theory. With the assumption that no heat is added to the air in the inlet duct and that no friction drop occurs in the annular space of the shroud-pipe system, a relation between the ratio of the air stagnation temperatures at the shroud exit $T_{a_{2_t}}$ and shroud inlet (assumed equal to T_{o_t}) and the choke factor

$$1.384 W_a \frac{\sqrt{T_{o_t}}}{\left(d_s^2 - d_p^2\right) H_{a_1}}$$ can be obtained from compressible-flow

theory for Mach numbers at the shroud exit up to 1.0. Data for curves of this relation were calculated for downstream cooling-air Mach numbers of 0.6, 0.7, and 1.0.

The given procedure for design is to determine the cooling-air flow rate for which the choke factor is at its limiting value based

on a downstream cooling-air Mach number of 0.6 instead of 1.0. The
value of W_a so obtained is not the maximum value that will exist
in the shroud before choking occurs; however, the use of the choke-
factor curve for a Mach number of 0.6 is recommended for the fol-
lowing reasons: (1) The pressure drop will increase with Mach
number. (2) The shroud-exit pressure losses are smaller for lower values
of M_{a_2}, thereby increasing the pressure drop available in the shroud
for cooling purposes. (3) The limiting choke factor is overesti-
mated by the stagnation-temperature ratio relation because the
latter relation is based on the assumption that no friction occurs
in the annulus. (4) The pressure-drop and heat-transfer formulas
are more applicable at low cooling-air exit Mach numbers than at
high cooling-air exit Mach numbers. At M_{a_2} equal to 0.6 or less
the assumption of cooling-air exit static pressure equal to the
free-stream static pressure, which is used in the pressure-drop
formulas, and of the heat-transfer equation being based on true
temperatures instead of stagnation temperatures (the latter being
the correct temperatures to use) will lead to little error in the
results. At the present time some aircraft shrouded exhaust-pipe
systems are not cooling satisfactorily, possibly because they are
at the choking limit.

Cooling drag.- When more than one shroud diameter will provide
adequate cooling of the installation the best selection of the shroud
diameter would be the one giving the lowest cooling drag if this
drag is appreciable as noted in the foregoing general considerations.
The drag power is obtained from the formula

$$\text{Drag power} = \frac{W_a}{g} V_0 \left(V_0 - V_2 \right) \tag{41}$$

where the velocity V_0 is that of the free stream, the velocity V_2
is that at the shroud exit, and the value of W_a corresponds to the
value of d_s selected.

Pressure at shroud entrance.- The total pressure at the shroud
entrance is determined by the following equation:

$$H_{a_1} = H_0 - \Delta H_{0-1} \tag{42}$$

where

ΔH_{o-1} pressure drop in inlet duct, pounds per square foot

H_o free-stream total pressure, pounds per square foot

The total pressure of the free stream is obtained from altitude tables in reference 8. Standard-air values were used in the present example as it was only given for illustrative purposes. In actual designs probably the summer-air values will be required, which are also given in reference 8. Although summer-air temperatures are higher than standard-air temperatures, a check calculation for the example showed that the use of the summer-air temperatures in place of those for standard air made no appreciable difference in the shroud dimensions necessary for adequate cooling. The details of determining the pressure loss in the inlet duct ΔH_{o-1} will be given in step (10) of the procedure for a single-segment shroud with parallel flow.

The static pressure at the shroud entrance p_{a_1} must also be determined. From compressible-flow relations given in reference 10 it can be shown that

$$\frac{\rho_{a_1} v_{a_1}}{\rho_{alt} a_{alt}} = \sqrt{\frac{2}{\gamma - 1}} \left(\frac{p_{a_1}}{H_{a_1}}\right)^{\frac{1}{\gamma}} \sqrt{1 - \left(\frac{p_{a_1}}{H_{a_1}}\right)^{\frac{\gamma-1}{\gamma}}} \tag{43}$$

where ρ_{alt} and a_{alt} are the density and velocity of sound of cooling air at station 1 based on stagnation conditions and γ is the ratio of specific heats. Now the stagnation temperature at station 1 is equal to the free-stream stagnation temperature. Then equation (43) reduces to

$$\frac{1.384 w_a \sqrt{T_{ot}}}{(d_s^2 - d_p^2) H_{a_1}} = \sqrt{\frac{2}{\gamma - 1}} \left(\frac{p_{a_1}}{H_{a_1}}\right)^{\frac{1}{\gamma}} \sqrt{1 - \left(\frac{p_{a_1}}{H_{a_1}}\right)^{\frac{\gamma-1}{\gamma}}} \tag{44}$$

This equation is represented by a curve in figure 16 where the left-hand side of the equation is the ordinate and the abscissa

is $\dfrac{H_{a1} - p_{a1}}{H_{a1}}$. The figure is divided into several parts for different ranges of $\dfrac{H_{a1} - p_{a1}}{H_{a1}}$. If the values of the ordinate and H_{a1} are known, p_{a1} may be determined from figure 16.

Temperature at shroud entrance.- The temperature of the cooling air at the shroud entrance is determined from the equation

$$T_a = T_{alt}\left(\frac{p_{a1}}{H_{a1}}\right)^{\frac{\gamma-1}{\gamma}} = T_{0t}\left(\frac{p_{a1}}{H_{a1}}\right)^{0.286} \tag{45}$$

where T_{0t} is the free-stream stagnation temperature.

Available pressure drop at shroud entrance.- The pressure drop available for forcing the air through the whole system (inlet duct and shroud) is equal to $H_0 - p_0$ with the assumptions that all the velocity head at the shroud exit is lost and that the static pressure at the exit is free-stream static pressure. The pressure drop required by the inlet duct is equal to ΔH_{0-1}. The pressure drop available for forcing the air through the shroud is the difference, or

$$\Delta H_{available} = \left(H_0 - p_0\right) - \Delta H_{0-1} \tag{46}$$

In the foregoing formulas the subscript 1 has been used to denote shroud entrance. This subscript is for parallel flow. For counter flow all subscripts referring to this station should be changed to 2.

SINGLE-SEGMENT SHROUD FOR PARALLEL FLOW

For a parallel-flow system the shroud must be designed so that imposed limiting values of downstream exhaust-gas temperatures t_{e2}, exhaust-pipe temperatures t_p, and downstream shroud temperatures t_{s2} will not be exceeded. (See fig. 2(a).) Values assumed or calculated for this example are given in the following steps:

Step 1 - Exhaust-gas flow rate W_e:

From manufacturer's data or the following approximate formula, obtain

$$W_e = \frac{7.5bhp(1 + f)}{3600} \tag{47}$$

where

f   fuel-air ratio

bhp   brake horsepower

Then, for the illustrative example,

$$W_e = 4.84 \text{ pounds per second}$$

Step 2 - Inlet exhaust-gas temperature t_{e_1}:

The value of t_{e_1} may be obtained from the equation

$$t_{e_1} = t_m - x\ell \tag{48}$$

where

t_m exhaust-gas temperature at manifold obtained from manufacturer's data or by analytical methods

x   cooling rate of gas in exposed exhaust pipe, approximately $2°$ per foot

ℓ length of exposed exhaust pipe between manifold and shroud entrance

For illustrative purposes, a value of t_{e_1} is assumed, as

$$t_{e_1} = 1800° \text{ F}$$

Step 3 - Exhaust-pipe diameter d_p:

The outside diameter of the exhaust pipe d_p is obtained from manufacturer's data or installation drawings.

Step 4 - Airplane and altitude conditions:

Airplane altitude and velocity are secured from manufacturer's data for the design flight condition. Free-stream conditions p_o, T_o, and ρ_o are obtained from altitude tables for standard air. (See reference 8.)

Step 5 - Design downstream exhaust-gas temperature t_{e_2}:

Obtain t_{e_2} from manufacturer's data on the safe operating temperatures of the turbine or, if a turbine is not used, the value selected by the designer for reasons peculiar to the installation. Decrease this design imposed maximum value of t_{e_2} by approximately $1\frac{1}{2}$ percent in the design procedure to correct for the slight underestimation of downstream exhaust-gas temperature by equation (13). For the example, the design maximum temperature is $1675°$ F and, therefore,

$$t_{e_2} = 1650° \text{ F}$$

Step 6 - Design exhaust-pipe temperature t_p:

Obtain from available data or estimate from experience the maximum temperature at which the exhaust pipe can operate without danger of failure. Approximate limits to use if no data are available are from $1200°$ F to $1450°$ F. Decrease this design imposed maximum value of t_p by approximately 4 percent in the design procedure to correct for the slight underestimation of downstream exhaust-gas temperature by equation (14). For an imposed maximum pipe temperature of $1450°$ F,

$$t_p = 1400° \text{ F}$$

Step 7 - Design shroud temperature t_s:

Obtain from the geometry and location of components of the installation the maximum shroud temperature that will not produce adverse effects of heat radiation. Limits to use, if none are specified by the airplane or engine manufacturer, are between $500°$ F and $800°$ F. If the shroud touches or passes close to rubber, neoprene, or other organic materials, use a lower limit of $500°$ F and shield the shroud at these points. This value of t_s is used for the critical downstream

cooling-air temperature t_{a_2} because, as brought out in the section entitled "Relation of measured shroud temperatures to measured cooling-air temperatures," a conservative design procedure to meet a limiting shroud temperature is to design for a limiting cooling-air temperature of the same value as the shroud-temperature limit. For the present illustration,

$$t_s = t_a = 800^\circ \text{ F}$$

Step 8 - Emissivity of exhaust pipe ϵ_p:

The emissivity ϵ_p for the most commonly used exhaust-pipe material, stainless steel, is about 0.70, and this value can be used inasmuch as small errors in the absolute value of ϵ_p will have a negligible effect on the design. If another material is used, refer to a standard heat-transfer test for values. The value used in the example is

$$\epsilon_p = 0.70$$

Step 9 - Cooling-air-flow rate W_a:

Assume a large range of values of cooling-air-flow rate (approximately 1/8 to 1/2 of value of W_e) and use with each assumed value of shroud diameter. Assumed values used for W_a are 0.50, 1.00, 1.50, 2.00, 2.50 pounds per second.

Step 10 - Selection of shroud-air-inlet duct size:

Assume an inlet duct cross-sectional area. For the values of cooling-air-flow rate W_a, use the equation for the pressure drop in the inlet duct

$$\Delta H_{0-1} = \underbrace{0.05 q_{c_0}}_{\text{Inlet loss}} + \underbrace{\sum 4 \frac{l_i}{D_i} q_i f}_{\substack{\text{Sum of} \\ \text{straight-} \\ \text{section} \\ \text{losses}}} + \underbrace{\sum K_b q_{i_b}}_{\substack{\text{Sum of} \\ \text{bend} \\ \text{losses}}} + \underbrace{\sum K_d \left(1 - \frac{A_{d_{inlet}}}{A_{d_{exit}}}\right)^2 q_{i_d}}_{\substack{\text{Sum of diffuser} \\ \text{losses}}}$$

and the methods and data of reference 9 to calculate the pressure drop available at the shroud entrance. (All or part of the equation is used depending on duct geometry.) Repeat these calculations for other assumed values of duct size. Plot $\Delta H_{available}$ against W_a for each duct size. (Fig. 17(a).) Select the inlet-duct area that shows no appreciable gain in pressure drop with further increase in duct area. When space limitations restrict the size of the inlet duct, use the largest area possible to get maximum $\Delta H_{available}$. From figure 17(a), the values selected for duct size are:

$$A_i = 0.2376 \text{ square foot}$$

$$d_i = 0.550 \text{ foot}$$

Step 11 - Length of shroud l:

Obtain l from installation geometry and purpose of shroud. The initial choice should be a single-segment shroud. The value of l for the present example is:

$$l = 18 \text{ feet}$$

Step 12 - Diameter of shroud d_s:

Assume a large range of practical shroud diameters, such as, for the present problem,

$$d_s = 0.542, \; 0.583, \; 0.625, \; 0.667, \; 0.710, \; 0.752 \text{ foot}$$

Step 13 - Curves of cooling-air static pressure at shroud inlet p_{a_1}:

Determine the value of p_{a_1} by computing items (30) to (36) of table 3 with values of W_a assumed in step 9. The calculations cannot be continued for any combination of d_s and W_a that causes item (34) to exceed 0.5907, for at this value choking occurs in the inlet duct to the shroud. Plot the choke factor (item (34)) against W_a for each d_s. (Shown, for the present examples, as the radial lines of figure 17(b).) The cooling-air-flow rate for each d_s is further limited by choking in the shroud due to heat addition to the air. Thus, the limiting value of choke factor (item (34)) must be obtained for the actual value of downstream cooling-air temperature that will result with each W_a. These temperatures are not yet known;

42

therefore, the calculations must be continued so that t_{a2} can be determined for all the assumed W_a values for each d_s that will not cause the inlet duct to choke. Plot p_{a1} against W_a for each d_s as in figure 17(c).

Step 14 - Curves of cooling-air temperature at shroud inlet t_{a1}:

Determine value of t_{a1} by computing item (37) of table 3. Plot t_{a1} against W_a for each d_s as in figure 17(d).

Step 15 - Curves of upstream exhaust-pipe temperature t_{p1}:

Determine value of t_{p1} by computing items (38) to (50) of table 3. Plot t_{p1} against W_a for each d_s (fig. 17(e)).

Step 16 - Curves of downstream exhaust-gas temperature t_{e2}:

Determine value of t_{e2} by computing items (52) to (64) of table 3. Plot t_{e2} against W_a for each d_s (fig. 17(f)).

Step 17 - Curves of downstream cooling-air temperature t_{a2}:

Determine value of t_{a2} by computing item (65) of table 3. Plot t_{a2} against W_a for each d_s (fig. 17(g)).

Step 18 - Curves of downstream exhaust-pipe temperature t_{p2}:

Determine t_{p2} by computing items (66) and (67) of table 3. Plot t_{p2} against W_a for each d_s (fig. 17(h)).

Step 19 - Design d_s and W_a combinations:

Select from the plots obtained in steps 15 to 18 (figs. 17(e) to 17(h)) the value of W_a needed for each d_s to make every installation temperature equal to its specified limiting value. (See steps 5 to 7.) All installation temperatures considered, the maximum value of W_a obtained for each d_s is the cooling-air-flow rate required to maintain all installation temperatures below specified limits. Plot these maximum values of W_a on the radial d_s lines of the plot obtained in step 13 (fig. 17(b)) to obtain the choke-factor curve for required cooling-air-flow rate. Select the value of t_{a2} for these same W_a and d_s combinations from the plot obtained in step 17 (fig. 17(g)).

Use these values of t_{a_2} to determine the cooling-air downstream stagnation temperature from the equation

$$T_{a_{2_t}} = T_{a_2} + 0.2361 \left(\frac{W_a T_{a_2}}{A_a p_{a_2}} \right)^2$$

where p_{a_2} is cooling-air downstream static pressure assumed equal to free-stream static pressure. Determine $T_{a_{2_t}}/T_{o_t}$ for each d_s and W_a combination. Obtain the value of the limiting approximate choke factor for each $T_{a_{2_t}}/T_{o_t}$ from the curve for $M_{a_2} = 0.6$ of figure 17(i). (Recommended design procedure is to limit M_{a_2} to a value of 0.6.) Plot these values of choke factor on the radial d_s lines of plot obtained in step 13 (fig. 17(b)) to obtain the choke-factor curve for the recommended design limit. Select from this plot the values of d_s for which the choke factors for required cooling-air-flow rate are less than the choke factors for the recommended design limit. (For the illustrative example, values of d_s selected from figure 17(b) were 0.667, 0.710, and 0.752.) Use these values of d_s and the corresponding values of required cooling-air-flow rate W_a in the shroud pressure-drop calculations (items (68) and (69) of table 3). For the d_s and required W_a combinations for which choke factors for required cooling-air-flow rate are greater than the recommended design limit choke factors, it is possible to determine the Mach number at the shroud exit. Those combinations for which M_{a_2} is less than 1.0 may possibly provide satisfactory cooling if sufficient pressure is available to force the air through the system. Such designs, however, are not recommended.

Step 20 - Curve of cooling-air pressure drop through shroud ΔH:

Determine the pressure drop for each d_s and W_a combination finally obtained in step 19 by computing items (70) to (88) of table 3. Select values of p_{a_1}, t_{a_1}, and t_{a_2} needed for this calculation from the plots obtained in steps 13, 14, and 17 (figs. 17(c), 17(d), and 17(g)). Plot the $\Delta H_{required}$ so obtained, the $\Delta H_{available}$ for the inlet-duct size previously selected (step 10), and d_s against W_a on the same curve.

The d_s values are plotted against their corresponding combination values of W_a that meet imposed limiting temperatures as obtained in step 19. The plot for the illustrative examples is given in figure 17(j).

Step 21 - Selection of shroud diameter d_s:

Compare the pressure-drop-required curve with the pressure-drop-available curve (from step 20). Three situations are possible:

(1) All of the pressure-drop-required curve is lower than the pressure-drop-available curve. For this case select the value of d_s corresponding to the value of W_a having the greatest excess available pressure drop or, if appreciable, the lowest cooling drag. Any shroud diameter will give adequate cooling.

(2) Only a part of the pressure-drop-required curve is lower than that available. For this case select the value of d_s in the range of the value of W_a for which the pressure-drop-required curve is lower than the available-pressure-drop curve. The best diameter to use in this range is determined as in the preceding case 1.

(3) All of the pressure-drop-required curve is higher than that available. For this case no single-segment shroud of any diameter used will provide satisfactory cooling. In order to obtain the required cooling the shroud must be divided into segments of shorter length. The design procedure for this case is continued in the section on multisegment shrouds.

The sample problem fell into the category of case 3 in step 21. (See fig. 17(j).) A two-segment shroud was assumed and the design continued as explained in a subsequent section on multisegment shrouds. The inlet ducts for both segments were assumed identical. The design procedure, calculations, and curves for the multisegment shroud are similar to those for the single-segment shroud; therefore, they are not given for the sample problem. A shroud divided into two segments of equal length, 9 feet long and 0.752 feet in diameter, was found to provide satisfactory cooling for the subject installation. Pertinent values are listed in the following table:

Segment	Value of W_a to provide required cooling (lb/sec)	ΔH in shroud for required cooling (lb/sq ft)	ΔH available for required W_a value (lb/sq ft)	Cooling-air-exit Mach number
First	1.92	85.6	91.5	0.32
Second	2.00	88.1	91.0	.31

The exit Mach number for both segments is noted to be far below the recommended design value of 0.6. The drag power for the two-segment shroud was less than $\frac{1}{2}$ percent of the brake horsepower of the engine. This drag power is an inappreciable power requirement and will have a very small effect on the airplane performance.

SINGLE-SEGMENT SHROUD FOR COUNTER FLOW

The design of a shroud for counter flow proceeds exactly as for parallel flow using, however, the calculation form given in table 4. For a counter-flow system the shroud must be designed to meet limiting values of downstream exhaust-gas temperature (in the exhaust-gas-flow direction) t_{e_2}, downstream cooling-air temperature (in the cooling-air-flow direction) t_{a_1}, and upstream exhaust-pipe temperature (in the exhaust-gas-flow direction) t_{p_1} illustrated in figure 2(b). This condition constitutes the only appreciable difference between the design for counter flow and parallel flow.

Steps 1 to 14 - Factors and curves required for shroud design:

The factors and curves required for shroud design are determined exactly as in parallel flow, steps 1 to 14, respectively. In steps 10, 13, and 14, station 1 is replaced by station 2.

Step 15 - Curves of downstream exhaust-gas temperature t_{e_2}:

Determine t_{e_2} by computing items (38) to (64) of table 4. Plot t_{e_2} against W_a for each d_s.

Step 16 - Curves of downstream cooling-air temperature t_{a_1}:

Determine t_{a_1} by computing item (65) of table 4. Plot t_{a_1} against W_a for each d_s.

Step 17 - Curves of upstream exhaust-pipe temperature t_{p_1}:

Determine t_{p_1} by computing items (66) and (67) of table 4. Plot t_{p_1} against W_a for each d_s.

Step 18 - Design d_s and W_a combinations:

Select from the preceding plots of installation temperature (steps 15 to 17) the value of W_a for each d_s giving a temperature equal to the limiting temperature. After all installation temperatures are considered, note the value of W_a which gives a temperature equal to one of the limiting values and lower than all the other limiting values for each d_s. The procedure given in step 19 of parallel flow is used to determine the d_s and W_a combinations that will not exceed the recommended limiting choke factor. These combinations of d_s and W_a are used in the pressure-drop calculation. (Items (68) and (69) of table 4.)

Step 19 - Curve of cooling-air pressure drop through shroud ΔH:

Determine the pressure drop for each d_s and W_a combination obtained in step 18 by computing items (70) to (88) of table 4. Select values of p_{a_2}, t_{a_2}, and t_{a_1} needed for this calculation from the previously drawn plots of these values against W_a (steps 13, 14, and 16). Plot the $\Delta H_{required}$ so obtained, the $\Delta H_{available}$ for the inlet duct size previously selected (step 10), and d_s against W_a on the same curve. The d_s values are plotted against their corresponding combination values of W_a that meet imposed limiting temperatures as obtained in step 18.

Step 20 - Selection of shroud diameter d_s:

Selection of shroud diameter is exactly the same as for parallel flow (step 21). Similarly, if no single-segment shroud of any diameter used will provide satisfactory cooling, the shroud must be divided into segments of shorter length. The design procedure for this case is continued in the following section on multisegment shrouds.

MULTISEGMENT SHROUD FOR PARALLEL OR COUNTER FLOW

The design of a multisegment shroud proceeds in much the same manner as that of the single-segment shroud for either parallel flow or counter flow, because each segment is treated as an individual shroud and is dependent only on the preceding segment for the inlet exhaust-gas temperature.

Step 1 - Diameter of shroud d_s:

Select the shroud diameter from the pressure-drop curve, obtained for the single-segment shroud, which requires the smallest pressure drop for adequate cooling. This value of d_s is used for all the shroud segments.

Step 2 - Segment inlet-exhaust-gas temperature t_{e_1}:

Determine the inlet-exhaust-gas temperature for each shroud segment by assuming linear gradient of exhaust-gas temperature. The exhaust-gas temperature at the shroud entrance and at the turbine inlet are the inlet-exhaust-gas temperature and the design downstream exhaust-gas temperature, respectively, obtained for a single-segment shroud from steps 2 and 5 of the parallel-flow or counter-flow design procedures.

Step 3 - Segment design downstream exhaust-gas temperature t_{e_2}:

The segment inlet temperatures obtained in step 2 are used as the limiting exhaust-gas temperatures to be met at the exit of the adjacent upstream segment; that is, t_{e_2} of first segment equals t_{e_1} of second segment, and so forth. (See fig. 12.)

Step 4 - Determination of shroud diameter d_s:

The design then proceeds exactly as explained previously, with table 3 used for parallel flow or table 4 for counter flow; each segment is treated as an individual shroud. The pressure drop in each shroud segment is calculated only for the value of d_s from step 1 and the value of W_a that gives the required cooling and for which the recommended limiting choke factor is not exceeded. The shroud diameter selected in step 1 will provide satisfactory cooling if the pressure drop in each shroud segment is less than the pressure drop available for that segment.

It is unlikely that more than two segments with two entrances and two exits will ever be used because of the complexity of the duct system, the additional weight, and the possible attendant drag increases.

DESIGN PROCEDURE WHEN MULTISEGMENT SHROUD SYSTEMS

PROVIDE UNSATISFACTORY COOLING

When the pressure drop available for cooling is less than the pressure drop required for adequate cooling, the available pressure drop can be increased by several methods: (1) locate the intake of the inlet duct in a region of higher dynamic pressure, (2) locate the shroud exit in a region of lower pressure, (3) use a fan or ejector pump, and (4) install diffuser at the shroud exit to recover some of the exit dynamic pressure. If such improvements are impossible or the resulting gain in available pressure drop is insufficient to provide the additional cooling required, the only alternative left is to select the most favorable shroud geometry based on the criterions set up in the foregoing procedure, to determine the cooling-air-flow rate and design temperatures that will be obtained for the pressure drop available, and then to adapt the installation by relocating components of the installation and selecting materials that can withstand these temperatures.

DISCUSSION OF DESIGN PROCEDURES

For this investigation the heat transfer from the exhaust gas to the cooling air was determined to be more greatly affected by the cooling-air-flow rate than by any other variable that may change with flight condition. Since the cooling-air-flow rate varies approximately as the square root of the density at the shroud inlet and the pressure drop available and since the density decreases so rapidly with altitude, in the usual case the most critical flight condition for design is maximum-power flight for the slowest speed (climb) at rated altitude.

In the procedures given herein all of the exhaust gas was assumed to flow through one exhaust pipe. In the cases in which two exhaust pipes carry the gases from the engine to the turbine or to the atmosphere, the exhaust-gas-flow rate for each pipe is assumed equal to one-half the exhaust-gas-flow rate through the engine.

In the design procedure a wide range of practical shroud diameter is assumed, as was illustrated when the sample problem was discussed. Since increasing the shroud diameter relative to the exhaust pipe decreases the downstream cooling-air temperatures and the cooling-air pressure drop for a shroud of constant length, (see figs. 17(g) and 17(j)) it would seem desirable to assume large

values of shroud diameter. The exhaust-pipe temperatures and the exhaust-gas temperatures, however, increase with increase of shroud diameter. (See figs. 17(e), 17(f), and 17(h).) The shroud diameter, therefore, is limited by the allowable exhaust-pipe and exhaust-gas temperatures and the weight and space limitations of the installation.

Analytical methods for determining the upstream exhaust-gas temperature t_{e_1} are not well developed and constitute another problem which is not considered herein. In the present work the manufacturer's data are assumed to exist. The flight condition for which the shroud is being designed will set the engine-operating conditions that will enable the designer to determine from the engine data the gas temperature at the exhaust manifold. The exhaust-gas temperature at the inlet to the shroud system can then be assumed equal to or slightly less than the temperature at the exhaust manifold, depending on the length of exposed pipe from the exhaust manifold to the shroud system entrance. The temperature drop in the uncooled length will probably be not more than a few degrees per foot of length.

For the case of a design in which a single-segment shroud does not provide satisfactory cooling it has been proposed that a multi-segment shroud be used. Another proposal for those cases in which shroud temperature is exceeded in a single-segment system would be to use a double shroud around the hot inner pipe. No calculations were made for such a system but it has definite possibilities provided that space is available. Again for those cases in which the shroud-temperature limit is exceeded, local heat shields may provide satisfactory protection of the installation at the critical points of the shroud system.

CONCLUDING REMARKS

The equations for predicting installation temperatures and cooling-air pressure loss for shrouded exhaust-pipe systems for parallel flow are considered to be verified within the limits of engineering requirements for one ratio of shroud diameter to exhaust-pipe diameter by experimental data. Since the equations have no diameter-ratio limitations, provided that turbulent cooling-air flow exists in the annulus, the verification of the equations for one diameter ratio lends support to the belief that the equations are applicable to all practical ratios of shroud diameter to exhaust-pipe diameter for which the cooling-air flow is expected to be turbulent. No experimental data were obtained for counter-flow systems. The counter-flow equations, however, are believed to be equally applicable because of their similarity to the parallel-flow equations.

The application of the equations to the design of shrouds has
been considerably simplified by the use of constant values of 0.24
and 0.30 for the specific heats of the cooling air and the exhaust
gas, respectively, and by the use of air properties in place of
exhaust-gas properties for determining the heat-transfer coefficient
of the exhaust gas. Calculations showed that these substitutions
have a negligible effect on the accuracy of the results.

The detailed procedures and charts, based on the derived equa-
tions, permit the determination of the proportions of an exhaust-
pipe shroud that provides desired or maximum cooling of an exhaust
installation for both parallel-flow and counter-flow systems. The
procedures for the initial choice of a single-segment shroud are
extended to multisegment shrouds for the case in which desired
cooling cannot be realized with a single-segment shroud. These
procedures are further extended to include the case in which desired
cooling cannot be attained with a multisegment shroud of practical
proportions. For this situation the procedures permit the deter-
mination of the shroud proportions that provide the maximum possible
cooling and the determination of the value of installation tempera-
tures that exist with that shroud. The results of the design
example, which is included to illustrate the use of the design
procedures, indicate that in well-designed shrouds adequate cooling
can be obtained with inappreciable cooling drag.

One problem of immediate significance for which the equations
and methods of shroud design are believed to be directly applicable
is the design of shrouds for the tail pipes of jet engines provided
that the luminosity of the gases in the tail pipe is negligible and
the cooling air exits to the atmosphere. If the luminosity of the
gases is not negligible for jet-engine installations, however, the
analysis presented in this paper must be extended to include the
heat transfer to the exhaust pipe by gas radiation. For installa-
tions in which flaps or ejector pumps are used the method of appli-
cation of the pressure-drop relations to shroud design must be
modified from that of the present method to account for the departure
of the cooling-air exit pressure from atmospheric pressure.

Langley Memorial Aeronautical Laboratory
    National Advisory Committee for Aeronautics
        Langley Field, Va., June 19, 1947

A P P E N D I X

PROPERTIES OF EXHAUST-GAS MIXTURES AND AIR

Status of Data on Properties

During the present investigation which led to the development
and verification by experiments of equations for the design of
exhaust-pipe shrouds and the development of shroud-design procedures
based on the equations, certain properties of air and exhaust-gas
mixtures for temperatures as high as 2300° F were required. These
properties were the enthalpy, instantaneous specific heat, viscosity,
and thermal conductivity.

Data existed on the enthalpy and instantaneous specific heat
of air from 80° F to 2240° F in reference 11 and on the instan-
taneous specific heat, viscosity, and thermal conductivity of air
from -100° F to 1600° F in reference 12. Equations were also given
in reference 12 for the determination of viscosity and thermal
conductivity. Some data on the properties of mixtures of two gases
are given in the literature, but only a small amount of data on
viscosity is available on mixtures of gases with as many constituents
as exist in exhaust gas from engines. Equations for the instan-
taneous specific heat and enthalpy of exhaust-gas mixtures, how-
ever, were derived in reference 11 based on classical thermodynamics
and tables of constants included for use in the equations. The data
of both references 11 and 12 were based on the work of many experi-
menters over a long period of years.

In order to meet the foregoing requirement for the shroud
design investigation values of viscosity and thermal conductivity
of air from 1600° F to 2300° F and values of instantaneous specific
heat and enthalpy of exhaust-gas mixtures from 500° F to 2300° F
had to be calculated by use of the equations of references 11 and 12.
In addition, formulas had to be derived for the viscosity and thermal
conductivity of exhaust-gas mixtures in a manner similar to the
derivation of the formulas for instantaneous specific heat and
enthalpy of exhaust-gas mixtures in reference 11, and values of the
properties had to be calculated with use of these newly derived
formulas over the same range of temperature as the other exhaust-
gas-mixture properties were calculated. The exhaust-gas-mixture
properties involved properties of individual gases such as carbon
monoxide which were obtained for the most part from reference 12.

The purpose of this appendix is to give tables or charts of the
foregoing properties and also the Prandtl numbers of air and exhaust-
gas mixtures over the range of temperature indicated and based on the

foregoing calculations and data. Details of methods for obtaining
the properties and the derivation of the formulas for the viscosity
and the thermal conductivity of exhaust-gas mixtures are included
herein. Although some of the results have been given in other
papers, these results have been replotted so that all results will
be in convenient form in one paper.

The accuracy of the calculated results is uncertain in most
cases because of the nonexistence of experimental data. Some indi-
cation of the accuracy can be obtained by noting the accuracy of
the properties of the individual gases in the references from which
they were obtained and the manner in which calculated data fair into
the experimental data. As far as the properties of exhaust-gas
mixtures are concerned, regardless of the accuracy of the individual
gas properties, the accuracy depends on the exactness of the classical
thermodynamic theory (presumably the best theory to date) which was
used in reference 11 and in the present paper. Until experimental
data are available, the calculated results presented herein are
considered to be the most accurate available.

Symbols

$$a_1 = \frac{\mu_{H_2O} - \frac{\mu_{O_2}}{2}}{2.016}$$

$$a_2 = \frac{k_{H_2O} - \frac{k_{O_2}}{2}}{2.016}$$

$$b_1 = \frac{\mu_{CO_2} - \mu_{O_2}}{12}$$

$$b_2 = \frac{k_{CO_2} - k_{O_2}}{12}$$

$$c_1 = \mu_{O_2} + 2\mu_{CO} - 2\mu_{CO_2}$$

$$C_2 = k_{O_2} + 2k_{CO} - 2k_{CO_2}$$

c_1, c_2 constants in formula for viscosity of air

c_{p_a} instantaneous specific heat of air at constant pressure, Btu/lb/°F

c_{p_e} instantaneous specific heat of exhaust gas at constant pressure, Btu/lb/°F

c_{v_a} instantaneous specific heat of air at constant volume, Btu/lb/°F

$c_{v_{H_2O}}$ instantaneous specific heat of water vapor at constant volume, Btu/lb/°F

$$D_1 = \frac{2\mu_{CO} - \mu_{CO_2}}{12}$$

$$D_2 = \frac{2k_{CO} - k_{CO_2}}{12}$$

$$E_1 = \frac{\mu_{H_2O} + \mu_{CO} - \mu_{CO_2}}{2.016}$$

$$E_2 = \frac{k_{H_2O} + k_{CO} - k_{CO_2}}{2.016}$$

f fuel-air ratio

g ratio of absolute to gravitational unit of mass, lb/slug, or acceleration due to gravity, ft/sec²

i_a heat content (enthalpy) of cooling air, Btu/lb (referred to 0° absolute)

i_e heat content (enthalpy) of exhaust gas, Btu/lb (referred to 0° absolute)

K constant in equation (A23)

K_1 constant in equation for k_a determined from μ_a and c_{v_a}

K_2 constant in equation for k_{H_2O}

k_a thermal conductivity of cooling air,
                                Btu/sec/sq ft/°F/ft

k_e thermal conductivity of exhaust gas,
                                Btu/sec/sq ft/°F/ft

k_{H_2O}, k_{N_2}, ...   thermal conductivity of exhaust-gas constituents
                                (designated by subscripts), Btu/sec/sq ft/°F/ft

M_a molecular weight of air (29)

m hydrogen-carbon ratio

S Sutherland constant in viscosity equation

T temperature, °C absolute or °F absolute

T_e exhaust-gas temperature, °F absolute

t temperature, °F

x mols of exhaust gas per mol of air

μ_a absolute viscosity of air, slugs/sec/ft

μ_e absolute viscosity of exhaust gas, slugs/sec/ft

μ_{H_2O}, μ_{N_2}, ... absolute viscosity of exhaust-gas constituents
                                (designated by subscripts), slugs/sec/ft

$\phi_1 = \mu_{CO_2} + \mu_{H_2} - \mu_{CO} - \mu_{H_2O}$

$\phi_2 = k_{CO_2} + k_{H_2} - k_{CO} - k_{H_2O}$

Pr_a Prandtl number of air $\left(c_{p_a}\mu_a g / k_a\right)$

Pr_e Prandtl number of exhaust gas $\left(c_{p_e}\mu_e g / k_e\right)$

Chemical Symbols

CO   mols of carbon monoxide in exhaust gas per mol of air burned

$(CO)' = CO + H_2$

CO_2 mols of carbon dioxide in exhaust gas per mol of air burned

$\left(CO_2\right)' = CO_2 - H_2$

H_2 mols of hydrogen in exhaust gas per mol of air burned

H_2O mols of water vapor in exhaust gas per mol of air burned

$\left(H_2O\right)' = H_2O + H_2$

$\left(H_2O\right)_a$ mols of water vapor in air per mol of air burned

N_2 mols of nitrogen in exhaust gas per mol of air burned

O_2 mols of oxygen required for combustion per mol of air burned

O_2' mols of excess oxygen in exhaust gas per mol of air burned

$\left(O_2\right)_a$ mols of oxygen in air per mol of air burned (0.2098)

Methods of Obtaining Properties of Air

Enthalpy i_a.- The enthalpy for air over a range of temperature from $80°$ to $2240°$ F has been reported in table II of reference 11. All enthalpy values were referred to a temperature of $0°$ absolute. The values given were based on information published in chemical journals from 1933 to 1939; the complete bibliography containing the information is given in reference 11. These values were plotted against temperature for use in the present paper in order that all of the data compiled herein would be available in one paper in a convenient manner.

Instantaneous specific heat c_{p_a}.- The instantaneous specific heats of air based on the same information as that for the enthalpy of air and over the same range of temperature are also given in table II of reference 11. In reference 12 the instantaneous specific heats of air are also given from -100° F to 1600° F. The results of references 11 and 12 are in excellent agreement for the overlapping range of temperature. A curve of instantaneous specific heat of air over a range of temperature from -100° F to 2240° F was then drawn based on the data of the two references. Further comparison of the data of references 11 and 12 with data on instantaneous specific heat in reference 13 up to 1600° F showed the latter data also agreed very well with the other values.

Viscosity μ_a.- Values of viscosity of air for a temperature range from -100° F to 1600° F have been reported in reference 12 in a table and a figure. These values were based on the work of many experimenters and a bibliography in reference 12 gives the reports used. The viscosity values given in reference 12 were replotted for presentation herein. At temperatures between 1600° F and 2300° F the following formula given in reference 12 was used to calculate the viscosity values which were also plotted on the curve of viscosity against temperature:

$$\mu_a = c_1 \frac{T_a^{\frac{3}{2}}}{T_a + c_2} \tag{A1}$$

where

T_a temperature of air, °F absolute

c_1 a constant

c_2 a constant

The constants in the formula were obtained from the data given for temperatures below 1600° F.

Conductivity k_a.- Values of conductivity of air are also given in reference 12 over a temperature range from -100° F to 1600° F. As for the viscosity μ_a these values of conductivity are based on

the work of many experimenters whose reports are listed in reference 12. The conductivity of air values given in this reference were replotted for use in the present paper. For temperatures between 1600° F and 2300° F the conductivity values were calculated by use of the following formula given in reference 12:

$$k_a = K_1 \mu_a c_{v_a} \qquad \qquad (A2)$$

The constant K_1 was calculated from the data on μ_a and k_a for temperatures below 1600° F in reference 12 and from values of c_{v_a}, the instantaneous specific heat at constant volume, calculated by means of the following formula given on page 178 of reference 13:

$$c_{v_a} = 0.1509 + 0.0000342 T_a - 0.00000000293 T_a^2 \qquad (A3)$$

where T_a is air temperature in °F absolute. Values of the conductivity of air for temperatures above 1600° F were then calculated by use of equations (A2) and (A3), the value of K_1 calculated by the method given, and the calculated values of μ_a for temperatures above 1600° F. The k_a values above 1600° F were then plotted with the values below 1600° F.

Prandtl number Pr_a.- The Prandtl number for air $c_{p_a} \mu_a g / k_a$ was calculated for a range of temperature from -100° F to 2300° F by use of the values of c_{p_a}, μ_a, and k_a that had been determined for this range of temperature.

Methods of Obtaining Exhaust-Gas Mixture Properties

Enthalpy i_e and instantaneous specific heat c_{p_e}.- Equations for the calculation of the enthalpy i_e and the instantaneous specific heat c_{p_e} of exhaust-gas mixtures for any fuel-air ratio and hydrogen-carbon ratio of the fuel are given in reference 11. The equations are based on classical thermodynamics and complete details of their derivation are given in the reference. Tables of constants to be used in the equations are included in the reference. The energy of combustion of CO and H_2 (carbon monoxide and hydrogen, respectively) at the absolute zero of temperature was

included in the constants to be used in the enthalpy equations of
reference 11. These constants were recalculated for the present
paper without this energy. The result is that the enthalpy cal-
culated with the new constants will be $\int c_{p_e} \, dT_e$ above the absolute
zero of temperature. Calculations of the enthalpy and instantaneous
specific heat were then made with the equations, the constants of
reference 11 for c_{p_e}, and the new constants for i_e over a range
of fuel-air ratio from 0.01 to 0.12, hydrogen-carbon ratios from 0.10
to 0.20, and exhaust-gas temperatures from 500° F to 2300° F.

It was intended to present faired curves based on these cal-
culations for the entire ranges of exhaust-gas temperatures, fuel-
air ratios, and hydrogen-carbon ratios. It was possible to do so
for the instantaneous specific heat and these curves are shown
herein. Since the hydrogen-carbon ratio is a constant for each
fuel, these curves and all the rest of the curves for exhaust-gas-
mixture properties are presented in families of constant hydrogen-
carbon ratio. The accuracy of interpolation for variables between
the given curves is limited only by the accuracy of the curves
themselves. Inasmuch as the fuel-air ratio for the stoichiometric
mixture varies with hydrogen-carbon ratio between the limits 0.06
and 0.08, the range of fuel-air ratio over which appropriate equa-
tions were applicable was indefinite. Consequently lean-mixture
equations were applied up to a fuel-air ratio of 0.06 and rich-
mixture equations down to a fuel-air ratio of 0.08, and the values
for a fuel-air ratio of 0.07 were obtained by cross plotting the
calculated values against fuel-air ratio and interpolating in the
range between 0.06 and 0.08. In order to present faired curves of
enthalpy of sufficient accuracy for use, the curves would have
required a greatly expanded scale and consequently a very large
figure. In order to avoid this large plot, the calculated values
of the enthalpy of exhaust gas for the ranges of temperatures, fuel-
air ratios, and hydrogen-carbon ratios are presented in a table.
One figure is given simply as an illustrative curve of enthalpy for
one hydrogen-carbon ratio to show the variation of enthalpy with
temperature and fuel-air ratio.

Viscosity μ_e.- Data on viscosity over only a limited range of
conditions (reference 14) were available for mixtures of gases with
a large number of constituents such as are found in exhaust-gas
mixtures. Mixtures of two constituents are about the only gas
mixtures usually reported in the literature. An equation was there-
fore derived for the viscosity μ_e by methods which were similar
to those used to arrive at the equations for i_e and c_{p_e} in

reference 11. This equation was then used to calculate μ_e over a range of exhaust-gas temperature, fuel-air ratio, and hydrogen-carbon ratio. The derivation of this equation is given herein.

Discussions in references 15 and 16 on the viscosity and thermal conductivity of mixed gases may be summarized as follows: For exhaust gases containing no hydrogen the viscosity of the mixture is very nearly the average of that of the components, weighted in proportion to their partial volumes. The absolute viscosity must be used for this calculation. When hydrogen is present, the averaging process yields too low a viscosity. The average viscosity computed by excluding hydrogen from the average is probably a little too large. The thermal conductivity is obtained by an averaging process similar to that for viscosity. The result is more nearly correct for thermal conductivity than for viscosity, particularly, when hydrogen is present. Then, approximately,

$$x\mu_e = \left(CO_2\right)\mu_{CO_2} + \left(H_2\right)\mu_{H_2} + \cdots \qquad (A4)$$

$$xk_e = \left(CO_2\right)k_{CO_2} + \left(H_2\right)k_{H_2} + \cdots \qquad (A5)$$

where

x mols of exhaust gas per mol of air

CO_2, H_2, $\cdots$ mols of exhaust-gas constituents per mol of air

μ_{CO_2}, k_{H_2}, $\cdots$ physical properties of exhaust-gas constituents

The equation involving k_e has been included at this point to show its similarity to the equation for μ_e. The conductivity, however, will be taken up in the next section.

The first part of the problem is the determination of the mols of constituents per mol of air and exhaust-gas mixture in terms of fuel-air and hydrogen-carbon ratios. These values are then substituted in an equation similar to equation (A4) and a formula derived for μ_e in terms of the fuel-air ratio f, the hydrogen-carbon ratio m, and the viscosities of the individual gases. Finally, values of μ for the individual gases are obtained and substituted in the equation for μ_e.

Formulas are given in reference 11 for the masses of exhaust-gas constituents formed when 1 mol of air is burned for ranges of mixtures leaner than the stoichiometric and richer than the stoichiometric. The masses of the constituents are functions of the fuel-air and hydrogen-carbon ratios. Various assumptions are made in reference 11 in order to determine these formulas. One assumption is that, in the range of mixtures leaner than stoichiometric, the fuel is completely converted to carbon dioxide CO_2 and water H_2O. A further assumption made is that the amount of water vapor in the combustion air is negligible and can be disregarded for both the lean and rich mixtures. The formula for μ_e in the lean-mixture range is

$$x\mu_e = \left(CO_2\right)\mu_{CO_2} + \left(H_2O\right)\mu_{H_2O} + \left(N_2\right)\mu_{N_2} + \left(O_2{}'\right)\mu_{O_2} \qquad (A6)$$

where

$O_2{}'$ mols of excess oxygen in exhaust gas per mol of air after combustion

N_2 mols of nitrogen in exhaust gas per mol of air

Now

$$\mu_a = \left(N_2\right)\mu_{N_2} + \left(O_2{}'\right)\mu_{O_2} + \left(O_2\right)\mu_{O_2}$$

where

O_2 mols of oxygen required for combustion per mol of air

or

$$\left(N_2\right)\mu_{N_2} + \left(O_2{}'\right)\mu_{O_2} = \mu_a - \left(O_2\right)\mu_{O_2} \qquad (A7)$$

Substituting equation (A7) in equation (A6) gives

$$x\mu_e = \mu_a + \left(CO_2\right)\mu_{CO_2} + \left(H_2O\right)\mu_{H_2O} - \left(O_2\right)\mu_{O_2} \qquad (A8)$$

From the formulas in reference 11 the following formulas were derived:

$$CO_2 = \frac{fM_a}{12(m + 1)} \tag{A9}$$

$$H_2O = \frac{fM_a m}{2.016(m + 1)} \tag{A10}$$

$$O_2 = \frac{fM_a \left(\frac{1}{12} + \frac{m}{2 \times 2.016} \right)}{(m + 1)} \tag{A11}$$

$$x = 1 + \left[\frac{fM_a m}{2 \times 2.016(m + 1)} \right] \tag{A12}$$

where

f   fuel-air ratio

m   hydrogen-carbon ratio

M_a molecular weight of air (29)

If equations (A9) to (A12) are substituted in equation (A8), the viscosity of the exhaust gas becomes

$$\mu_e = \frac{\dfrac{\mu_a}{M_a} + \dfrac{f(a_1 m + b_1)}{m + 1}}{\dfrac{1}{M_a} + \dfrac{fm}{2 \times 2.016(m + 1)}} \tag{A13}$$

where

$$a_1 = \frac{\mu_{H_2O} - \dfrac{\mu_{O_2}}{2}}{2.016} \tag{A14}$$

$$b_1 = \frac{\mu_{CO_2} - \mu_{O_2}}{12} \tag{A15}$$

In the range of mixtures richer than stoichiometric one of the assumptions made is that the constituents of the exhaust gas are CO_2, H_2O, H_2, CO, and N_2. (See reference 11.) Then,

$$x\mu_e = \left(CO_2\right)\mu_{CO_2} + \left(H_2O\right)\mu_{H_2O} + \left(H_2\right)\mu_{H_2} + (CO)\mu_{CO} + \left(N_2\right)\mu_{N_2} \qquad (A16)$$

Now

$$\left(N_2\right)\mu_{N_2} = \mu_a - \left(O_2\right)_a \mu_{O_2} \qquad (A17)$$

where

$\left(O_2\right)_a$ mols of oxygen in air per mol of air (0.2098)

Equation (A16) then becomes

$$x\mu_e = \left(CO_2\right)\mu_{CO_2} + \left(H_2O\right)\mu_{H_2O} + \left(H_2\right)\mu_{H_2} + (CO)\mu_{CO} + \mu_a - \left(O_2\right)_a \mu_{O_2} \qquad (A18)$$

From reference 11 the following equations for the mols of exhaust gas and constituents were derived:

$$CO_2 = 2\left(O_2\right)_a - \frac{fM_a}{12(m+1)} - \frac{fM_a m}{2.016(m+1)} + H_2 \qquad (A19)$$

$$H_2O = \frac{fmM_a}{2.016(m+1)} - H_2 \qquad (A20)$$

$$CO = \frac{fM_a m}{2.016(m+1)} + \frac{fM_a}{6(m+1)} - 2\left(O_2\right)_a - H_2 \qquad (A21)$$

$$N_2 = 1 - \left(O_2\right)_a \qquad (A22)$$

$$H_2 = \frac{\sqrt{\left[K(CO_2)' + (CO)' + (H_2O)'\right]^2 + 4(K-1)(CO)'(H_2O)'}}{2(K-1)}$$

$$- \frac{K(CO_2)' + (CO)' + (H_2O)'}{2(K-1)} \tag{A23}$$

where

$$K = 3.8$$

$$(CO_2)' = (CO_2) - (H_2) \tag{A24}$$

$$(CO)' = (CO) + (H_2) \tag{A25}$$

$$(H_2O)' = (H_2O) + (H_2) \tag{A26}$$

$$x = 1 - (O_2)_a + \frac{fM_a}{12(m+1)} + \frac{fM_a m}{2.016(m+1)} \tag{A27}$$

Substitution of equations (A19) to (A27) in equation (A18) leads to the following expression for μ_e in the mixture range richer than stoichiometric:

$$\mu_e = \frac{\left[\dfrac{\mu_a}{M_a} - \dfrac{(O_2)_a}{M_a}C_1 + \dfrac{f}{1+m}(D_1 + mE_1) + \dfrac{H_2}{M_a}\phi_1\right]}{\left[\dfrac{1}{M_a} - \dfrac{(O_2)_a}{M_a} + \dfrac{f}{1+m}\left(\dfrac{1}{12} + \dfrac{m}{2.016}\right)\right]} \tag{A28}$$

where

$$C_1 = \mu_{O_2} + 2\mu_{CO} - 2\mu_{CO_2} \tag{A29}$$

$$D_1 = \frac{(2\mu_{CO} - \mu_{CO_2})}{12} \tag{A30}$$

$$E_1 = \frac{(\mu_{H_2O} + \mu_{CO} - \mu_{CO_2})}{2.016} \tag{A31}$$

$$\phi_1 = (\mu_{CO_2} + \mu_{H_2} - \mu_{CO} - \mu_{H_2O}) \tag{A32}$$

The viscosities of the individual gases were next determined for use in finding the constants a_1, b_1, and so forth in the equations for μ_e. The viscosities of H_2, N_2, O_2, CO_2, and CO were obtained by means of formulas and values given in tables in reference 12. The viscosity of H_2O was calculated by use of the Sutherland equation obtained from reference 17, page 1. This equation is

$$\frac{(\mu_{H_2O})_T}{(\mu_{H_2O})_{0^\circ C}} = \left(\frac{T}{273.1}\right)^{\frac{3}{2}} \left(\frac{273.1 + S}{T + S}\right) \tag{A33}$$

where

T   temperature, 0° C absolute

S   Sutherland constant (from reference 17, table 1, p. 4,
         S for H_2O = 650)

The viscosity of H_2O at 100° C is 0.2527×10^{-6} slugs per second-foot. (See reference 15, p. 180, units changed to British engineering.) This value and the value of S were used in equation (A33) to calculate the viscosity of water at 0° C. Since the value of $(\mu_{H_2O})_{0^\circ C}$

was known, values of the viscosity over a large range of temperature were calculated by use of equation (A33).

The constants in the equations for μ_e were then calculated by use of the viscosities of the individual gases and equations (A14), (A15), (A29), (A30), (A31), and (A32). These constants were then used to calculate μ_e over ranges of fuel-air and hydrogen-carbon ratios and temperatures by use of equations (A13) and (A28).

Conductivity k_e.- No data on the conductivity of mixtures of gases with a large number of constituents were available. Consequently, derivations of equations for k_e in a manner identical to that used for the equations of μ_e, on the basis of equations (A4) and (A5), were made. The derivations led to equations, for the range of mixtures leaner than stoichiometric, identical to equations (A13) to (A15) and for the range of mixtures richer than stoichiometric to equations identical to equations (A28) to (A32), with the exception that every value of μ in the foregoing equations is replaced with a k. The constants in the equations for k_e are denoted a_2, b_2, C_2, D_2, E_2, and ϕ_2 which correspond to the constants in the equations containing μ_e.

The conductivities of the individual gases were then determined. The conductivities of CO_2, N_2, CO, O_2, and H_2 were determined in the same manner that was used to determine the conductivity of air, which has already been described, by use of the data on the conductivities of the individual gases at temperatures below $1600°$ F in reference 12, the data on the viscosities of the individual gases calculated in the manner given in the preceding section of this paper, and equations for instantaneous specific heat at constant volume given in reference 13 for the individual gases. The conductivity of H_2O was calculated from the formula

$$k_{H_2O} = K_2 \mu_{H_2O} c_{v_{H_2O}} \tag{A34}$$

where K_2 was obtained from reference 15, p. 180, and values of $c_{v_{H_2O}}$ were calculated from an equation given in reference 13. The values of viscosity μ_{H_2O} already described were also used.

The constants in the equations for k_e were then calculated by use of the conductivities of the individual gases and equations similar to equations (A14), (A15), (A29) to (A32) with the term μ

replaced with k in all instances. These constants were then used
to calculate k_e over ranges of fuel-air ratios, hydrogen-carbon
ratios, and temperatures from equations similar to equations (A13)
and (A28). The thermal-conductivity curves were extrapolated
between the fuel-air ratios of 0.06 and 0.08; the curves are dashed
in this range.

Prandtl number Pr_e.- The Prandtl number $c_{p_e}\mu_e g/k_e$ for the
gas mixtures was calculated by use of the values of instantaneous
specific heat, viscosity, and conductivity that were read from
faired curves of these properties. Because of the excessive over-
lapping and crossing of faired curves of the calculated Prandtl
numbers of exhaust gases that were plotted for a range of tempera-
ture, fuel-air ratio, and hydrogen-carbon ratio, the data are pre-
sented in a table. One plot of Prandtl number for one hydrogen-
carbon ratio was prepared to illustrate the variation of Prandtl
number with fuel-air ratio and temperature. Values at the fuel-air
ratio of 0.07 were calculated from the interpolated values of
specific heat, viscosity, and thermal conductivity.

Properties of Exhaust-Gas Mixtures and Air

Air properties.- The instantaneous specific heat and enthalpy
of air over a range of temperature up to 2300° F are given in
figure 18 and the viscosity, conductivity, and Prandtl number of
air up to the same temperature are given in figure 19. The cal-
culated values of viscosity and conductivity above 1600° F fair
very well into the values below 1600° F (fig. 19); thus, confidence
is provided in the formulas used in the calculations.

The instantaneous specific heat (fig. 18) varied from about 0.24
at room temperature to 0.29 at 2300° F. Consequently, the value
of 0.24 usually used may be in error as much as 15 percent.

The Prandtl number is also usually assumed a constant with a
value of about 0.73. Figure 19 shows that use of this value at
room temperatures will lead to little error, but its use at high
temperatures will lead to some error because the Prandtl number
falls to a value of about 0.62.

Exhaust-gas-mixture properties.- Values of the enthalpy i_e
of exhaust-gas mixtures are given in table 6. Figure 20 illustrates
the type of variation obtained with fuel-air ratio and temperature
for a hydrogen-carbon ratio of 0.10. From table 6 and figure 20 it
is apparent that the main change in enthalpy occurs because of
temperature change.

The variation of the specific heat of exhaust-gas mixtures
with temperature, fuel-air ratio, and hydrogen-carbon ratio is
given in figures 21(a) and 21(b). An appreciable change in c_{p_e}
occurs for a wide variation in temperature and fuel-air ratio, but
the change with hydrogen-carbon ratio is much less. Appreciable
error could possibly be introduced in a problem dealing with
exhaust-gas mixtures if a constant value of c_{p_e} such as 0.30,
which is sometimes assumed, is used.

Curves similar to those of figure 21 for c_{p_e} are given in
figure 22 for the viscosity μ_e. Values of μ_a and of the constants
to be used in the exhaust-gas-mixture viscosity equations are given
in table 7 for a temperature range from 500° F to 2300° F. Only the
values of μ_e for the extreme ranges of hydrogen-carbon ratio, 0.10
and 0.20, are given in figure 22 because the change in μ_e was small
enough such that interpolation between the values given for other
ratios will result in good estimates of viscosity.

As stated previously, some data on the viscosity of exhaust-
gas mixtures are given in reference 14. The ranges of conditions
for which these data were obtained were from 75° F to 890° F and
fuel-air ratios from 0.0625 to 0.167. The hydrogen-carbon ratio of
the fuel used was not given. For the ranges tested the viscosity
was found to be nearly independent of the fuel-air ratio used. No
mention is made in reference 14 of the effect of hydrogen-carbon
ratio on the viscosity μ_e. Figure 22 shows that the viscosity is
affected to some extent by both fuel-air ratio and hydrogen-carbon-
ratio variations. In order to compare the results of reference 14
with those of figure 22 it was assumed that gasoline with a hydrogen-
carbon ratio of 0.17, a normal value for aviation gasoline, was used
in the tests of reference 14. The comparison showed that the
average differences between the two sets of results varied from
about 3 percent to 4 percent; the experimental values are higher
than the calculated values. Inasmuch as reference 14 states that
the experimental values can be as much as 2 percent too high because
of experimental errors and also because the hydrogen-carbon ratio
had to be assumed, the agreement is very good.

Curves of exhaust-gas-mixture conductivity k_e against fuel-
air ratio for several constant temperatures are given in figure 23(a)
for a hydrogen-carbon ratio of 0.10 and in figure 23(b) for a ratio
of 0.20. Only results for the two H/C ratios are given for the
same reason that only curves of μ_e for these two ratios were given.
Values for any intermediate hydrogen-carbon ratio obtained by inter-
polation will differ from the calculated values by less than $\frac{1}{2}$ percent.

Constants and values of conductivity of air k_a used in the
k_e formulas are given in table 8 for a range of temperatures
from 500° F to 2300° F. In the range of fuel-air ratio leaner than
the stoichiometric from 0.01 to 0.06, the conductivity changed very
little with fuel-air-ratio change. (See figs. 23(a) and 23(b).)
Above the range of the stoichiometric mixture the conductivity
increased rapidly with increases of fuel-air ratio. The increase
of conductivity with temperature was rapid in both the lean and
rich fuel-air-ratio ranges.

Values of Prandtl number for exhaust-gas mixtures, for a tem-
perature range from 500° F to 2300° F and a fuel-air ratio range
from 0.01 to 0.12, at a hydrogen-carbon ratio of 0.10 are given in
figure 24 to illustrate the type of curves obtained. Values for
other hydrogen-carbon ratios are given in table 9.

A summary table is given below for easy reference to the
figures and tables for obtaining the properties.

Property	Symbol	Units	Location
Enthalpy of air	i_a	Btu/lb	Fig. 18
Instantaneous specific heat of air	c_{p_a}	Btu/(lb)(°F)	Fig. 18
Viscosity of air	μ_a	slugs/(sec)(ft)	Fig. 19
Conductivity of air	k_a	Btu/(sec)(ft²)(°F/ft)	Fig. 19
Prandtl number of air	Pr_a	------------------	Fig. 19
Enthalpy of exhaust gas	i_e	Btu/lb	Table 6
Instantaneous specific heat of exhaust gas	c_{p_e}	Btu/(lb)(°F)	Fig. 21
Viscosity of exhaust gas	μ_e	slugs/(sec)(ft)	Fig. 22
Conductivity of exhaust gas	k_e	Btu/(sec)(ft²)(°F/ft)	Fig. 23
Prandtl number of exhaust gas	Pr_e	------------------	Table 9

REFERENCES

1. McAdams, William H.: Heat Transmission. Second ed., McGraw-Hill Book Co., Inc., 1942.

2. Martinelli, R. C., Weinberg, E. B., Morrin, E. H., and Boelter, L. M. K.: An Investigation of Aircraft Heaters. III - Measured and Predicted Performance of Double Tube Heat Exchangers. NACA ARR, Oct. 1942.

3. Monrad, C. C., and Pelton, J. F.: Heat Transfer by Convection in Annular Spaces. Trans. American Inst. Chem. Eng., vol. 38, sec. A, no. 3, June 25, 1942, pp. 593-611.

4. Wiegand, J. H., and Baker, E. M.: Transfer Processes in Annuli. Trans. American Inst. Chem. Eng., vol. 38, sec. A, no. 3, June 25, 1942, pp. 569-592.

5. McAdams, William H.: Heat Transmission. First ed., McGraw-Hill Book Co., Inc., 1933.

6. Bakhmeteff, Boris A.: The Mechanics of Turbulent Flow. Princeton Univ. Press, 1941.

7. Joyner, Upshur T.: Mathematical Analysis of Aircraft Intercooler Design. NACA TN No. 781, 1940.

8. Silverstein, Abe: High-Altitude Cooling. I - Résumé of the Cooling Problem. NACA ARR No. L4I11, 1944.

9. Henry, John R.: Design of Power-Plant Installations. Pressure-Loss Characteristics of Duct Components. NACA ARR No. L4F26, 1944.

10. Taylor, G. I., and Maccoll, J. W.: The Mechanics of Compressible Fluids. Steady Flow through Channels. Vol. III of Aerodynamic Theory, div. H, ch. II, secs. 2 and 3, W. F. Durand, ed., Julius Springer (Berlin), 1935, pp. 222-226.

11. Pinkel, Benjamin, and Turner, L. Richard: Thermodynamic Data for the Computation of the Performance of Exhaust-Gas Turbines. NACA ARR No. 4B25, 1944.

12. Tribus, Myron, and Boelter, L. M. K.: An Investigation of Aircraft Heaters. II - Properties of Gases. NACA ARR, Oct. 1942.

13. Faires, Virgil Moring: Applied Thermodynamics. The Macmillan
      Co., 1943.

14. Boelter, L. M. K., and Sharp, W. H.: An Investigation of Aircraft
      Heaters. XVI - Determination of the Viscosity of Exhaust
      Gases from a Gasoline Engine. NACA ARR No. 4F24, 1944.

15. Kennard, Earle H.: Kinetic Theory of Gases. McGraw-Hill Book
      Co., Inc., 1938.

16. Chapman, Sydney, and Cowling, T. G.: The Mathematical Theory of
      Non-Uniform Gases. Cambridge Univ. Press, 1939.

17. National Research Council: International Critical Tables.
      Vol. V. McGraw-Hill Book Co., Inc., 1929.

TABLE 1

APPROXIMATE VALUES OF VARIABLES INVOLVED IN ISOTHERMAL

AND HEAT-TRANSFER TESTS

Test	Type of test	Range of variables				
		Cooling-air Reynolds number, $\rho V(d_s - d_p)/\mu$	Exhaust-gas Reynolds number, $\rho V d/\mu$	Exhaust-gas Prandtl number, $\mu c_p g/k$	Exhaust-gas temperature $^\circ F$	Fuel-air ratio
A	Iso-thermal	100,000 to 324,000	----------------	----------------	------------	--------
B	Heat transfer	265,000	220,000	0.59 to 0.66	1160 to 1500	0.063 to 0.090
C_1	Heat transfer	170,000	120,000 to 220,000	0.64 to 0.65	920 to 1270	0.078
C_2	Heat transfer	250,000	215,000 to 360,000	0.58 to 0.61	1150 to 1420	0.089
D	Heat transfer	170,000 to 280,000	189,000	0.64	1170	0.078

NATIONAL ADVISORY
COMMITTEE FOR AERONAUTICS

TABLE 2

EFFECTS OF APPROXIMATIONS AND FAIRING METHODS ON

DESIGN TEMPERATURES AND PRESSURE LOSSES

(a) Effect of using air properties in place of gas properties		
Design temperatures	Station	Percent error due to use of air properties
Exhaust gas, t_e	2 3	0.2 0.2
Cooling air, t_a	2 3	-1.0 -1.5
Exhaust pipe, t_p	1 2 3	-4.5 -3.5 -3.0

(b) Effect of using constant values of specific heat in place of integrated mean values		
Design temperatures	Station	Percent error due to use of constant values of specific heats
Exhaust gas, t_e	2 3	-0.3 to 0.0 -0.4 to 0.2
Cooling air, t_a	2 3	-0.3 to 0.8 -0.6 to 0.5
Exhaust pipe, t_p	1 2 3	-0.3 to 0.3 -0.5 to 0.3 -0.6 to 0.5

(c) Effect of fairing method on measured pressure losses			
Shroud-segment length	Percent deviation from results on original fairing - methods of reference 6		
	Arithmetic mean	Extreme fairing	Coinciding rake fairing
ΔH_{1-2}	±2.0	1.1	-2.0
ΔH_{1-3}	±3.0	-1.3	-0.3

(d) Effect of fairing method on design temperatures				
Design temperatures	Station	Percent deviation from results on original fairing - methods of reference 6		
		Arithmetic mean	Extreme fairing	Coinciding rake fairing
Exhaust gas, t_e	2 3	1.3 1.0	-0.3 -0.3	-1.0 -1.0
Cooling air, t_a	2 3	3.0 3.5	0.8 0.6	2.0 1.4
Exhaust pipe, t_p	1 2 3	0.3 1.3 1.1	-1.0 -0.8 -0.4	-0.7 -1.2 -0.8

TABLE 3

CALCULATION FORM FOR SHROUD DESIGN - PARALLEL FLOW

Step	Item[1]	Quantity	Source	Symbol	Units	
			Factors for design			
	(1)	Brake horsepower	Manufacturer	bhp	hp	2142
	(2)	Fuel-air ratio	Manufacturer	f		0.0961
1	(3)	Exhaust-gas-flow rate through engine	Manufacturer's data or equation (47)	W_e	lb/sec	4.84
2	(4)	Exhaust-gas temperature at shroud entrance	Manufacturer's data and equation (48) or analytical method	t_{e_1}	°F	1800
3	(5)	Exhaust-pipe diameter (outer)	Manufacturer	d_p	ft	0.4583
4	(6)	Velocity of airplane	Performance data	V_o	ft/sec	468
	(7)	Altitude	Performance data		ft	30,000
	(8)	Exhaust-pipe material	Manufacturer			18-8 stainless steel
5	(9)	Design exhaust-gas temperature	Manufacturer	t_{e_2}	°F	1650
6	(10)	Design exhaust-pipe temperature	Manufacturer	t_p	°F	1400
7	(11)	Design shroud temperature	Manufacturer	t_{s_2}	°F	800
			Pressure drop available at shroud entrance			
4	(12)	Free-stream static pressure	(7) and reference 8	p_o	lb/ft^2	628.1
	(13)	Free-stream temperature	(7) and reference 8	T_o	°F abs.	411.4
	(14)	Free-stream density	(7) and reference 8	ρ_o	slugs/ft^3	0.000889
	(15)	Free-stream dynamic pressure	(14) × (6)^2 × F_{c_o}/2	q_o	lb/ft^2	102.8

[1]Items are carried in parentheses to indicate row used in calculations.

TABLE 3 - Continued

CALCULATION FORM FOR SHROUD DESIGN - PARALLEL FLOW - Continued

Step	Item[1]	Quantity	Source	Symbol	Units										
					Pressure drop available at shroud entrance										
9	(16)	Cooling-air-flow rate	Assumed (approximately 1/8 to 1/2 of (3))	W_a	lb/sec	0.50	1.00	1.50	2.00	2.50	0.50	1.00	1.50	2.00	2.50
	(17)	Cross-sectional area of inlet duct straight section	Area of straight section of assumed inlet duct	A_1	ft²	0.1647					0.1964				
	(18)	Length of inlet duct straight section	Length of straight section of assumed inlet duct	l_1	ft	6					6				
	(19)	Hydraulic diameter of inlet duct straight section	4 × (17)/Perimeter of inlet duct straight section	D_1	ft	0.458					0.50				
	(20)	Dynamic pressure in straight section	$0.00048 \times [(16)/(17)]^2/(14)$	q_1	lb/ft²	4.98	19.90	44.79	79.62	124.41	3.50	14.00	31.49	55.99	87.49
	(21)	μ_{a_o}	$[(13) - 460]$ and figure 19	μ_{a_o}	slugs/(sec)(ft)	0.317×10^{-6}					0.317×10^{6}				
10	(22)	R_1	$0.031 \times (16) \times (19)/[(17) \times (21)]$	R_1		135,970	271,940	407,910	543,880	679,850	124,480	248,960	373,440	497,920	622,400
	(23)	Friction factor	(22) and reference 9	f_1		0.00512	0.00445	0.00412	0.00392	0.00377	0.00521	0.00452	0.00421	0.00398	0.00383
	(24)	Friction pressure loss in straight-section inlet duct	$4 \times (18) \times (20) \times (23)/(19)$	ΔH_1	lb/ft²	1.33	4.62	9.60	16.10	24.07	0.87	3.03	6.30	10.57	15.79
		Where the inlet duct contains more than one straight section, the calculations of items (16) to (24) are repeated to determine the pressure loss in each straight section. If the intake duct contains bends and/or diffusers, supplementary calculation forms will be needed to calculate the pressure losses in each bend and/or diffuser as given by the equation and method of step 10 of the single-segment design procedure.														
	(25)	Total pressure drop in inlet duct	$0.05 \times (15) + \sum (24) + \sum$ Bend and diffuser losses	ΔH_{o-1}	lb/ft²	6.47	9.76	14.74	21.24	29.21	6.01	8.17	11.44	15.71	20.93
	(26)	Pressure drop available at shroud entrance	(15) - (25)	$\Delta H_{available}$	lb/ft²	96.33	93.04	88.06	81.56	73.59	96.79	94.63	91.36	87.09	81.87

[1]Items are carried in parentheses to indicate row used in calculations.

NATIONAL ADVISORY
COMMITTEE FOR AERONAUTICS

TABLE 3 - Continued

CALCULATION FORM FOR SHROUD DESIGN - PARALLEL FLOW - Continued

Step	Item[1]	Quantity	Source	Symbol	Units										
				Pressure drop available at shroud entrance											
9	(16)	Cooling-air-flow rate	Assumed (approximately 1/8 to 1/2 of (3))	W_a	lb/sec	0.50	1.00	1.50	2.00	2.50	0.50	1.00	1.50	2.00	2.50
	(17)	Cross-sectional area of inlet duct straight section	Area of straight section of assumed inlet duct	A_1	ft^2			0.2376					0.2827		
	(18)	Length of inlet duct straight section	Length of straight section of assumed inlet duct	l_1	ft			6					6		
	(19)	Hydraulic diameter of inlet duct straight section	4 × (17)/Perimeter of inlet duct straight section	D_i	ft			0.55					0.60		
	(20)	Dynamic pressure in straight section	$0.00048 \times \left[(16)/(17)\right]^2/(14)$	q_1	lb/ft^2	2.39	9.56	21.52	38.25	59.78	1.69	6.75	15.20	27.02	42.22
	(21)	μ_{a_o}	$\left[(13) - 460\right]$ and figure 19	μ_{a_o}	$\dfrac{\text{slugs}}{(\text{sec})(\text{ft})}$			0.317×10^6					0.317×10^6		
10	(22)	R_1	$0.031 \times (16) \times (19)/\left[(17) \times (21)\right]$	R_1		113,190	226,370	339,560	452,740	565,930	103,780	207,560	311,330	415,100	518,880
	(23)	Friction factor	(22) and reference 9	f_1		0.00531	0.00461	0.00428	0.00403	0.00390	0.00541	0.00469	0.00433	0.00412	0.00395
	(24)	Friction pressure loss in straight-section inlet duct	4 × (18) × (20) × (23)/(19)	ΔH_1	lb/ft^2	0.55	1.92	3.99	6.69	10.00	0.36	1.26	2.62	4.40	6.58
		Where the inlet duct contains more than one straight section, the calculations of items (16) to (24) are repeated to determine the pressure loss in each straight section. If the intake duct contains bends and/or diffusers, supplementary calculation forms will be needed to calculate the pressure losses in each bend and/or diffuser as given by the equation and method of step 10 of the single-segment design procedure.														
	(25)	Total pressure drop in inlet duct	$0.05 \times (15) + \sum (24) + \sum \begin{array}{c}\text{Bend and}\\\text{diffuser}\\\text{losses}\end{array}$	ΔH_{0-1}	lb/ft^2	5.69	7.06	9.13	11.83	15.14	5.50	6.41	7.76	9.54	11.72
	(26)	Pressure drop available at shroud entrance	(15) - (25)	$\Delta H_{available}$	lb/ft^2	97.11	95.74	93.67	90.97	87.66	97.30	96.40	95.04	93.26	91.08

[1]Items are carried in parentheses to indicate row used in calculations.

TABLE 3 - Continued

CALCULATION FORM FOR SHROUD DESIGN - PARALLEL FLOW - Continued

Step	Item[1]	Quantity	Source	Symbol	Units															
						Design variables														
11	(27)	Length of shroud segment	Assumed	l	ft			18					18					18		
12	(28)	Shroud diameter	Assumed	d_s	ft			0.583					0.625					0.667		
9	(29)	Cooling-air-flow rate	Assumed	W_a	lb/sec	0.50	1.00	1.50	2.00	2.50	0.50	1.00	1.50	2.00	2.50	0.50	1.00	1.50	2.00	2.50
						Cooling-air conditions at shroud entrance														
13	(30)	Free-stream stagnation temperature	$(13) + 0.0000832(6)^2$	T_{o_t}	°F abs.			429.6					429.6					429.6		
	(31)	Pressure drop available at shroud entrance	(29) and curve of $\Delta H_{available}$ for inlet duct size selected by step 10	$\Delta H_{available}$	lb/ft²	97.11	95.74	93.67	90.97	87.66	97.11	95.74	93.67	90.97	87.66	97.11	95.74	93.67	90.97	87.66
	(32)	Total pressure at shroud entrance	(12) + (31)	H_{a_1}	lb/ft²	725.21	723.84	721.77	719.07	715.76	725.21	723.84	721.77	719.07	715.76	725.21	723.84	721.77	719.07	715.76
	(33)	$\left(d_s^2 - d_p^2\right)$	$(28)^2 - (5)^2$					0.1299					0.1806					0.2349		
	(34)	$\dfrac{1.384 W_a \sqrt{T_{o_t}}}{\left[\left(d_s^2 - d_p^2\right) \times H_{a_1}\right]}$	$1.384 \times (29) \times (30)^{1/2}/[(32) \times (33)]$			0.1523	0.3053	0.4594	0.6151	--------	0.1095	0.2195	0.3303	0.4423	0.5557	0.0842	0.1688	0.2540	0.3401	0.4273
	(35)	$\left(H_{a_1} - p_{a_1}\right)/H_{a_1}$	(34) and figure 16			0.01652	0.0705	0.1840	--------	--------	0.0086	0.0350	0.0839	0.1670	0.3345	0.0050	0.0204	0.0473	0.0890	0.1525
	(36)	Cooling-air static pressure at shroud entrance	$(32)[1 - (35)]$	p_{a_1}	lb/ft²	713.1	672.6	588.6	--------	--------	718.9	698.3	660.8	598.3	475.6	721.5	708.8	687.2	654.4	605.7
14	(37)	Cooling-air temperature at shroud entrance	$(30)\left[(36)/(32)\right]^{0.286} - 460$	t_{a_1}	°F	-32.4	-39.3	-54.7	--------	--------	-31.5	-34.7	-41.0	-52.3	-77.6	-31.0	-32.9	-36.3	-41.7	-51.0
						Upstream exhaust-pipe temperature														
15	(38)	$W_e^{0.8}$	(3) and table 5					3.531					3.531					3.531		
	(39)	$d_p^{1.8}$	(5) and table 5					0.2456					0.2456					0.2456		
	(40)	$\left[k_a(Pr_a)^{0.4}/\mu_a^{0.8}\right]$	(4) and figure 14					0.758					0.758					0.758		
	(41)	Heat-transfer coefficient on gas side	$0.001735 \times (38) \times (40)/(39)$	h_e	Btu/(sec)(ft²)(°F)			0.01891					0.01891					0.01891		
	(42)	Factor depending on ratio of pipe diameters	(28)/(5) and figure 15	ϕ				1.088					1.114					1.138		
	(43)	$\mu_a^{0.2}$	(37) and figure 13			0.0503	0.0502	0.0499	--------	--------	0.0504	0.0503	0.0502	0.0499	0.0494	0.0504	0.0503	0.0502	0.0501	0.0500
	(44)	$W_a^{0.8}$	(29) and table 5			0.574	1.000	1.383	--------	--------	0.574	1.000	1.383	1.741	2.081	0.574	1.000	1.383	1.741	2.081
	(45)	$\left(d_s + d_p\right)^{0.8}$	$[(28) + (5)]$ and table 5					1.033					1.0663					1.099		
	(46)	$\left(d_s - d_p\right)$	(28) - (5)					0.1250					0.1667					0.2087		
	(47)	Heat-transfer coefficient on air side	$\dfrac{0.01528 \times (42) \times (43) \times (44)}{(45) \times (46)}$	h_a	Btu/(sec)(ft²)(°F)	0.00373	0.00648	0.00889	--------	--------	0.00277	0.00482	0.00665	0.00832	0.00984	0.00219	0.00381	0.00526	0.00662	0.00786
	(48)	$h_e t_{o_1} + h_a t_{a_1}$	$(4) \times (41) + (37) \times (47)$			33.92	33.82	33.55	--------	--------	33.95	33.87	33.76	33.60	33.27	33.97	33.91	33.84	33.76	33.59
	(49)	$h_e + h_a$	(41) + (47)			0.02264	0.0254	0.0278	--------	--------	0.0217	0.0237	0.0256	0.0272	0.0288	0.02110	0.0227	0.0242	0.0255	0.0268
	(50)	Upstream exhaust-pipe temperature	(48)/(49)	t_{p_1}	°F	1498	1332	1206	--------	--------	1566	1427	1321	1234	1155	1610	1493	1400	1322	1253

[1]Items are carried in parentheses to indicate row used in calculations.

NATIONAL ADVISORY
COMMITTEE FOR AERONAUTICS

76

NACA TN No. 1495

TABLE 3 - Continued

CALCULATION FORM FOR SHROUD DESIGN - PARALLEL FLOW - Continued

Step	Item[1]	Quantity	Source	Symbol	Units										
			Design variables												
11	(27)	Length of shroud segment	Assumed	l	ft			18					18		
12	(28)	Shroud diameter	Assumed	d_s	ft			0.710					0.752		
9	(29)	Cooling-air-flow rate	Assumed	W_a	lb/sec	0.50	1.00	1.50	2.00	2.50	0.50	1.00	1.50	2.00	2.50
				Cooling-air conditions at shroud entrance											
	(30)	Free-stream stagnation temperature	$(13) + 0.0000832(6)^2$	T_{o_t}	°F abs.			429.6					429.6		
	(31)	Pressure drop available at shroud entrance	(29) and curve of $\Delta H_{available}$ for inlet duct size selected by step 10	$\Delta H_{available}$	lb/ft²	97.11	95.74	93.67	90.97	87.66	97.11	95.74	93.67	90.97	87.66
	(32)	Total pressure at shroud entrance	(12) + (31)	H_{a_1}	lb/ft²	725.21	723.84	721.77	719.07	715.76	725.21	723.84	721.77	719.07	715.76
13	(33)	$\left(d_s^2 - d_p^2\right)$	$(28)^2 - (5)^2$					0.2941					0.3555		
	(34)	$\dfrac{1.384 W_a \sqrt{T_{o_t}}}{\left[\left(d_s^2 - d_p^2\right) \times H_{a_1}\right]}$	$1.384 \times (29) \times (30)^{1/2}/[(32) \times (33)]$			0.0673	0.13481	0.2029	0.2716	0.3412	0.05570	0.1115	0.1678	0.2247	0.2823
	(35)	$\left(H_{a_1} - p_{a_1}\right)/H_{a_1}$	(34) and figure 16			0.00318	0.01290	0.0298	0.0544	0.0896	0.0022	0.0088	0.0200	0.0366	0.0594
	(36)	Cooling-air static pressure at shroud entrance	$(32)\left[1 - (35)\right]$	p_{a_1}	lb/ft²	722.8	714.3	699.8	679.2	650.7	723.5	717.2	706.9	692.0	672.2
14	(37)	Cooling-air temperature at shroud entrance	$(30)\left[(36)/(32)\right]^{0.286} - 460$	t_{a_1}	°F	-30.8	-32.0	-34.1	-37.2	-41.8	-30.7	-31.5	-32.9	-35.0	-37.9
				Upstream exhaust-pipe temperature											
	(38)	$W_e^{0.8}$	(3) and table 5					3.531					3.531		
	(39)	$d_p^{1.8}$	(5) and table 5					0.2456					0.2456		
	(40)	$\left[k_a(Pr_a)^{0.4}/\mu_a^{0.8}\right]$	(4) and figure 14					0.758					0.758		
	(41)	Heat-transfer coefficient on gas side	$0.001735 \times (38) \times (40)/(39)$	h_e	$\dfrac{Btu}{(sec)(ft^2)(°F)}$			0.01891					0.01891		
	(42)	Factor depending on ratio of pipe diameters	(28)/(5) and figure 15	ϕ				1.161					1.184		
15	(43)	$\mu_a^{0.2}$	(37) and figure 13			0.0504	0.0503	0.0503	0.0502	0.0501	0.0504	0.0504	0.0503	0.0503	0.0502
	(44)	$W_a^{0.8}$	(29) and table 5			0.574	1.000	1.383	1.741	2.081	0.574	1.000	1.383	1.741	2.081
	(45)	$\left(d_s + d_p\right)^{0.8}$	$\left[(28) + (5)\right]$ and table 5					1.133					1.167		
	(46)	$\left(d_s - d_p\right)$	(28) - (5)					0.2517					0.2937		
	(47)	Heat-transfer coefficient on air side	$\dfrac{0.01528 \times (42) \times (43) \times (44)}{(45) \times (46)}$	h_a	$\dfrac{Btu}{(sec)(ft^2)(°F)}$	0.00180	0.00313	0.00433	0.00544	0.00650	0.00153	0.00266	0.00367	0.00462	0.00552
	(48)	$h_e t_{e_1} + h_a t_{a_1}$	(4) × (41) + (37) × (47)			33.98	33.94	33.89	33.84	33.76	33.99	33.95	33.92	33.88	33.83
	(49)	$h_e + h_a$	(41) + (47)			0.02071	0.02204	0.02324	0.02435	0.02541	0.02044	0.02157	0.02258	0.02353	0.02443
	(50)	Upstream exhaust-pipe temperature	(48)/(49)	t_{p_1}	°F	1641	1540	1458	1390	1329	1663	1574	1502	1440	1385

[1]Items are carried in parentheses to indicate row used in calculations.

TABLE 3 - Continued

CALCULATION FORM FOR SHROUD DESIGN - PARALLEL FLOW - Continued

Step	Item[1]	Quantity	Source	Symbol	Units																
						Downstream exhaust-gas temperature															
8	(51)	Emissivity of exhaust pipe	(8) and literature	ϵ_p			0.70					0.70					0.70				
	(52)	$(t_{p1} - t_{a1})$	(50) - (37)			1530	1371	1261	-------	-------	1593	1462	1363	1286	1233	1640	1526	1437	1364	1304
	(53)	$(T_{p1}/100)^4$	$\{[(50) + 460]/100\}^4$			146,980	102,660	77,040	-------	-------	168,470	126,870	100,570	82,540	68,030	183,590	145,340	119,710	101,290	86,100
	(54)	$(T_{a1}/100)^4$	$\{[(37) + 460]/100\}^4$			334	312	263	-------	-------	337	327	305	276	214	339	332	321	306	264
	(55)	Radiant heat-transfer coefficient	$0.000048 \times (51) \times [(53) - (54)]/(52)$	h_r	$\frac{Btu}{(sec)(ft^2)(°F)}$	0.00322	0.00251	0.00204	-------	-------	0.003540	0.002908	0.00247	0.002157	0.001856	0.00375	0.00319	0.00279	0.002494	0.002211
	(56)	$\left(\frac{1}{h_a + h_r} + \frac{1}{h_e}\right)$	$\frac{1}{(47) + (55)} + \frac{1}{(41)}$			196.9	164.2	144.4	-------	-------	211.5	182.3	162.5	148.3	138.4	221.0	195.6	177.0	162.6	152.2
	(57)	$m_{p}l/\left(\bar{c}_{p_e}W_e\right)$	$10.47 \times (5) \times (27)/(3)$					17.86					17.86					17.86		
16	(58)	$\bar{c}_{p_e}W_e/\bar{c}_{p_a}W_a$	$1.25 \times (3)/(29)$	z		12.10	6.05	4.033	-------	-------	12.10	6.05	4.033	3.025	2.42	12.1	6.05	4.033	3.025	2.42
	(59)	ω	$(57)[1 + (58)]/(56)$			1.1890	0.7671	0.6225	-------	-------	1.1064	0.6906	0.5531	0.4853	0.4413	1.0586	0.6438	0.5078	0.4427	0.4012
	(60)	e^ω	$e^{(59)}$			3.2838	2.1535	1.8636	-------	-------	3.024	1.995	1.739	1.625	1.555	2.882	1.904	1.662	1.557	1.494
	(61)	$t_{e1} - t_{a1}$	(4) - (37)			1833	1840	1857	-------	-------	1832	1835	1842	1852	1878	1831	1833	1837	1842	1857
	(62)	$(t_{e1} - t_{a1})/e^\omega$	(61)/(60)			558	854	997	-------	-------	606	920	1061	1140	1208	635	963	1105	1183	1243
	(63)	$z t_{e1} + t_{a1}$	$(4) \times (58) + (37)$			21,750	10,850	7220	-------	-------	21,748	10,855	7217	5402	4278	21,750	10,857	7223	5412	4299
	(64)	Downstream exhaust-gas temperature	$[(62) + (63)]/[1 + (58)]$	t_{e2}	°F	1703	1660	1629	-------	-------	1706	1670	1645	1623	1604	1709	1677	1655	1636	1621
						Downstream cooling-air temperature															
17	(65)	Downstream cooling-air temperature	$(58)[(4) - (64)] + (37)$	t_{a2}	°F	1141	807	632	-------	-------	1106	752	583	484	379	1070	711	548	455	397
						Downstream exhaust-pipe temperature															
18	(66)	$h_e t_{e2} + h_a t_{a2}$	$(41) \times (64) + (47) \times (65)$			36.45	36.62	36.42	-------	-------	35.32	35.20	34.99	34.72	34.24	34.67	34.42	34.18	33.95	33.61
	(67)	Downstream exhaust-pipe temperature	(66)/(49)	t_{p2}	°F	1610	1442	1310	-------	-------	1629	1483	1369	1275	1191	1643	1515	1414	1330	1256

[1] Items are carried in parentheses to indicate row used in calculations.

TABLE 3 - Continued

CALCULATION FORM FOR SHROUD DESIGN - PARALLEL FLOW - Continued

Step	Item[1]	Quantity	Source	Symbol	Units										
						Downstream exhaust-gas temperature									
8	(51)	Emissivity of exhaust pipe	(8) and literature	ϵ_p		0.70					0.70				
	(52)	$(t_{p_1} - t_{a_1})$	(50) - (37)			1672	1572	1492	1427	1371	1694	1606	1535	1475	1423
	(53)	$(T_{p_1}/100)^4$	$\{[(50) + 460]/100\}^4$			194,850	160,000	135,330	117,130	102,430	203,140	171,160	148,180	130,320	115,870
	(54)	$(T_{a_1} 100)^4$	$\{[(37) + 460]/100\}^4$			339	336	329	319	304	340	337	333	327	317
	(55)	Radiant heat-transfer coefficient	$0.000048 \times (51) \times [(53) - (54)]/(52)$	h_r	$\dfrac{\text{Btu}}{(\text{sec})(\text{ft}^2)(°F)}$	0.00391	0.00341	0.00304	0.00275	0.00250	0.00402	0.00357	0.00324	0.00296	0.00273
	(56)	$\left(\dfrac{1}{h_a + h_r} + \dfrac{1}{h_e}\right)$	$\dfrac{1}{(47) + (55)} + \dfrac{1}{(41)}$			228.0	205.7	188.6	175.0	164.0	233.0	213.3	197.7	184.8	174.0
16	(57)	$ml_p{}^l/(\bar{c}_{p_e} W_e)$	$10.47 \times (5) \times (27)/(3)$			17.86					17.86				
	(58)	$\bar{c}_{p_e} W_e / \bar{c}_{p_a} W_a$	$1.25 \times (3)/(29)$	z		12.1	6.05	4.033	3.025	2.42	12.1	6.05	4.033	3.025	2.42
	(59)	ω	$(57)[1 + (58)]/(56)$			1.0260	0.6121	0.4764	0.4109	0.3726	1.0043	0.5903	0.4545	0.3890	0.3510
	(60)	e^ω	$e^{(59)}$			2.790	1.844	1.610	1.508	1.452	2.730	1.805	1.576	1.476	1.421
	(61)	$t_{e_1} - t_{a_1}$	(4) - (37)			1831	1832	1834	1837	1842	1831	1832	1833	1835	1838
	(62)	$(t_{e_1} - t_{a_1})/e^\omega$	(61)/(60)			656	993	1139	1218	1269	671	1015	1164	1244	1293
	(63)	$z t_{e_1} + t_{a_1}$	$(4) \times (58) + (37)$			21,750	10,858	7220	5408	4314	21,750	10,858	7221	5412	4318
	(64)	Downstream exhaust-gas temperature	$[(62) + (63)]/[1 + (58)]$	t_{e_2}	°F	1710	1681	1662	1646	1632	1711	1684	1667	1654	1641
						Downstream cooling-air temperature									
17	(65)	Downstream cooling-air temperature	$(58)[(4) - (64)] + (37)$	t_{a_2}	°F	1058	688	522	428	364	1046	670	503	407	345
						Downstream exhaust-pipe temperature									
18	(66)	$h_e t_{e_2} + h_a t_{a_2}$	$(41) \times (64) + (47) \times (65)$			34.24	33.94	33.69	33.46	33.23	33.96	33.62	33.37	33.16	32.92
	(67)	Downstream exhaust-pipe temperature	(66)/(49)	t_{p_2}	°F	1653	1540	1450	1374	1308	1661	1559	1478	1409	1345

[1]Items are carried in parentheses to indicate row used in calculations.

NATIONAL ADVISORY
COMMITTEE FOR AERONAUTICS

TABLE 3 - Concluded

CALCULATION FORM FOR SHROUD DESIGN - PARALLEL FLOW - Concluded

Step	Item[1]	Quantity	Source	Symbol	Units					
				Cooling-air pressure drop in shroud						
19	(68)	Shroud diameter	Selected from critical tempera-ture plots such that no limiting temperature is exceeded, as per instructions in step 19	d_s	ft	--------	--------	0.667	0.710	0.752
	(69)	Cooling-air-flow rate		W_a	lb/sec	--------	--------	1.62	1.94	2.37
	(70)	Upstream cooling-air static pressure	(68), (69) and curves plotted against W_a	p_{a_1}	lb/ft^2	--------	--------	678	680	680
	(71)	Upstream cooling-air temperature		t_{a_1}	°F	--------	--------	-38	-37	-36.5
	(72)	Downstream cooling-air temperature		t_{a_2}	°F	--------	--------	520	440	368
	(73)	Downstream cooling-air static pressure	$p_{a_2} = p_o = (12)$	p_{a_2}	lb/ft^2			628.1		
	(74)	Upstream cooling-air density	$0.000583 \times (70)/[(71) + 460]$	ρ_{a_1}	slugs/ft^3	--------	--------	0.000937	0.000937	0.000936
	(75)	Downstream cooling-air density	$0.000583 \times (73)/[(72) + 460]$	ρ_{a_2}	slugs/ft^3	--------	--------	0.000374	0.000407	0.000442
	(76)	$\left(1 + \dfrac{\rho_{a_1}}{\rho_{a_2}}\right)$	$1 + [(74)/(75)]$			--------	--------	3.507	3.303	3.117
	(77)	$W_a^{1.8}$	(69) and table 5			--------	--------	2.383	3.298	4.72
	(78)	$\left(d_s + d_p\right)^{1.8}$	$[(68) + (5)]$ and table 5			--------	--------	1.237	1.323	1.411
20	(79)	$\left(d_s - d_p\right)^3$	$[(68) - (5)]^3$			--------	--------	0.00909	0.0160	0.0253
	(80)	$\mu_a^{0.2}$	(71) and figure 13			--------	--------	0.0502	0.0502	0.0503
	(81)	Friction pressure drop referred to standard density	$\dfrac{0.0879 \times (27) \times (76) \times (77) \times (80)}{(78) \times (79)}$	$\sigma_{a_1} \Delta p_f$	lb/ft^2	--------	--------	59.07	40.97	33.10
	(82)	$2\dfrac{\rho_{a_1}}{\rho_{a_2}} - 1$	$[2 \times (74)/(75)] - 1$			--------	--------	4.015	3.606	3.233
	(83)	W_a^2	$(69)^2$			--------	--------	2.624	3.764	5.617
	(84)	$\left(d_s + d_p\right)^2$	$[(68) + (5)]^2$			--------	--------	1.266	1.365	1.465
	(85)	$\left(d_s - d_p\right)^2$	$[(68) - (5)]^2$			--------	--------	0.0436	0.0634	0.0863
	(86)	Heating and exiting pressure drop referred to standard density	$0.3284 \times (82) \times (83)/[(84) \times (85)]$	$\sigma_{a_1}\left(\Delta H_h + \Delta H_e\right)$	lb/ft^2	--------	--------	62.68	51.50	47.20
	(87)	Total pressure drop referred to standard density	$(81) + (86)$	$\sigma_{a_1} \Delta H$	lb/ft^2	--------	--------	121.75	92.47	80.3
	(88)	Cooling-air pressure drop in shroud	$0.002378 \times (87)/(74)$	ΔH	lb/ft^2	--------	--------	309.0	234.7	207.1

[1]Items are carried in parentheses to indicate row used in calculations.

NATIONAL ADVISORY
COMMITTEE FOR AERONAUTICS

TABLE 4

CALCULATION FORM FOR SHROUD DESIGN - COUNTERFLOW

Step	Item[1]	Quantity	Source	Symbol	Units
Factors for design					
	(1)	Brake horsepower	Manufacturer	bhp	hp
	(2)	Fuel-air ratio	Manufacturer	f	
1	(3)	Exhaust-gas-flow rate through engine	Manufacturer's data or equation (47)	W_e	lb/sec
2	(4)	Exhaust-gas temperature at shroud entrance	Manufacturer's data and equation (48) or analytical method	t_{e_1}	°F
3	(5)	Exhaust-pipe diameter (outer)	Manufacturer	d_p	ft
4	(6)	Velocity of airplane	Performance data	V_o	ft/sec
	(7)	Altitude	Performance data		ft
	(8)	Exhaust-pipe material	Manufacturer		
5	(9)	Design exhaust-gas temperature	Manufacturer	t_{e_2}	°F
6	(10)	Design exhaust-pipe temperature	Manufacturer	t_{p_1}	°F
7	(11)	Design shroud temperature	Manufacturer	t_{s_1}	°F
Pressure drop available at shroud entrance					
4	(12)	Free-stream static pressure	(7) and reference 8	p_o	lb/ft²
	(13)	Free-stream temperature	(7) and reference 8	T_o	°F abs
	(14)	Free-stream density	(7) and reference 8	ρ_o	slugs/ft³
	(15)	Free-stream dynamic pressure	(14) × (6)² × F_{c_o}/2	q_{c_o}	lb/ft²
9	(16)	Cooling-air-flow rate	Assumed (approximately 1/8 to 1/2 of (3))	W_a	lb/sec
10	(17)	Cross-sectional area of inlet-duct straight section	Area of straight section of assumed inlet duct	A_i	ft²
	(18)	Length of inlet duct straight section	Length of straight section of assumed inlet duct	l_i	ft
	(19)	Hydraulic diameter of inlet duct straight section	4 × (17)/Perimeter of inlet duct straight section	D_i	ft
	(20)	Dynamic pressure in straight section	0.00048 × [(16)/(17)]²/(14)	q_i	lb/ft²
	(21)	μ_{a_o}	[(13) - 460] and figure 19	μ_{a_o}	$\dfrac{\text{slugs}}{\text{(sec)(ft)}}$
	(22)	R_i	0.031 × (16) × (19)/[(17) × (21)]	R_i	
	(23)	Friction factor	(22) and reference 9	f_i	
	(24)	Friction pressure loss in straight-section inlet duct	4 × (18) × (20) × (23)/(19)	ΔH_i	lb/ft²

Where the inlet duct contains more than one straight section, the calculations of items (16) to (24) are repeated to determine the pressure loss in each straight section. If the intake duct contains bends and/or diffusers, supplementary calculation forms will be needed to calculate the pressure losses in each bend and/or diffuser as given by the equation and method of step 10 of the single-segment design procedure.

| | (25) | Total pressure drop in inlet duct | 0.05 (15) + $\sum$ (24) + $\sum$ Bend and diffuser losses | ΔH_{o-2} | lb/ft² |
| | (26) | Pressure drop available at shroud entrance | (15) - (25) | $\Delta H_{available}$ | lb/ft² |

[1]Items are carried in parentheses to indicate row used in calculations.

NATIONAL ADVISORY
COMMITTEE FOR AERONAUTICS

TABLE 4 - Continued

CALCULATION FORM FOR SHROUD DESIGN - COUNTERFLOW - Continued

Step	Item[1]	Quantity	Source	Symbol	Units
		Design variables			
11	(27)	Length of shroud segment	Assumed	l	ft
12	(28)	Shroud diameter	Assumed	d_s	ft
9	(29)	Cooling-air-flow rate	Assumed	W_a	lb/sec
		Cooling-air conditions at shroud entrance			
	(30)	Free-stream stagnation temperature	(13) + 0.0000832 (6)^2	T_{o_t}	°F abs
	(31)	Pressure drop available at shroud entrance	(29) and curve of $\Delta H_{available}$ for inlet duct selected by step (10)	$\Delta H_{available}$	lb/ft^2
	(32)	Total pressure at shroud entrance	(12) + (31)	H_{a_2}	lb/ft^2
13	(33)	$d_s{}^2 - d_p{}^2$	(28)^2 - (5)^2		
	(34)	$1.384 W_a \sqrt{T_{o_t}} / \left[\left(d_s{}^2 - d_p{}^2 \right) \times H_{a_2} \right]$	1.384 × (29) × (30)$^{1/2}$ /$\left[(32) \times (33) \right]$		
	(35)	$\left(H_{a_2} - p_{a_2} \right) / H_{a_2}$	(34) and figure 16		
	(36)	Cooling-air static pressure at shroud entrance	(32)$\left[1 - (35) \right]$	p_{a_2}	lb/ft^2
14	(37)	Cooling-air temperature at shroud entrance	(30)$\left[(36)/(32) \right]^{0.286} - 460$	t_{a_2}	°F
		Downstream exhaust-gas temperature			
	(38)	$W_e{}^{0.8}$	(3) and table 5		
	(39)	$d_p{}^{1.8}$	(5) and table 5		
	(40)	$k_a (Pr_a)^{0.4} / \mu_a{}^{0.8}$	(4) and figure 14		
	(41)	Heat-transfer coefficient on gas side	0.001735 × (38) × (40)/(39)	h_e	$\dfrac{Btu}{(sec)(ft^2)(°F)}$
	(42)	Factor depending on ratio of pipe diameters	(28)/(5) and figure 15	ϕ	
	(43)	$\mu_a{}^{0.2}$	(37) and figure 13		
	(44)	$W_a{}^{0.8}$	(29) and table 5		
15	(45)	$\left(d_s + d_p \right)^{0.8}$	$\left[(28) + (5) \right]$ and table 5		
	(46)	$\left(d_s - d_p \right)$	(28) - (5)		
	(47)	Heat-transfer coefficient on air side	$\dfrac{0.01528 \times (42) \times (43) \times (44)}{(45) \times (46)}$	h_a	$\dfrac{Btu}{(sec)(ft^2)(°F)}$
	(48)	$h_e t_{e_1} + h_a t_{a_2}$	(4) × (41) + (37) × (47)		
	(49)	$h_e + h_a$	(41) + (47)		
	(50)	Downstream exhaust-pipe temperature	(48)/(49)	t_{p_2}	°F
8	(51)	Emissivity of exhaust pipe	(8) and literature	ϵ_p	
	(52)	$\left(t_{p_2} - t_{a_2} \right)$	(50) - (37)		
15	(53)	$\left(T_{p_2}/100 \right)^4$	$\left\{ \left[(50) + 460 \right]/100 \right\}^4$		
	(54)	$\left(T_{a_2}/100 \right)^4$	$\left\{ \left[(37) + 460 \right]/100 \right\}^4$		

[1]Items are carried in parentheses to indicate row used in calculations.

TABLE 4 - Concluded

CALCULATION FORM FOR SHROUD DESIGN - COUNTERFLOW - Concluded

Step	Item[1]	Quantity	Source	Symbol	Units
		Downstream exhaust-gas temperature			
15	(55)	Radiant heat-transfer coefficient	$0.000048 \times (51) \times [(53) - (54)]/(52)$	h_r	$\dfrac{\text{Btu}}{(\text{sec})(\text{ft}^2)(°\text{F})}$
	(56)	$\left(\dfrac{1}{h_a + h_r} + \dfrac{1}{h_e}\right)$	$\dfrac{1}{(47) + (55)} + \dfrac{1}{(41)}$		
	(57)	$\pi d_p l / (\bar{c}_{p_e} W_e)$	$10.47 \times (5) \times (27)/(3)$		
	(58)	$\bar{c}_{p_e} W_e / (\bar{c}_{p_a} W_a)$	$1.25 \times (3)/(29)$	Z	
	(59)	ψ	$(57)[1 - (58)]/(56)$		
	(60)	e^ψ	$e^{(59)}$		
	(61)	$t_{e_2}(1 - e^\psi)$	$(37)[1 - (60)]$		
	(62)	$t_{e_1}(1 - Z)$	$(4)[1 - (58)]$		
	(63)	$Z - e^\psi$	$(58) - (60)$		
	(64)	Downstream exhaust-gas temperature	$[(61) - (62)]/(63)$	t_{e_2}	$°\text{F}$
		Downstream cooling-air temperature			
16	(65)	Downstream cooling-air temperature	$(58)[(4) - (64)] + (37)$	t_{a_1}	$°\text{F}$
		Upstream exhaust-pipe temperature			
17	(66)	$h_e t_{e_1} + h_a t_{a_1}$	$(4) \times (41) + (47) \times (65)$		
	(67)	Upstream exhaust-pipe temperature	$(66)/(49)$	t_{p_1}	$°\text{F}$
		Cooling-air pressure drop in shroud			
18	(68)	Shroud diameter	Selected from critical temperature plots such that no limiting temperature is exceeded, as per instructions in step 18	d_s	ft
	(69)	Cooling-air-flow rate		W_a	lb/sec
19	(70)	Upstream cooling-air static pressure	from (68), (69), and curves plotted against W_a	p_{a_2}	lb/ft²
	(71)	Upstream cooling-air temperature		t_{a_2}	$°\text{F}$
	(72)	Downstream cooling-air temperature		t_{a_1}	$°\text{F}$
	(73)	Downstream cooling-air static pressure	$p_{a_1} = p_0 = (12)$	p_{a_1}	lb/ft²
	(74)	Upstream cooling-air density	$0.000583 \times (70)/[(71) + 460]$	ρ_{a_2}	slugs/ft³
	(75)	Downstream cooling-air density	$0.000583 \times (73)/[(72) + 460]$	ρ_{a_1}	slugs/ft³
	(76)	$1 + \dfrac{\rho_{a_2}}{\rho_{a_1}}$	$1 + (74)/(75)$		
	(77)	$W_a^{1.8}$	(69) and table 5		
	(78)	$(d_s + d_p)^{1.8}$	$[(68) + (5)]$ and table 5		
	(79)	$(d_s - d_p)^3$	$[(68) - (5)]^3$		
	(80)	$\mu_a^{0.2}$	(71) and figure 13		
	(81)	Friction pressure drop referred to standard density	$\dfrac{0.0879 \times (27) \times (76) \times (77) \times (80)}{(78) \times (79)}$	$\sigma_{a_2} \Delta p_f$	lb/ft²
	(82)	$2\dfrac{\rho_{a_2}}{\rho_{a_1}} - 1$	$[2 \times (74)/(75)] - 1$		
	(83)	W_a^2	$(69)^2$		
	(84)	$(d_s + d_p)^2$	$[(68) + (5)]^2$		
	(85)	$(d_s - d_p)^2$	$[(68) - (5)]^2$		
	(86)	Heating and exiting pressure drop referred to standard density	$0.3284 \times (82) \times (83)/[(84) \times (85)]$	$\sigma_{a_2}(\Delta H_h + \Delta H_e)$	lb/ft²
	(87)	Total pressure drop referred to standard density	$(81) + (86)$	$\sigma_{a_2} \Delta H$	lb/ft²
	(88)	Cooling-air pressure drop in shroud	$0.002378 \, (87)/(74)$	ΔH	lb/ft²

[1]Items are carried in parentheses to indicate row used in calculations.

TABLE 5

VALUES OF N RAISED TO THE 0.8 AND 1.8 POWERS

N	0	1	2	3	4	5	6	7	8	9
					$N^{0.8}$					
0.2	0.2759	0.2869	0.2978	0.3086	0.3193	0.3299	0.3404	0.3508	0.3612	0.3715
.3	.3817	.3918	.4019	.4119	.4219	.4318	.4416	.4514	.4611	.4708
.4	.4804	.4900	.4996	.5091	.5185	.5279	.5373	.5466	.5559	.5651
.5	.5743	.5835	.5927	.6018	.6108	.6199	.6289	.6378	.6468	.6557
.6	.6645	.6734	.6822	.6910	.6998	.7085	.7172	.7259	.7345	.7432
.7	.7518	.7603	.7689	.7774	.7859	.7944	.8029	.8113	.8197	.8281
.8	.8365	.8449	.8532	.8615	.8698	.8781	.8863	.8946	.9028	.9110
.9	.9192	.9273	.9355	.9436	.9517	.9598	.9679	.9759	.9840	.9920
1.0	1.000	1.008	1.016	1.024	1.032	1.040	1.048	1.056	1.064	1.071
1.1	1.079	1.087	1.095	1.103	1.111	1.118	1.126	1.134	1.142	1.149
1.2	1.157	1.165	1.172	1.180	1.188	1.195	1.203	1.211	1.218	1.226
1.3	1.234	1.241	1.249	1.256	1.264	1.271	1.279	1.286	1.294	1.301
1.4	1.309	1.316	1.324	1.331	1.339	1.346	1.354	1.361	1.368	1.376
1.5	1.383	1.391	1.398	1.405	1.413	1.420	1.427	1.435	1.442	1.449
1.6	1.456	1.464	1.471	1.478	1.486	1.493	1.500	1.507	1.514	1.522
2.0	1.741	1.810	1.879	1.947	2.015	2.081	2.148	2.214	2.279	2.344
3.0	2.408	2.472	2.536	2.599	2.662	2.724	2.786	2.848	2.910	2.971
4.0	3.031	3.092	3.151	3.212	3.272	3.331	3.390	3.449	3.508	3.566
5.0	3.624	3.682	3.739	3.797	3.854	3.911	3.968	4.024	4.081	4.137
6.0	4.193	4.249	4.304	4.360	4.415	4.470	4.525	4.580	4.635	4.690
7.0	4.743	4.797	4.851	4.905	4.959	5.012	5.066	5.119	5.172	5.225
8.0	5.278	5.331	5.383	5.436	5.488	5.540	5.592	5.644	5.696	5.748
9.0	5.800	5.851	5.902	5.954	6.005	6.056	6.107	6.158	6.208	6.259
10.0	6.310	6.360	6.410	6.461	6.511	6.561	6.611	6.660	6.710	6.760
					$N^{1.8}$					
0.2	0.05519	0.06026	0.06552	0.07098	0.07663	0.08247	0.08850	0.09472	0.1011	0.1077
.3	.1145	.1215	.1286	.1359	.1434	.1511	.1590	.1670	.1752	.1836
.4	.1922	.2009	.2098	.2189	.2281	.2376	.2472	.2569	.2668	.2769
.5	.2872	.2976	.3082	.3189	.3299	.3409	.3522	.3636	.3751	.3868
.6	.3987	.4108	.4230	.4353	.4478	.4605	.4733	.4863	.4995	.5128
.7	.5262	.5398	.5535	.5675	.5816	.5958	.6102	.6247	.6394	.6542
.8	.6692	.6843	.6996	.7151	.7306	.7464	.7622	.7783	.7945	.8108
.9	.8272	.8439	.8606	.8775	.8946	.9118	.9292	.9466	.9643	.9821
1.0	1.000	1.018	1.036	1.055	1.073	1.092	1.111	1.130	1.149	1.168
1.1	1.187	1.207	1.226	1.246	1.266	1.286	1.306	1.327	1.347	1.368
1.2	1.388	1.410	1.430	1.452	1.473	1.494	1.516	1.538	1.559	1.581
1.3	1.604	1.626	1.648	1.671	1.694	1.716	1.739	1.762	1.786	1.809
1.4	1.832	1.856	1.880	1.904	1.928	1.952	1.976	2.001	2.025	2.050
1.5	2.075	2.100	2.125	2.150	2.175	2.201	2.227	2.252	2.278	2.304
1.6	2.330	2.357	2.383	2.410	2.436	2.463	2.490	2.517	2.544	2.572
2.0	3.482	3.802	4.134	4.478	4.835	5.204	5.584	5.977	6.381	6.797
3.0	7.225	7.664	8.115	8.577	9.050	9.535	10.031	10.538	11.056	11.586
4.0	12.126	12.677	13.239	13.812	14.395	14.989	15.594	16.210	16.836	17.472
5.0	18.119	18.777	19.445	20.123	20.812	21.511	22.220	22.939	23.669	24.408
6.0	25.158	25.918	26.687	27.467	28.257	29.057	29.866	30.686	31.515	32.354
7.0	33.203	34.062	34.930	35.808	36.696	37.594	38.500	39.417	40.344	41.279
8.0	42.224	43.179	44.143	45.117	46.100	47.093	48.095	49.106	50.126	51.157
9.0	52.196	53.244	54.302	55.359	56.446	57.531	58.626	59.730	60.842	61.965
10.0	63.096	64.236	65.386	66.554	67.711	68.888	70.073	71.267	72.471	73.683

NATIONAL ADVISORY
COMMITTEE FOR AERONAUTICS

TABLE 6

VARIATION OF EXHAUST-GAS ENTHALPY REFERRED TO 0° ABSOLUTE WITH EXHAUST-GAS

TEMPERATURE, FUEL-AIR RATIO, AND HYDROGEN-CARBON RATIO

t, °F \ f	0.01	0.02	0.03	0.04	0.05	0.06	0.07	0.08	0.09	0.10	0.11	0.12
(Btu/lb)												
$\frac{H}{C} = 0.10$												
440	217.0	217.6	218.2	218.8	219.4	220.0	221.6	223.2	227.2	231.1	234.9	238.7
620	262.2	263.2	264.2	265.1	266.1	267.0	269.1	271.1	275.5	279.9	284.3	288.7
800	308.3	309.8	311.2	312.6	314.0	315.4	317.8	320.2	325.1	330.0	334.9	339.8
980	355.6	357.6	359.5	361.4	363.2	365.0	367.9	370.7	376.0	381.3	386.7	392.1
1160	403.9	406.4	408.8	411.2	413.6	415.9	418.9	421.8	426.1	433.9	439.8	445.7
1340	453.2	456.2	459.2	462.2	465.1	467.9	471.7	475.4	481.5	487.7	493.9	500.3
1520	503.3	507.0	510.6	514.1	517.6	521.0	525.8	529.5	535.9	542.5	549.2	556.1
1700	554.1	558.4	562.7	566.8	570.9	574.9	579.7	584.4	591.2	598.2	605.4	612.7
1880	605.2	610.2	615.0	619.9	624.6	629.2	634.5	639.8	645.0	654.4	662.0	669.8
2060	657.7	663.4	669.0	674.5	679.9	685.1	691.0	696.8	704.4	712.2	720.2	728.4
2240	710.4	716.8	723.1	729.3	735.3	741.3	747.7	754.0	762.0	770.2	778.7	787.4
$\frac{H}{C} = 0.12$												
440	217.3	218.2	219.1	220.0	220.9	221.7	224.9	226.3	230.6	234.9	239.1	243.2
620	262.5	263.9	265.2	266.5	267.8	269.1	271.9	274.6	279.6	284.4	289.2	294.0
800	308.8	310.7	312.5	314.3	316.1	317.8	321.1	324.3	329.7	335.2	340.6	346.0
980	356.1	358.5	360.9	363.3	365.6	367.8	371.6	375.3	381.2	387.2	393.2	399.2
1160	404.5	407.5	410.5	413.4	416.3	419.1	423.3	427.5	434.0	440.5	447.0	453.6
1340	453.8	457.5	461.1	464.6	468.1	471.5	476.3	481.0	487.9	494.9	502.0	509.1
1520	504.0	508.3	512.6	516.8	520.9	525.0	530.3	535.5	543.0	550.4	558.1	565.7
1700	554.9	560.0	565.0	569.9	574.6	579.3	585.2	591.0	598.9	606.9	615.1	623.3
1880	606.0	611.8	617.6	623.2	628.7	634.1	635.0	646.9	655.0	659.1	672.5	681.4
2060	658.7	665.3	671.8	678.1	684.4	690.5	697.5	704.5	713.4	722.4	731.8	741.0
2240	711.4	718.8	726.1	733.2	740.2	747.1	754.7	762.3	771.7	781.2	791.0	800.9
$\frac{H}{C} = 0.14$												
440	217.6	218.8	220.0	221.2	222.3	223.4	226.4	229.3	233.9	238.5	243.1	247.6
620	262.9	264.6	266.3	267.9	269.5	271.1	274.3	278.4	283.4	288.7	294.7	299.3
800	309.2	311.5	313.7	315.9	318.1	320.2	324.3	328.3	334.1	340.1	346.1	352.1
980	356.6	359.5	362.3	365.1	367.9	370.6	375.0	379.7	386.2	393.8	399.5	406.1
1160	405.0	408.6	412.1	415.5	418.9	422.2	427.4	432.5	439.5	446.8	454.1	461.5
1340	454.4	458.7	462.9	467.0	471.0	475.0	480.7	486.4	494.0	501.9	509.8	517.9
1520	504.6	509.7	514.6	519.4	524.2	528.8	535.1	541.4	549.7	558.1	566.7	575.4
1700	555.7	561.5	567.2	572.8	578.2	583.6	590.6	597.5	606.2	615.3	624.6	633.9
1880	606.8	613.5	620.0	626.4	632.6	638.8	646.4	654.0	663.3	672.9	682.9	692.9
2060	659.6	667.1	674.4	681.6	688.7	695.7	704.0	712.2	722.0	732.3	742.8	753.4
2240	712.4	720.8	729.0	737.1	745.0	752.8	761.7	770.0	781.0	791.9	803.0	814.3
$\frac{H}{C} = 0.16$												
440	217.9	219.4	220.8	222.3	223.7	225.0	228.6	232.1	237.1	242.1	247.0	251.8
620	263.2	265.3	267.3	269.3	271.2	273.1	277.3	281.5	287.2	292.9	298.6	304.2
800	309.6	312.3	314.9	317.5	320.0	322.5	327.3	332.1	338.5	345.0	351.5	357.9
980	357.0	360.4	363.7	366.9	370.1	373.2	378.6	384.0	391.2	398.4	405.6	412.8
1160	405.5	409.6	413.6	417.5	421.4	425.2	431.3	437.3	445.1	453.0	460.9	468.9
1340	455.0	459.8	464.6	469.3	473.8	478.3	485.0	491.7	500.1	508.8	517.4	526.1
1520	505.3	511.0	516.5	522.0	527.3	532.6	540.0	547.3	556.4	565.7	575.1	584.6
1700	556.4	562.9	569.3	575.6	581.7	587.8	595.8	603.8	613.6	623.6	633.7	643.9
1880	607.6	615.1	622.3	629.5	636.5	643.4	652.2	660.9	671.3	682.0	692.8	703.8
2060	660.4	668.8	677.0	685.0	692.9	700.7	710.2	719.6	730.7	742.0	753.6	765.3
2240	713.4	722.7	731.8	740.8	749.6	758.2	768.3	778.5	790.3	802.4	814.7	827.1
$\frac{H}{C} = 0.18$												
440	218.2	219.9	221.7	223.3	225.0	226.6	230.8	234.9	240.3	245.5	250.7	255.9
620	263.6	265.9	268.3	270.5	272.8	275.0	279.9	284.7	290.9	297.0	303.1	309.2
800	310.0	313.0	316.0	319.0	321.9	324.7	330.3	335.8	342.8	349.7	353.0	363.6
980	357.5	361.3	365.0	368.6	372.2	375.7	382.0	388.2	396.0	403.7	411.5	419.3
1160	406.0	410.6	415.1	419.5	423.8	428.0	435.0	441.9	450.4	458.9	467.6	476.3
1340	455.6	461.0	466.3	471.5	476.5	481.6	489.2	496.8	506.1	515.4	524.9	534.4
1520	506.0	512.2	518.4	524.4	530.4	536.2	544.6	552.9	562.9	573.0	583.3	593.6
1700	557.1	564.3	571.4	578.3	585.1	591.8	600.9	610.0	620.7	631.6	642.7	653.9
1880	608.4	616.6	624.6	632.5	640.2	647.8	658.4	668.9	681.9	695.1	708.8	722.7
2060	661.3	670.5	679.5	688.3	697.0	705.5	716.2	726.8	739.1	751.5	764.2	777.0
2240	714.3	724.5	734.5	744.4	754.0	763.5	774.4	786.3	799.4	812.5	826.1	839.8
$\frac{H}{C} = 0.20$												
440	218.5	220.5	222.5	224.4	226.3	228.2	234.0	239.8	243.3	248.8	254.4	259.8
620	263.9	266.6	269.2	271.8	274.3	276.8	282.4	287.9	294.4	300.9	307.5	313.9
800	310.3	313.8	317.1	320.4	323.6	326.8	333.1	339.4	346.8	354.3	361.8	369.1
980	357.9	362.1	366.3	370.3	374.3	378.2	385.3	392.3	400.6	408.9	417.3	425.6
1160	406.5	411.6	416.5	421.4	426.1	430.8	438.7	446.5	455.6	464.8	474.2	483.4
1340	456.1	462.0	466.9	473.6	479.2	484.7	493.3	501.9	511.8	521.9	532.2	542.3
1520	506.6	513.4	520.2	526.8	533.3	539.7	549.1	558.5	569.2	580.2	591.4	602.3
1700	557.5	565.6	573.3	580.9	588.3	595.6	605.8	616.0	627.7	639.4	651.5	663.4
1880	609.2	618.1	626.8	635.4	643.8	652.0	664.1	676.2	690.6	705.4	720.6	735.8
2060	662.1	672.1	681.9	691.5	700.9	710.2	722.1	733.9	747.1	760.7	774.6	788.3
2240	715.2	726.3	737.2	747.8	758.3	768.6	781.3	794.0	808.1	822.6	837.3	851.9

TABLE 7

CONSTANTS FOR THE CALCULATION OF ABSOLUTE

VISCOSITY OF EXHAUST GAS

Temperature (°F)	μ_a	a_1	b_1	c_1	D_1	E_1	ϕ_1
	(slugs/(sec)(ft) × 10^6)						
500	0.587	0.0223	-0.0112	0.726	0.0493	0.202	-0.133
700	.663	.0399	-.0116	.783	.0537	.234	-.159
900	.732	.0580	-.0121	.854	.0591	.270	-.197
1100	.800	.0756	-.0121	.903	.0632	.300	-.223
1300	.864	.0945	-.0124	.955	.0672	.331	-.255
1500	.928	.1116	-.0128	1.008	.0712	.362	-.286
1700	.977	.1280	-.0131	1.046	.0741	.387	-.308
1900	1.028	.1443	-.0133	1.088	.0774	.414	-.332
2100	1.077	.1602	-.0135	1.130	.0806	.440	-.358
2300	1.125	.1753	-.0138	1.169	.0837	.465	-.380

TABLE 8

CONSTANTS FOR THE CALCULATION OF THERMAL

CONDUCTIVITY OF EXHAUST GAS

Temperature (°F)	k_a	a_2	b_2	c_2	D_2	E_2	ϕ_2
	(Btu/(sec)(sq ft)(°F/ft) × 10^5)						
500	0.695	0.0921	-0.0127	0.861	0.0590	0.306	4.08
700	.814	.1315	-.0118	.919	.0648	.360	4.39
900	.928	.1748	-.0118	1.014	.0727	.426	4.84
1100	1.045	.2214	-.0111	1.078	.0787	.489	5.35
1300	1.164	.2772	-.0099	1.153	.0861	.563	5.87
1500	1.281	.3333	-.0093	1.231	.0933	.639	6.32
1700	1.392	.3947	-.0085	1.271	.0974	.710	6.94
1900	1.500	.4597	-.0078	1.345	.1043	.793	7.48
2100	1.607	.5293	-.0068	1.415	.1111	.880	8.01
2300	1.707	.6033	-.0051	1.472	.1175	.968	8.60

NATIONAL ADVISORY
COMMITTEE FOR AERONAUTICS

TABLE 9

VARIATION OF EXHAUST-GAS PRANDTL NUMBER WITH EXHAUST-GAS TEMPERATURE,

FUEL-AIR RATIO, AND HYDROGEN-CARBON RATIO

$\dfrac{H}{C} = 0.10$

t, °F \ f	0.01	0.02	0.03	0.04	0.05	0.06	0.07	0.08	0.09	0.10	0.11	0.12
500	0.679	0.683	0.686	0.689	0.692	0.695	0.699	0.682	0.646	0.608	0.573	0.536
700	.672	.676	.679	.683	.686	.690	.693	.678	.645	.608	.573	.539
900	.666	.670	.674	.678	.682	.685	.688	.674	.643	.607	.573	.539
1100	.662	.666	.670	.673	.677	.681	.684	.669	.640	.605	.572	.538
1300	.656	.660	.664	.668	.672	.676	.679	.663	.635	.602	.569	.536
1500	.650	.654	.658	.662	.666	.670	.673	.658	.629	.597	.565	.532
1700	.644	.647	.651	.655	.659	.663	.665	.651	.623	.591	.559	.527
1900	.636	.640	.644	.647	.652	.656	.657	.643	.616	.584	.552	.520
2100	.627	.631	.635	.639	.643	.647	.648	.635	.607	.576	.544	.513
2300	.619	.623	.627	.630	.634	.638	.639	.627	.597	.568	.535	.504

$\dfrac{H}{C} = 0.12$

t, °F \ f	0.01	0.02	0.03	0.04	0.05	0.06	0.07	0.08	0.09	0.10	0.11	0.12
500	0.679	0.683	0.687	0.691	0.695	0.699	0.698	0.671	0.629	0.588	0.552	0.514
700	.672	.676	.680	.685	.689	.693	.691	.668	.629	.589	.554	.519
900	.667	.671	.675	.680	.684	.689	.687	.664	.628	.589	.554	.520
1100	.662	.667	.671	.675	.680	.684	.682	.660	.626	.588	.554	.520
1300	.656	.660	.665	.670	.674	.679	.676	.654	.621	.585	.552	.517
1500	.650	.655	.660	.664	.669	.673	.671	.649	.616	.581	.547	.514
1700	.644	.648	.653	.657	.661	.666	.664	.643	.610	.575	.541	.509
1900	.636	.641	.645	.649	.654	.658	.655	.635	.603	.568	.534	.501
2100	.627	.632	.637	.641	.645	.650	.646	.626	.594	.560	.526	.495
2300	.620	.624	.628	.632	.636	.640	.636	.617	.584	.552	.518	.487

$\dfrac{H}{C} = 0.14$

t, °F \ f	0.01	0.02	0.03	0.04	0.05	0.06	0.07	0.08	0.09	0.10	0.11	0.12
500	0.679	0.684	0.689	0.693	0.698	0.703	0.698	0.660	0.613	0.568	0.530	0.493
700	.673	.677	.682	.687	.692	.697	.690	.657	.613	.571	.534	.499
900	.667	.672	.677	.682	.687	.692	.685	.655	.613	.572	.535	.501
1100	.662	.668	.673	.677	.682	.687	.681	.651	.612	.571	.536	.502
1300	.656	.661	.666	.671	.677	.682	.674	.644	.606	.568	.533	.498
1500	.651	.656	.661	.666	.671	.676	.670	.640	.602	.564	.530	.496
1700	.644	.649	.654	.659	.664	.669	.663	.635	.597	.559	.524	.491
1900	.637	.642	.647	.651	.656	.661	.654	.627	.590	.553	.517	.482
2100	.628	.633	.638	.643	.648	.653	.645	.617	.581	.543	.509	.477
2300	.621	.625	.630	.634	.638	.643	.634	.608	.571	.535	.500	.469

$\dfrac{H}{C} = 0.16$

t, °F \ f	0.01	0.02	0.03	0.04	0.05	0.06	0.07	0.08	0.09	0.10	0.11	0.12
500	0.679	0.685	0.690	0.696	0.701	0.707	0.697	0.649	0.597	0.548	0.508	0.471
700	.673	.678	.683	.689	.694	.700	.688	.647	.597	.552	.515	.479
900	.667	.672	.678	.684	.690	.695	.684	.645	.598	.554	.516	.482
1100	.663	.668	.674	.679	.685	.690	.680	.642	.598	.554	.518	.484
1300	.656	.662	.668	.673	.679	.684	.672	.635	.592	.551	.514	.479
1500	.651	.657	.662	.668	.674	.679	.668	.631	.589	.548	.513	.478
1700	.645	.650	.655	.661	.666	.672	.662	.627	.584	.543	.506	.473
1900	.637	.642	.648	.653	.658	.664	.652	.619	.577	.537	.499	.466
2100	.629	.634	.640	.645	.650	.655	.643	.608	.568	.527	.491	.459
2300	.622	.626	.631	.636	.640	.645	.631	.598	.558	.519	.483	.452

$\dfrac{H}{C} = 0.18$

t, °F \ f	0.01	0.02	0.03	0.04	0.05	0.06	0.07	0.08	0.09	0.10	0.11	0.12
500	0.680	0.685	0.692	0.698	0.704	0.711	0.695	0.638	0.582	0.531	0.490	0.453
700	.673	.679	.685	.691	.697	.703	.687	.636	.584	.537	.497	.461
900	.667	.674	.680	.686	.692	.698	.682	.635	.585	.539	.499	.465
1100	.663	.669	.675	.681	.687	.693	.677	.632	.584	.539	.501	.466
1300	.657	.663	.669	.675	.682	.688	.671	.627	.580	.536	.498	.463
1500	.652	.658	.664	.670	.676	.682	.666	.623	.576	.532	.496	.461
1700	.645	.651	.657	.663	.669	.675	.659	.618	.570	.527	.490	.456
1900	.638	.644	.650	.655	.661	.667	.650	.610	.564	.521	.483	.449
2100	.630	.636	.641	.647	.652	.658	.641	.600	.556	.513	.476	.444
2300	.623	.628	.633	.637	.642	.647	.629	.591	.547	.506	.469	.438

$\dfrac{H}{C} = 0.20$

t, °F \ f	0.01	0.02	0.03	0.04	0.05	0.06	0.07	0.08	0.09	0.10	0.11	0.12
500	0.680	0.687	0.694	0.700	0.707	0.714	0.693	0.627	0.568	0.515	0.472	0.436
700	.673	.680	.686	.693	.700	.706	.686	.626	.571	.522	.479	.443
900	.668	.675	.681	.688	.695	.701	.679	.624	.572	.524	.482	.447
1100	.663	.670	.676	.683	.690	.696	.674	.622	.572	.523	.484	.447
1300	.658	.664	.671	.677	.684	.691	.670	.619	.571	.521	.484	.448
1500	.652	.658	.665	.671	.678	.684	.664	.614	.568	.517	.482	.447
1700	.646	.652	.658	.665	.671	.684	.657	.608	.563	.512	.479	.444
1900	.639	.645	.651	.657	.664	.677	.649	.601	.557	.506	.474	.440
2100	.631	.637	.643	.649	.655	.670	.639	.593	.551	.499	.468	.435
2300	.624	.629	.634	.639	.644	.660	.628	.584	.544	.492	.462	.430
						.649			.535		.455	.424
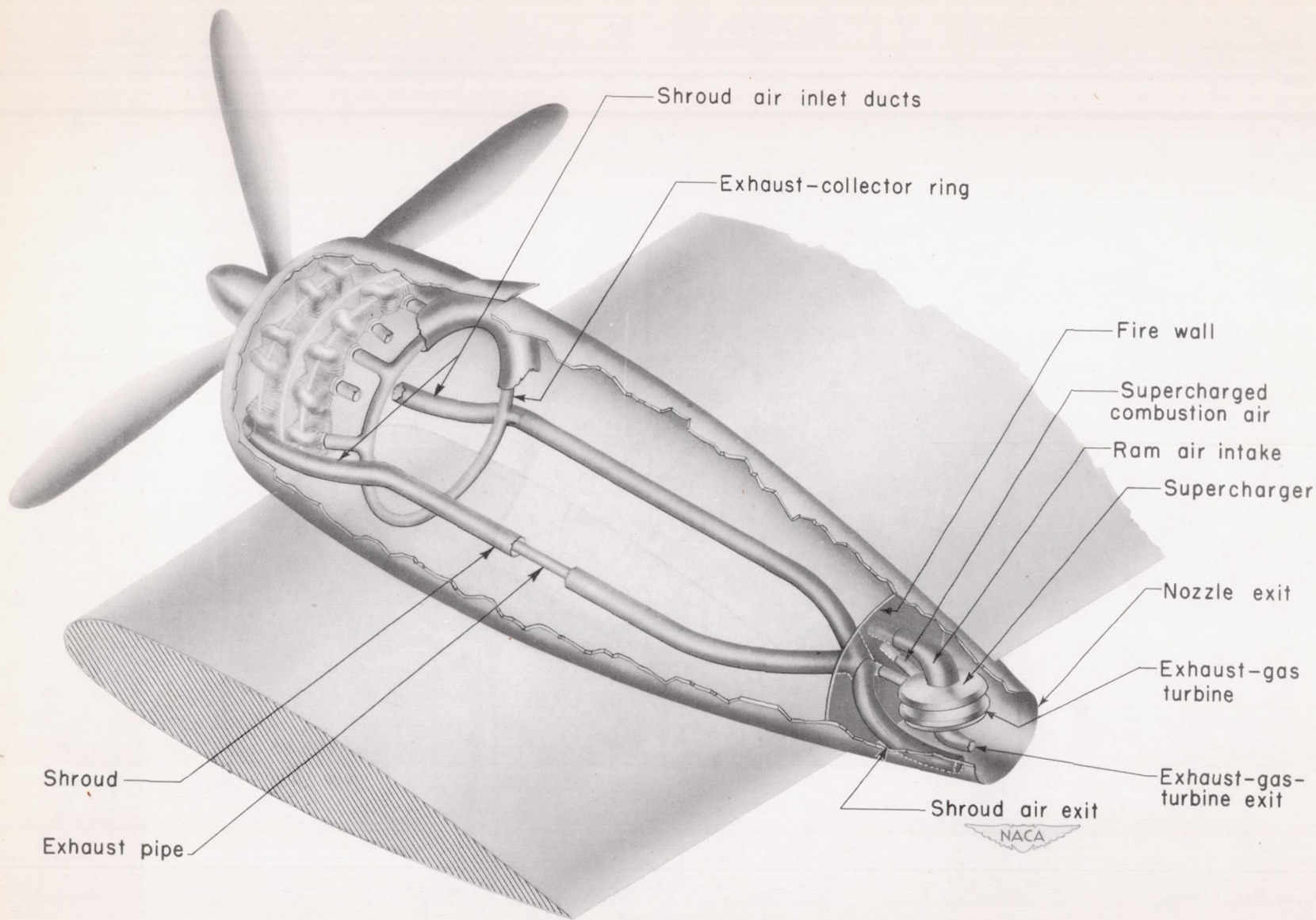
Figure 1.- Illustration of a shrouded exhaust-pipe system in an airplane.
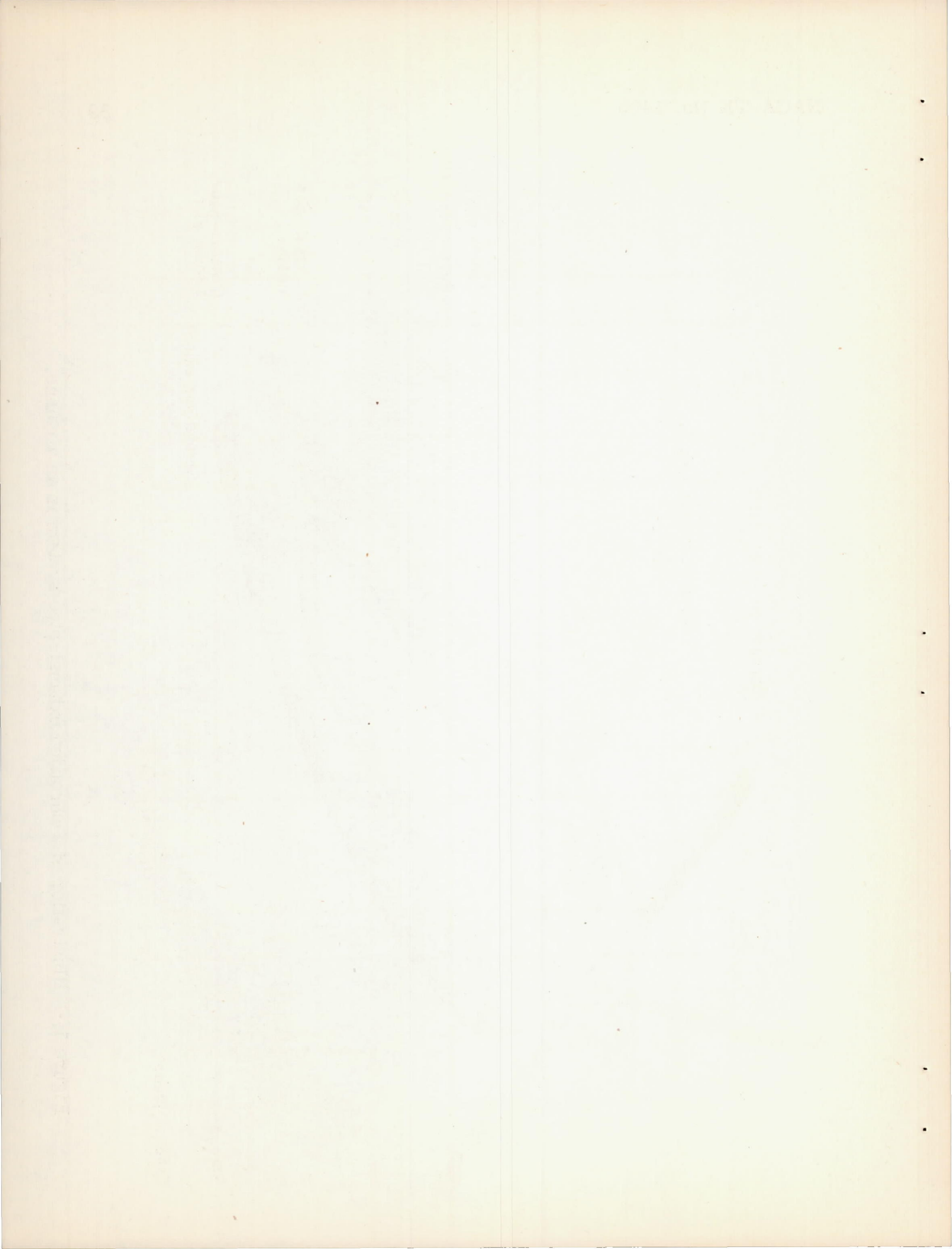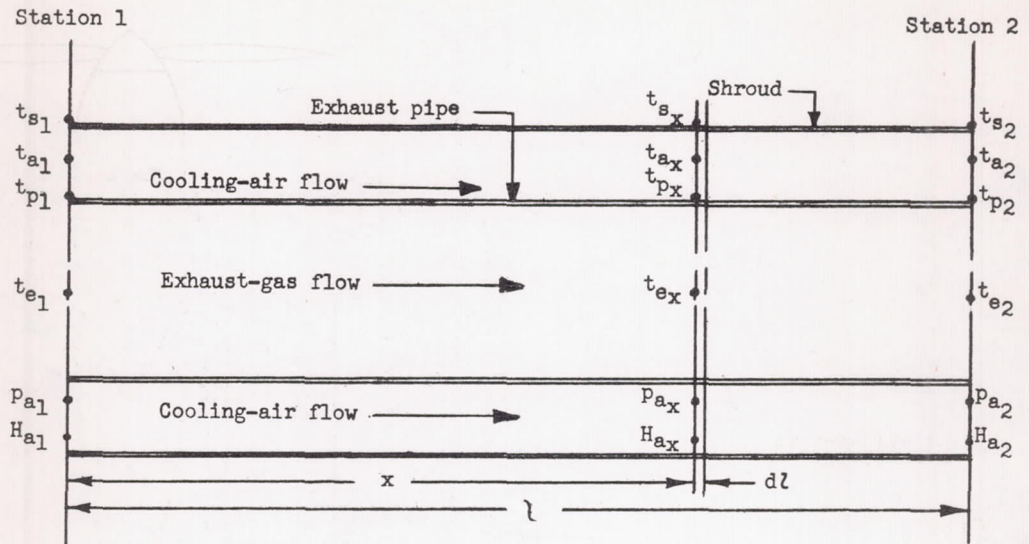
(a) Parallel flow.
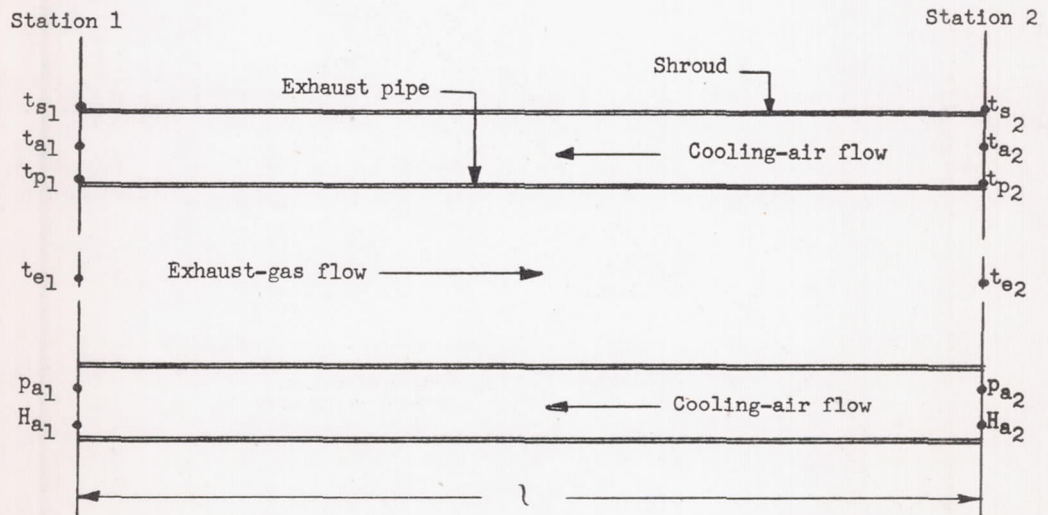
(b) Counter flow.

Figure 2.- Illustration of symbols defined for a shrouded
exhaust-pipe system.
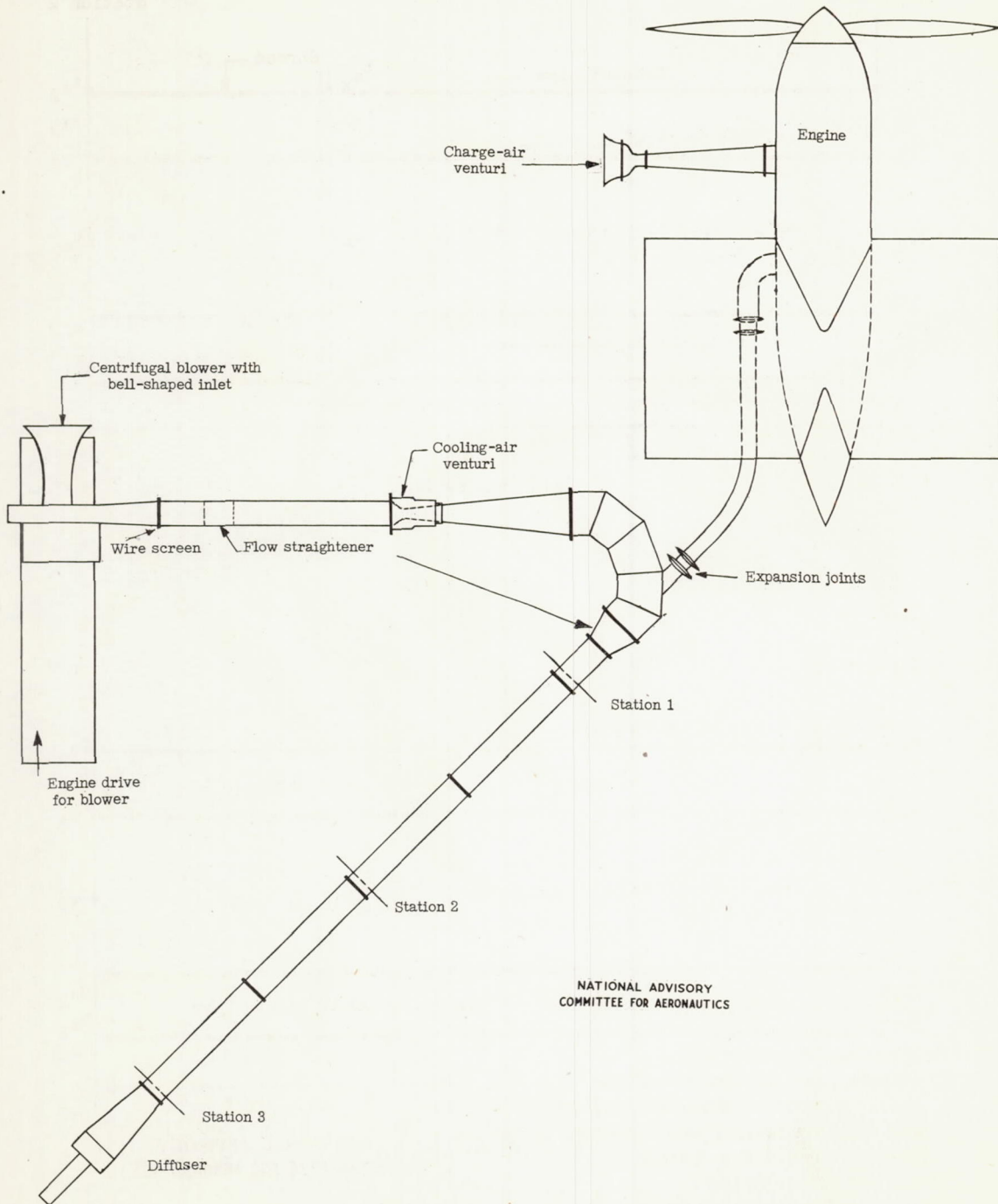
Figure 3.- Schematic diagram of experimental exhaust-pipe-shroud
test setup.
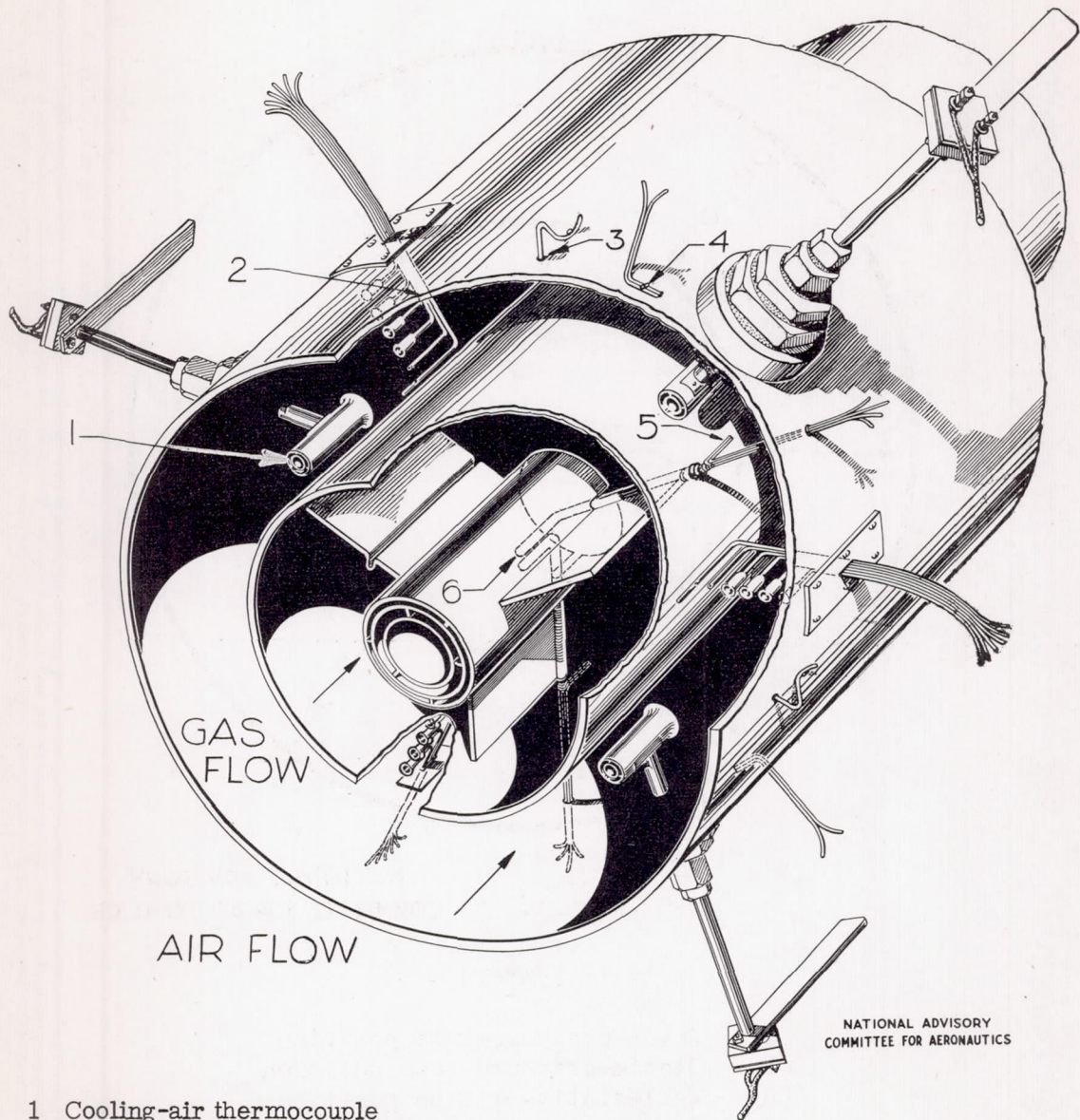
1   Cooling-air thermocouple
2   Pressure rake consisting of one
        static-pressure tube, one unshielded
        and four shielded total-pressure tubes
3   Wall static-pressure orifice
4   Shroud thermocouple
5   Exhaust-pipe thermocouple
6   Exhaust-gas thermocouple

Figure 4.- Sketch of typical instrument station showing temperature-
            and pressure-measuring devices.
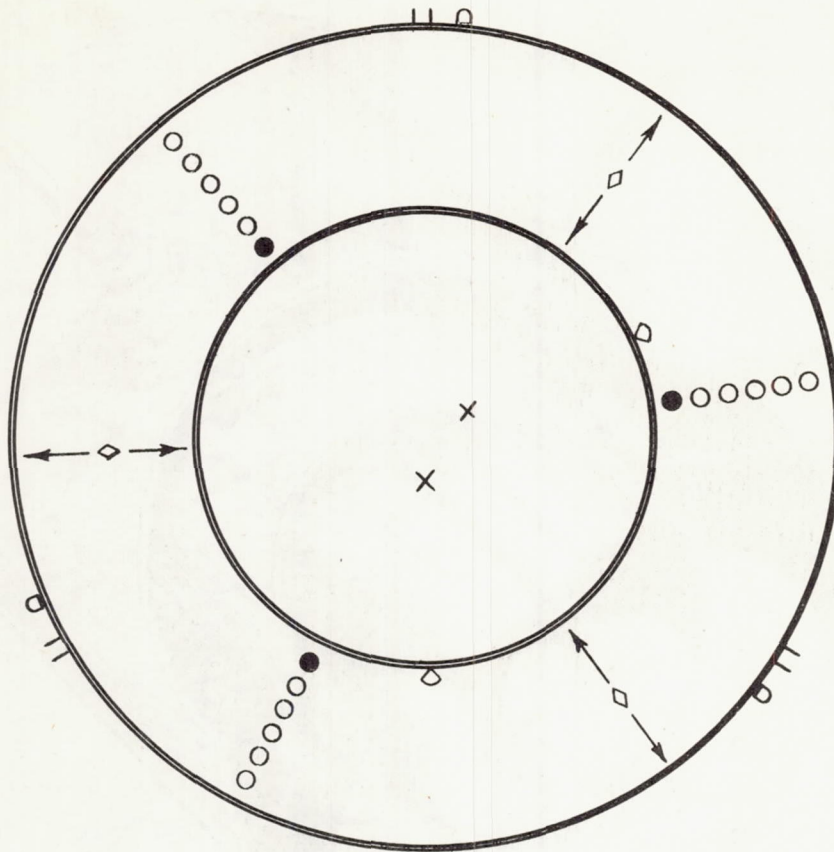
**NATIONAL ADVISORY
COMMITTEE FOR AERONAUTICS**

Symbols

O   Total-pressure-tube position
●   Static-pressure-tube position
⊥⊥   Wall-static-orifice position
✕   Exhaust-gas thermocouple position
◇   Exhaust-pipe-thermocouple position
◊   Cooling-air-thermocouple position
       (←—— ——▸ indicates direction
       of traverse)
◠   Shroud-thermocouple position

Figure 5.-   Sketch of typical instrument station showing relative
location of instruments.

(a) Station 2.
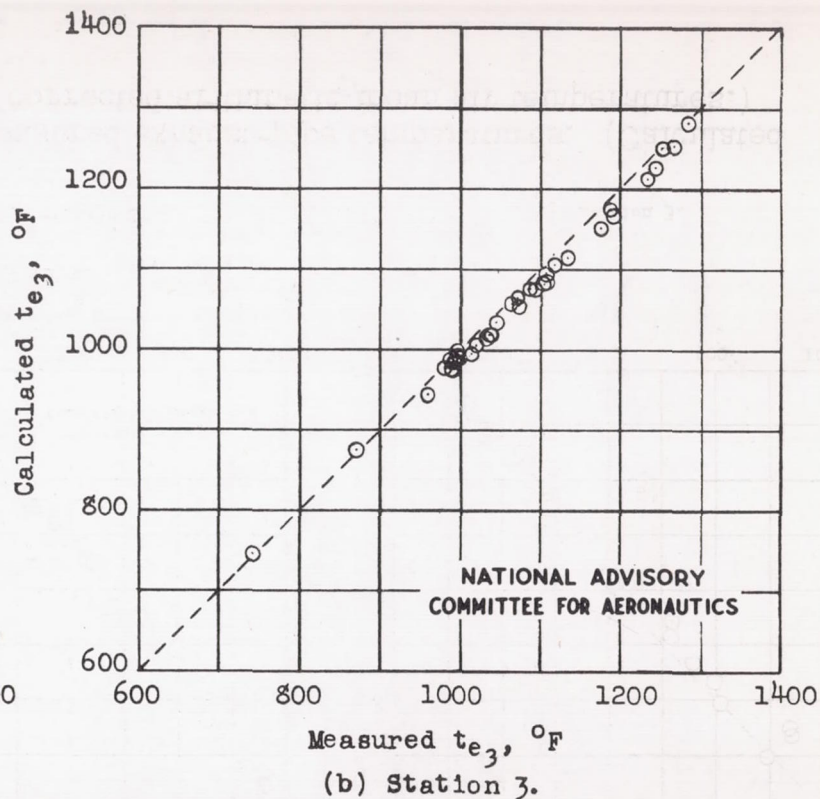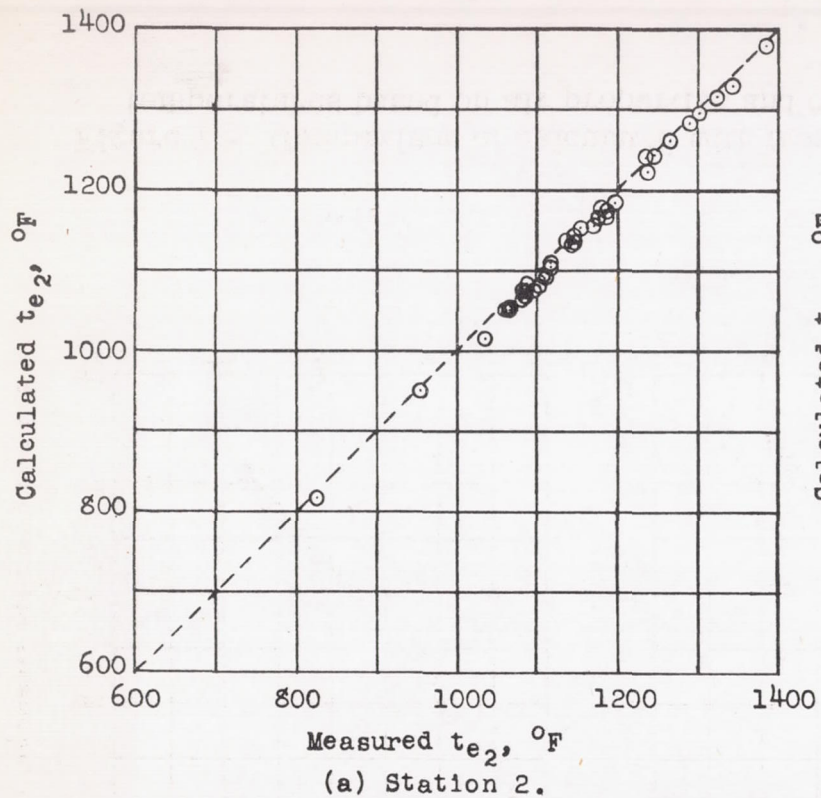
(b) Station 3.

Figure 6.- Comparison of calculated with measured downstream exhaust-gas temperatures. (Calculated temperatures based on air properties and corrected arithmetic mean air temperatures.)
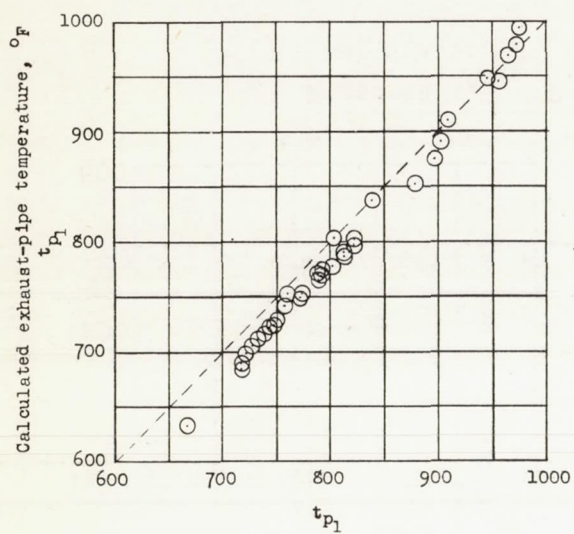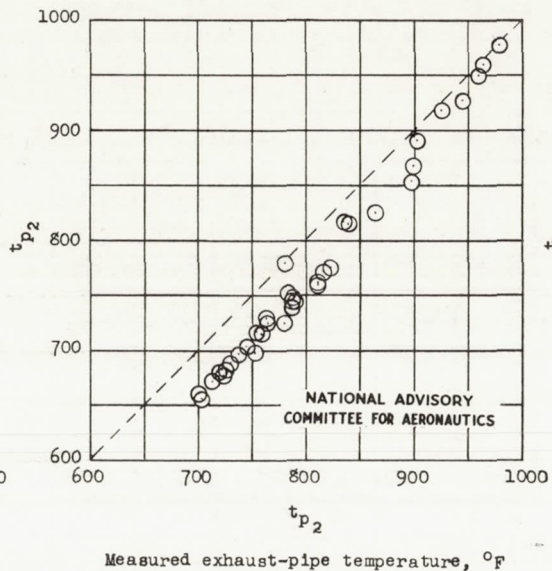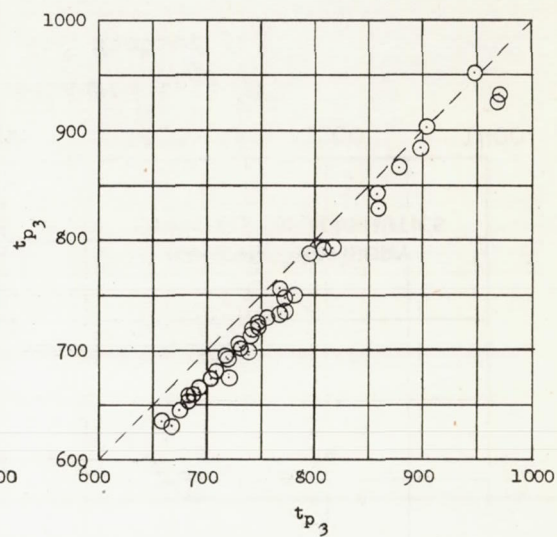
(a) Station 1.　　　　　　　(b) Station 2.　　　　　　　(c) Station 3.

Figure 7.- Comparison of calculated with measured exhaust-pipe temperatures. (Calculated temperatures based on air properties and corrected arithmetic mean air temperatures.)

(a) Station 2.

(b) Station 3.
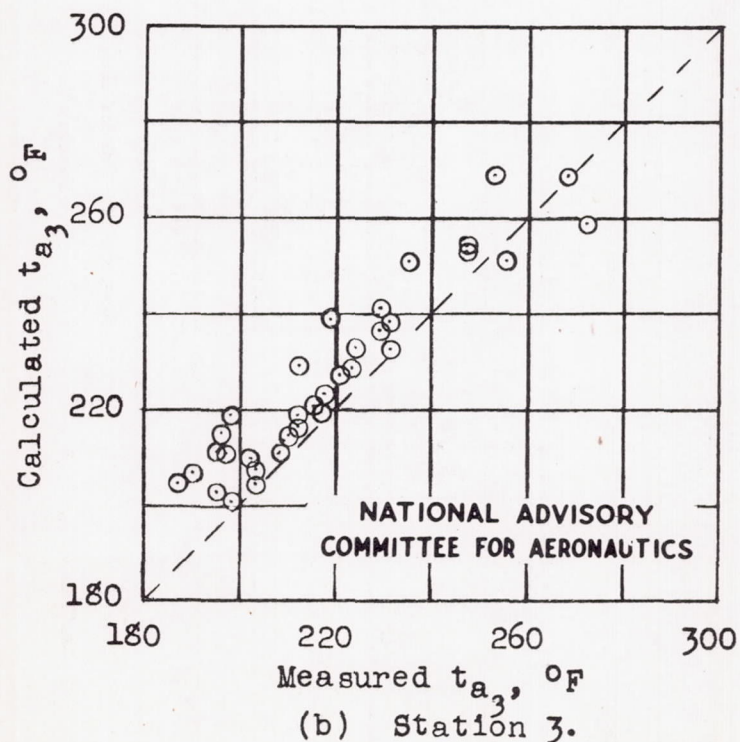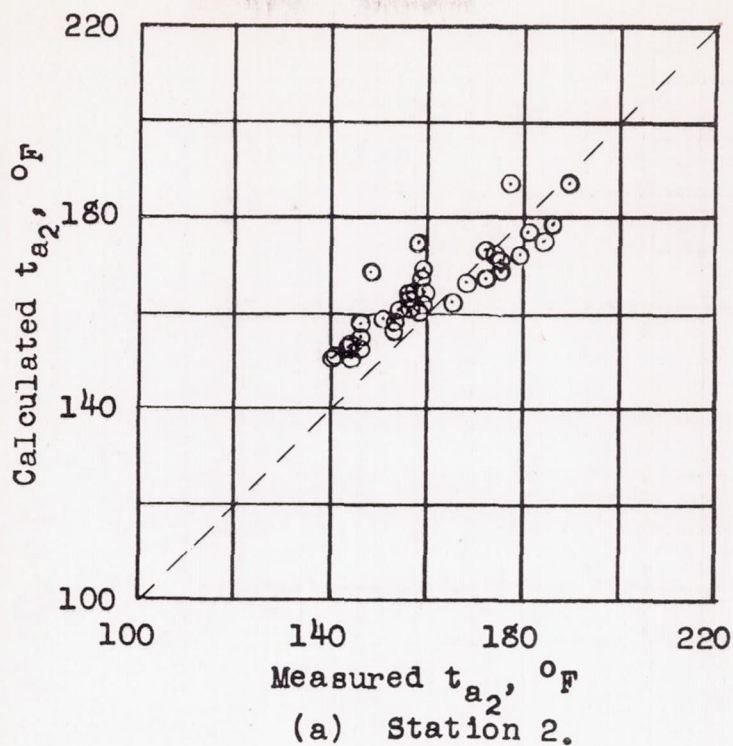
Figure 8.- Comparison of calculated with measured downstream
cooling-air temperatures. (Calculated temperatures based on
air properties and corrected arithmetic mean air temperatures.
Measured temperatures are corrected arithmetic means.)
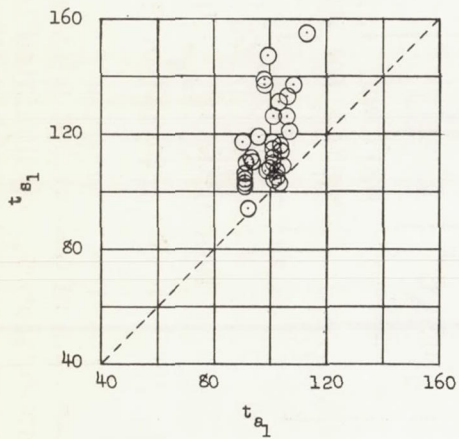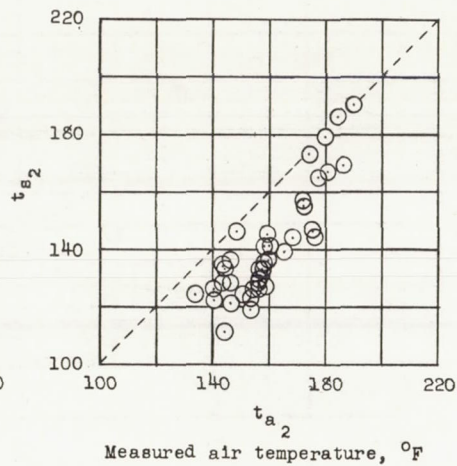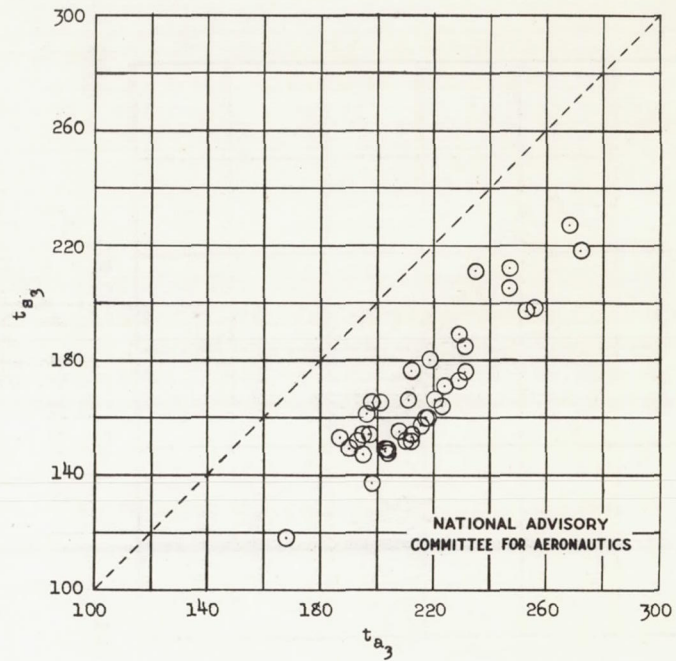
(a) Station 1. (b) Station 2. (c) Station 3.

Figure 9.- Relation of the measured shroud temperature to the measured cooling-air temperature.
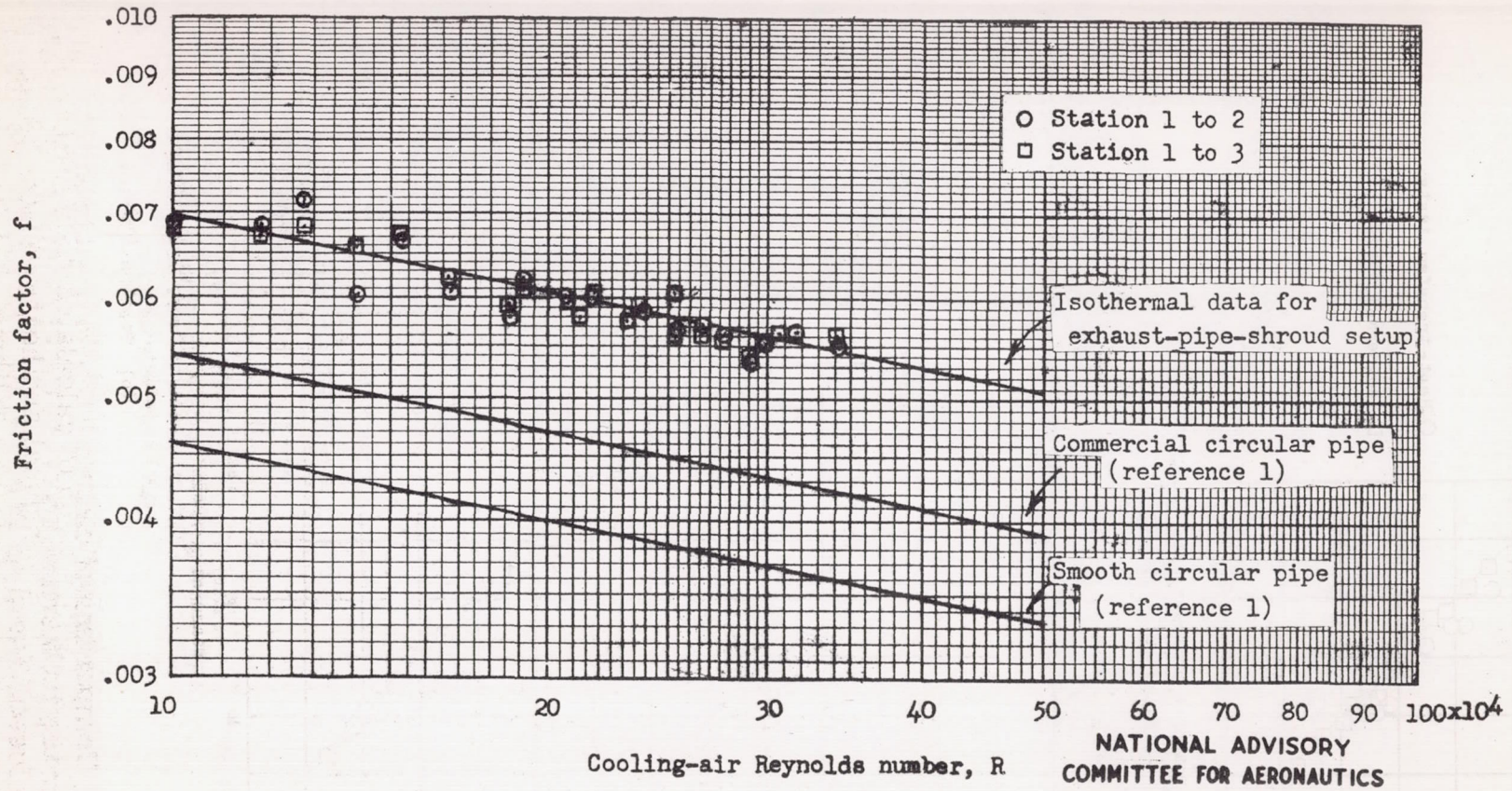
Figure 10.- Variation of friction factors for the exhaust-pipe-shroud setup and for commercial and smooth circular pipes with cooling-air Reynolds number.
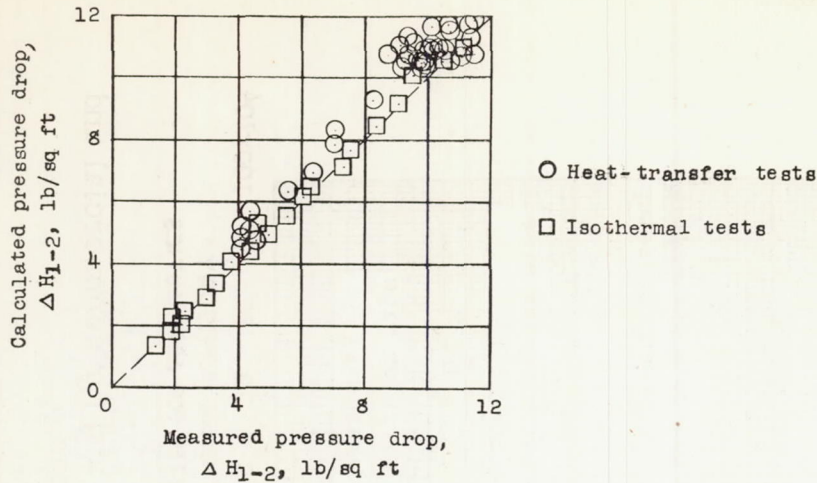
(a) Station 1 to 2.
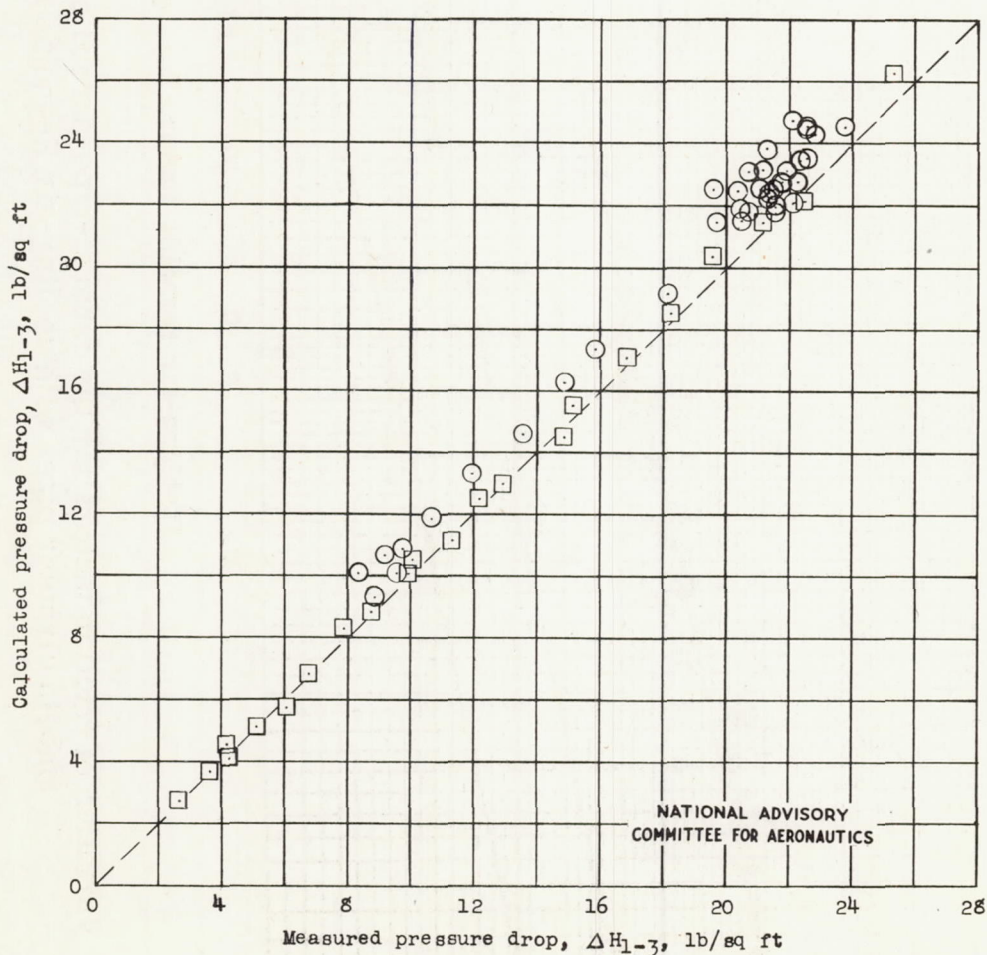
(b) Station 1 to 3.

Figure 11.- Comparison of calculated with measured total-pressure
losses for the isothermal and heat-transfer tests. (Calculated
pressure losses based on arithmetic mean pressures and
calculated downstream air temperatures based on air properties
and corrected arithmetic mean air temperatures.)
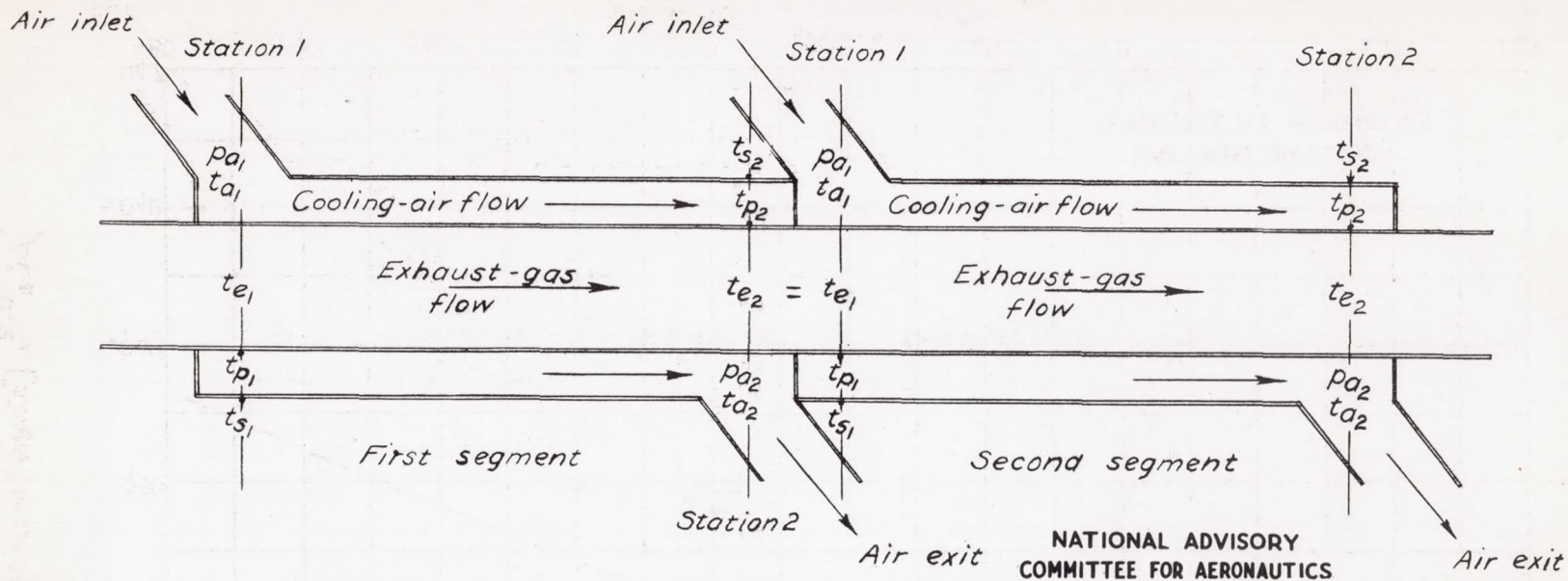
Figure 12.- Diagrammatic sketch of a multisegment exhaust-pipe-shroud system for parallel flow.
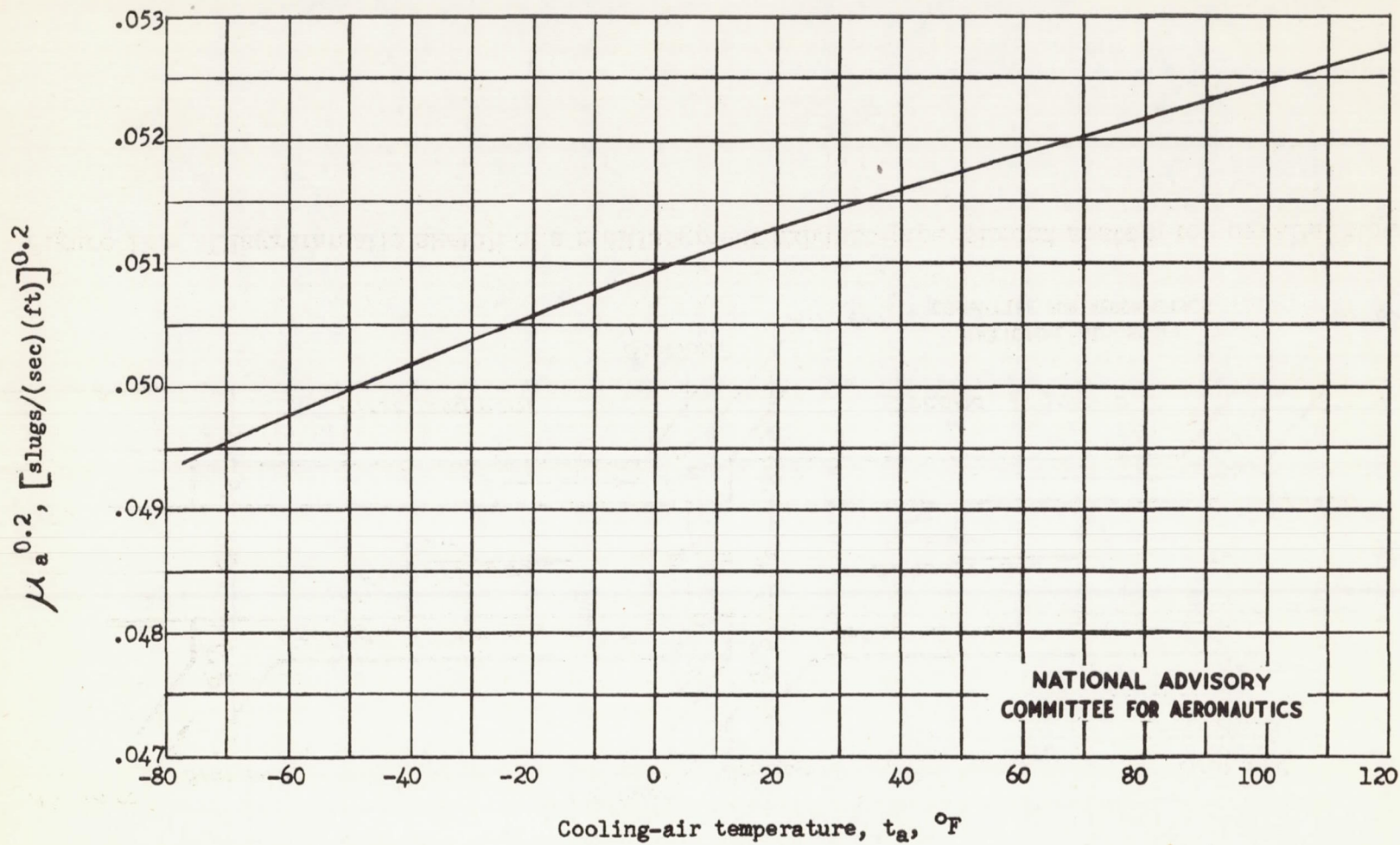
Figure 13.- Variation of $\mu_a^{0.2}$ with cooling-air temperature.
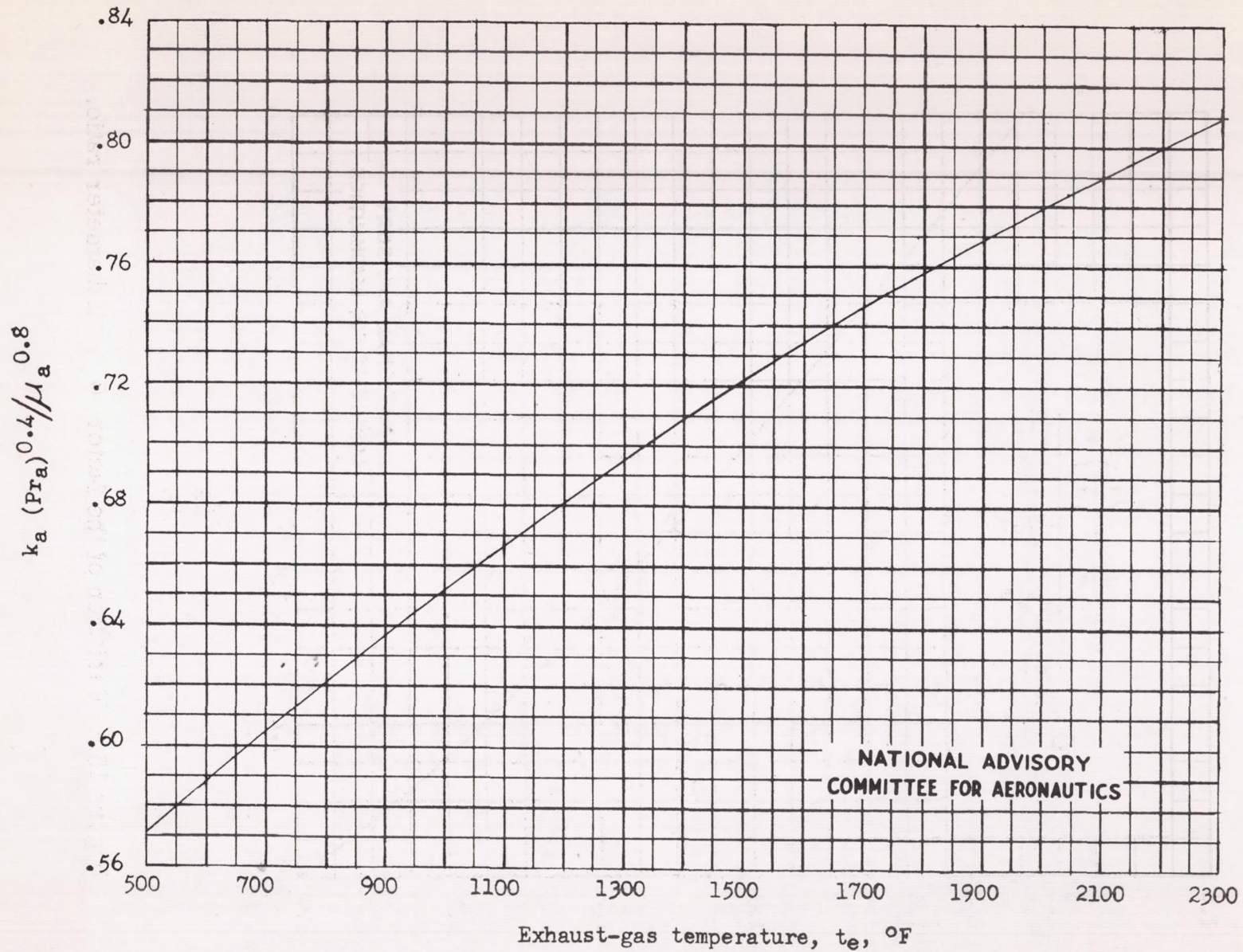
Figure 14.- Variation of the factor $k_a \left(\mathrm{Pr}_a\right)^{0.4} \Big/ \mu_a^{0.8}$ with exhaust-gas temperature.

$$\phi = \cfrac{2 \log_e \cfrac{d_s}{d_p} - \left(\cfrac{d_s}{d_p}\right)^2 + 1}{\cfrac{d_s}{d_p} - \cfrac{d_p}{d_s} - 2\cfrac{d_s}{d_p} \log_e \cfrac{d_s}{d_p}}$$

$$\frac{d_s}{d_p}$$
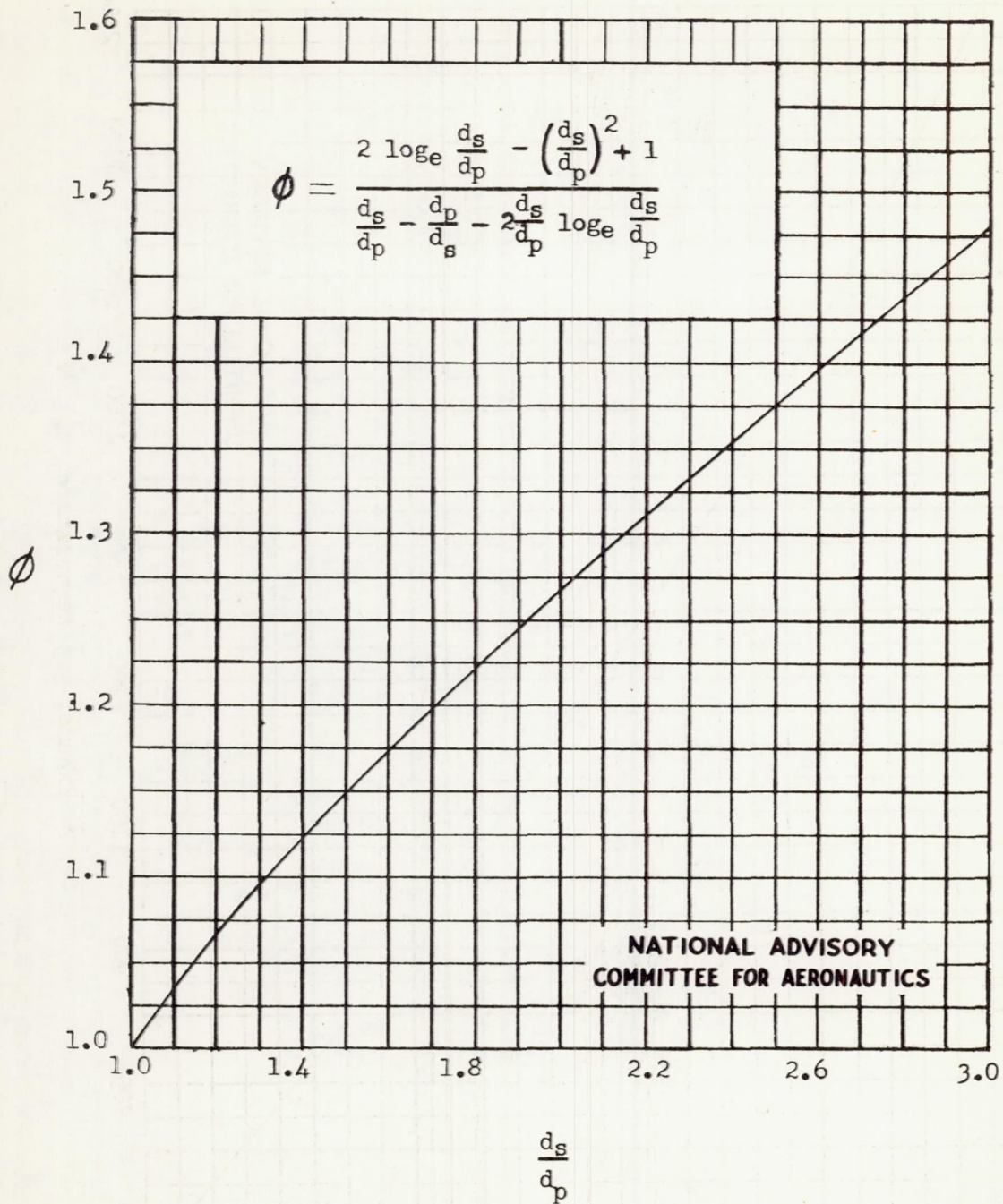
Figure 15.- Variation of the factor ϕ with diameter ratio.
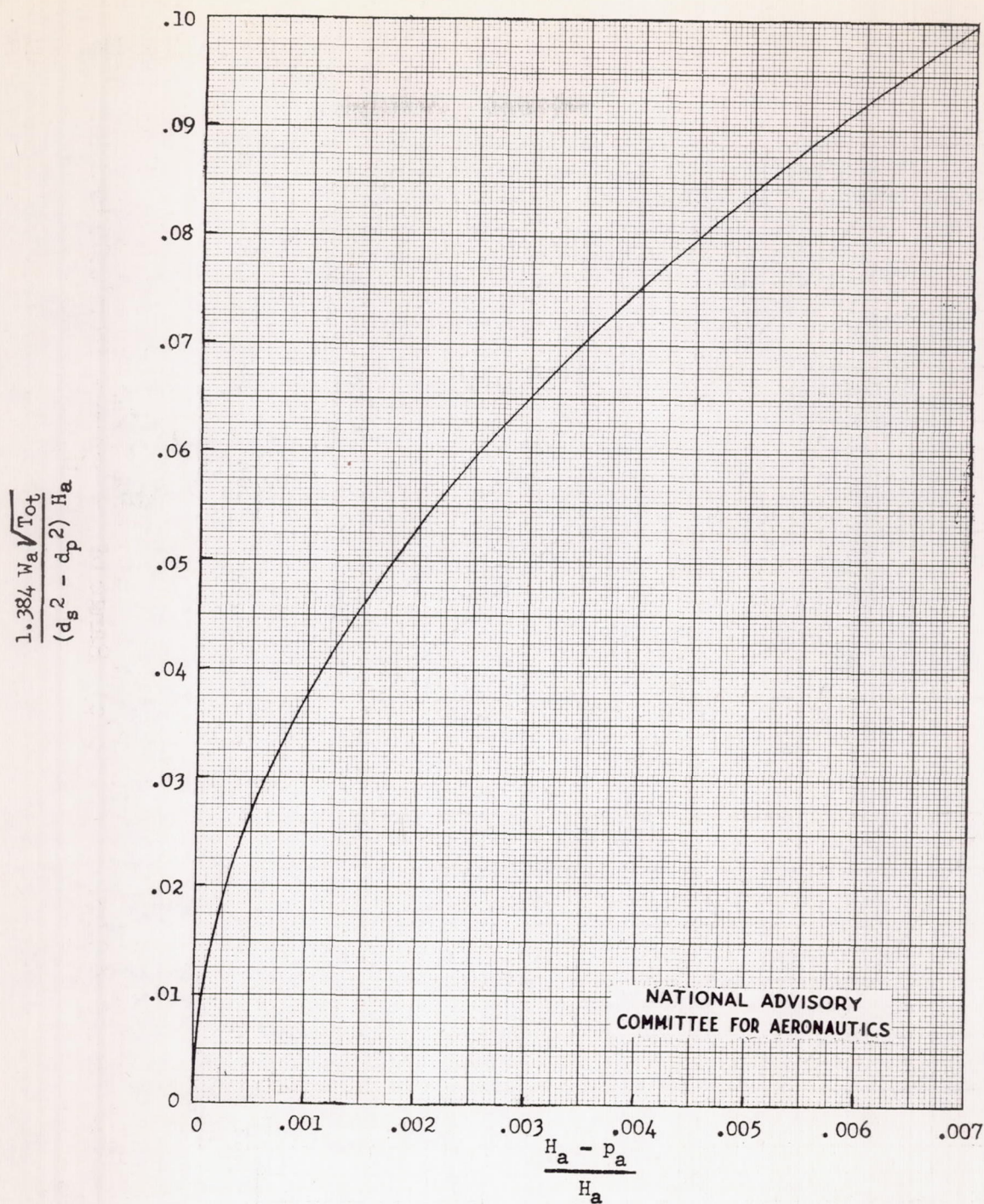
(a)   Range of $\dfrac{H_a - p_a}{H_a}$ from 0 to 0.007.

Figure 16.-   Variation of the choke factor $\dfrac{1.384\ W_a\sqrt{T_{o_t}}}{\left(d_s^2 - d_p^2\right)H_a}$

with $\dfrac{H_a - p_a}{H_a}$.
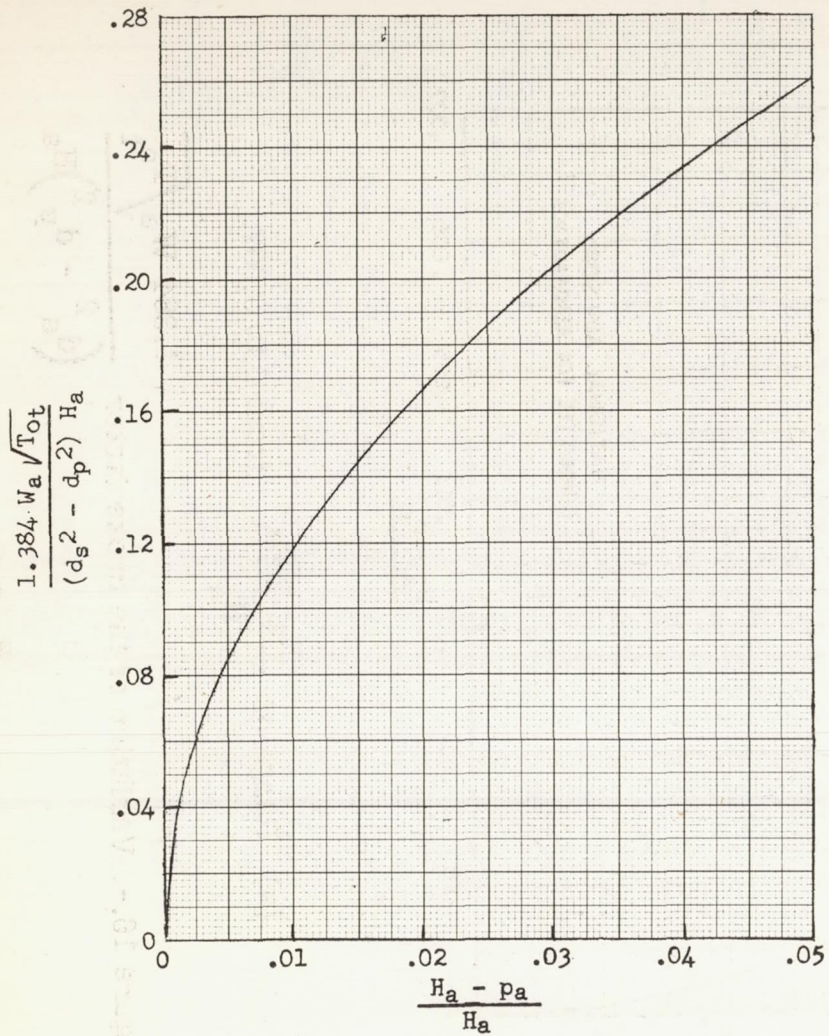
(b) Range of $\dfrac{H_a - p_a}{H_a}$ from 0 to 0.05.
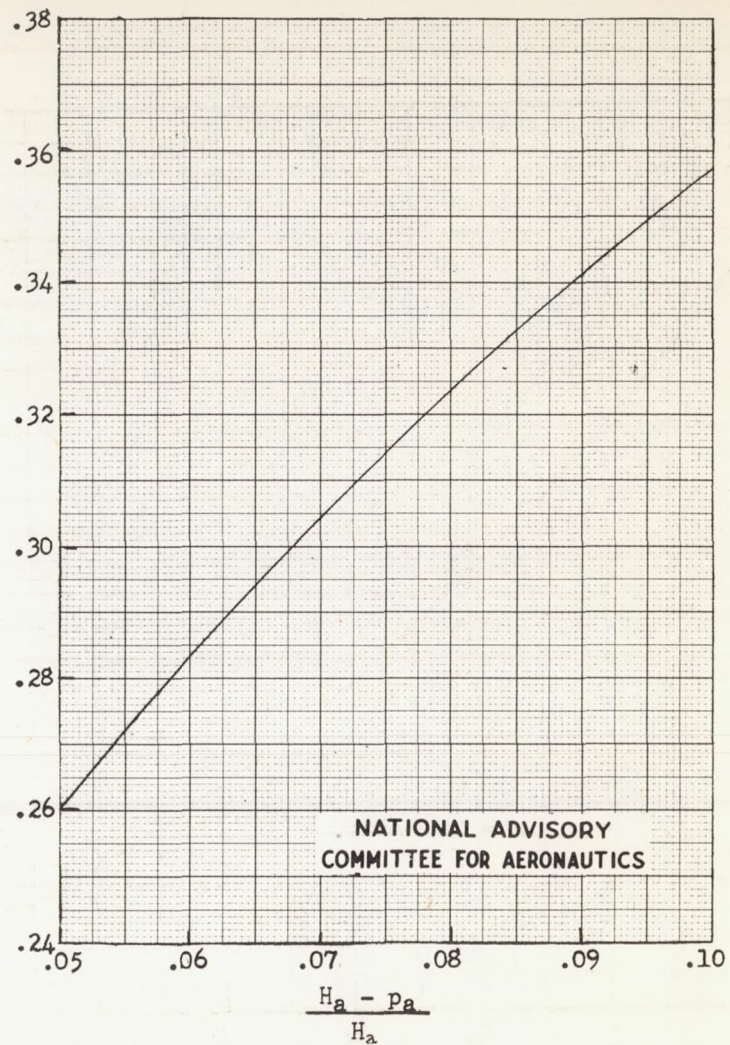
(c) Range of $\dfrac{H_a - p_a}{H_a}$ from 0.05 to 0.10.

Figure 16.- Continued.

$$\frac{1.384 \ W_a \sqrt{T_{ot}}}{(d_s{}^2 - d_p{}^2) \ H_a}$$

$$\frac{H_a - p_a}{H_a}$$

NATIONAL ADVISORY
COMMITTEE FOR AERONAUTICS
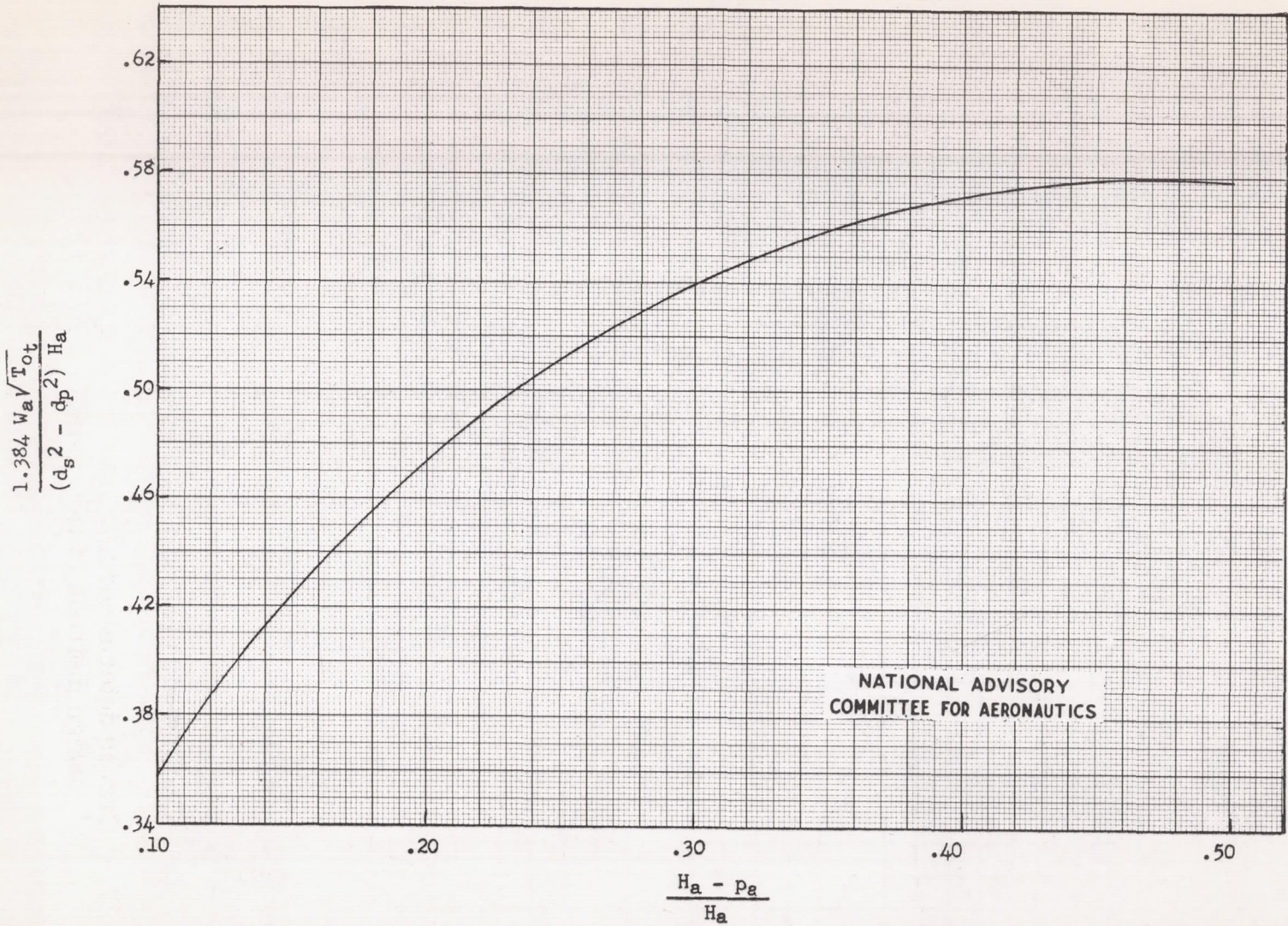
(d)   Range of $\dfrac{H_a - p_a}{H_a}$ from 0.10 to 0.50.

Figure 16.-   Concluded.
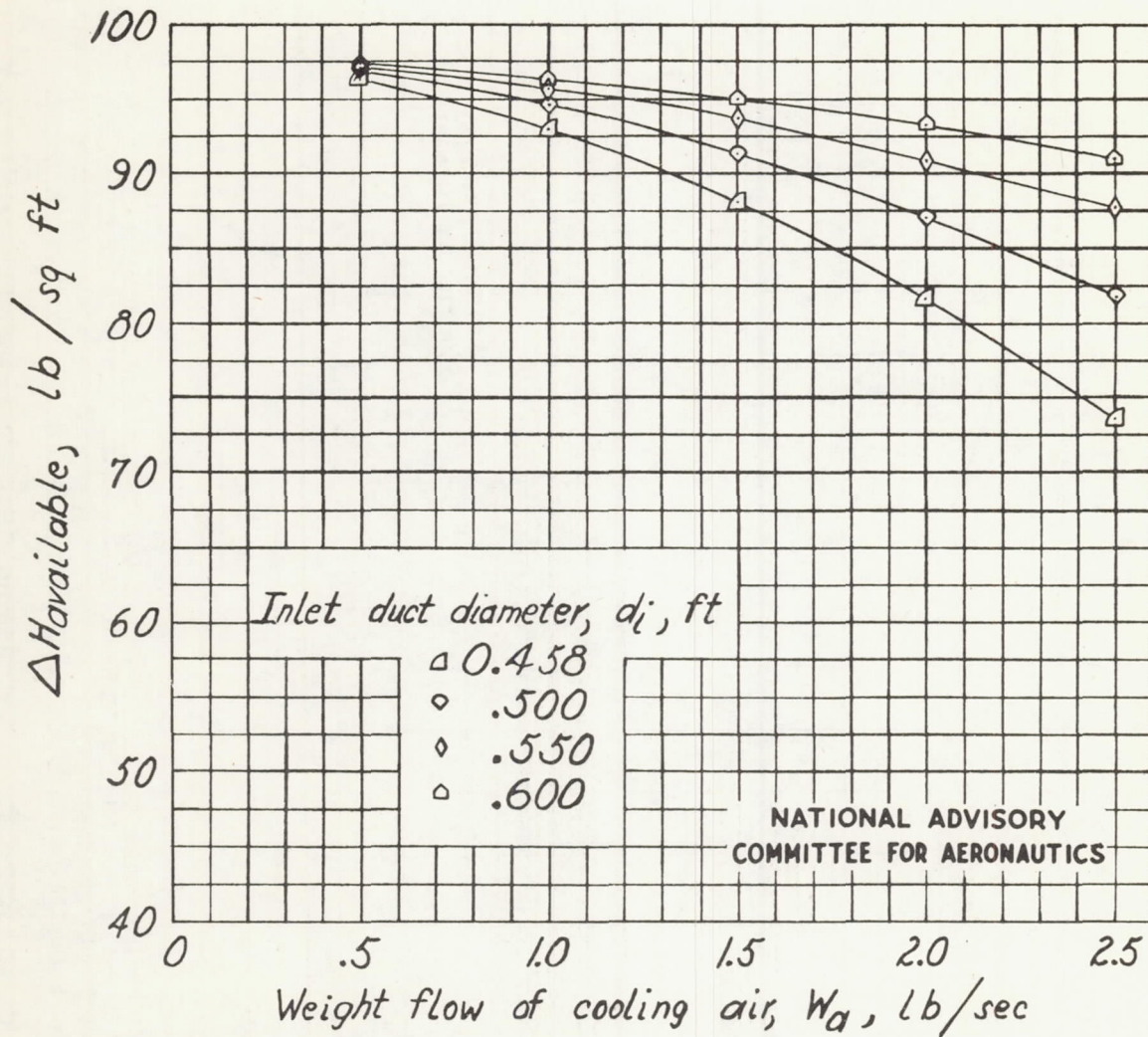
(a) Cooling-air pressure drop available at shroud entrance.

Figure 17.- Curves determined and used in the application of the
design methods to the example.
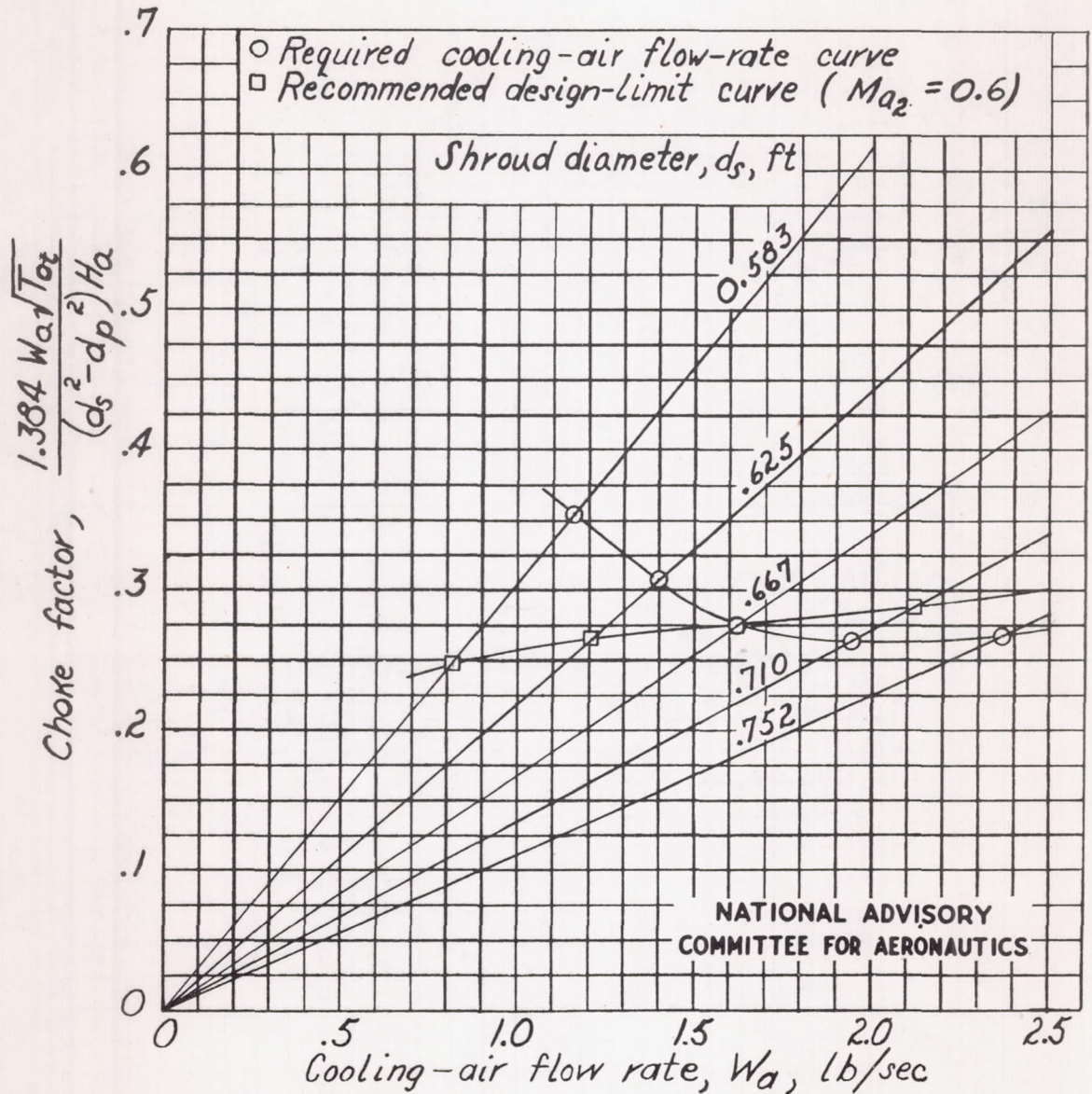
(b) Variation of choke factor with cooling-air flow rate.

Figure 17.- Continued.
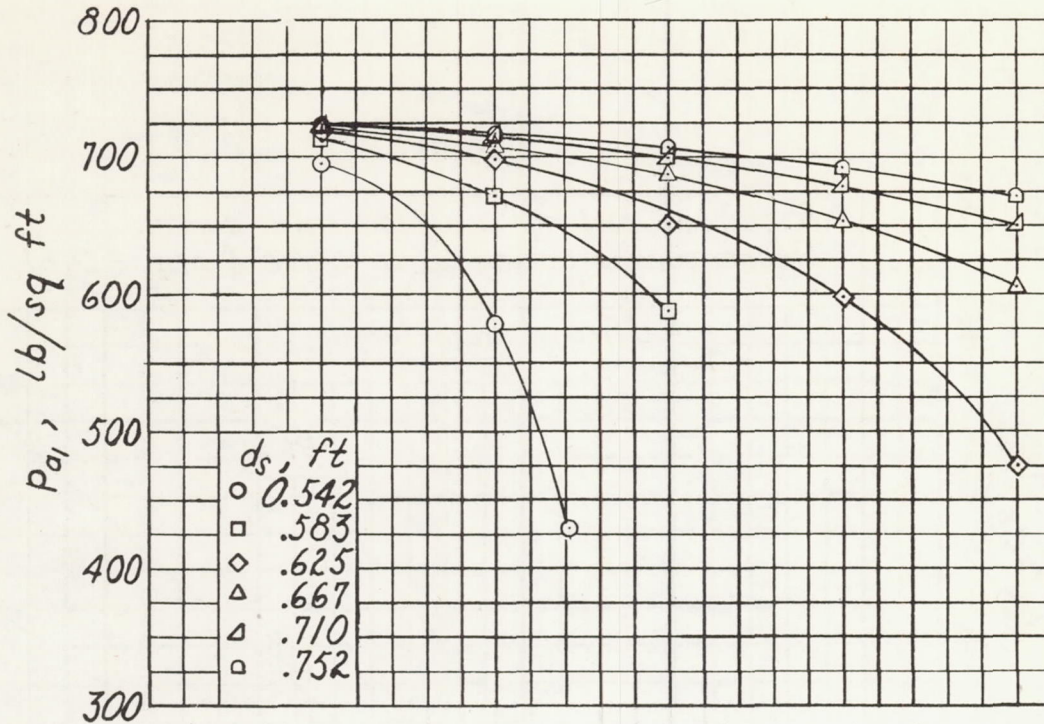
(c) Cooling-air static pressure at shroud entrance.

(d) Cooling-air temperature at shroud entrance.
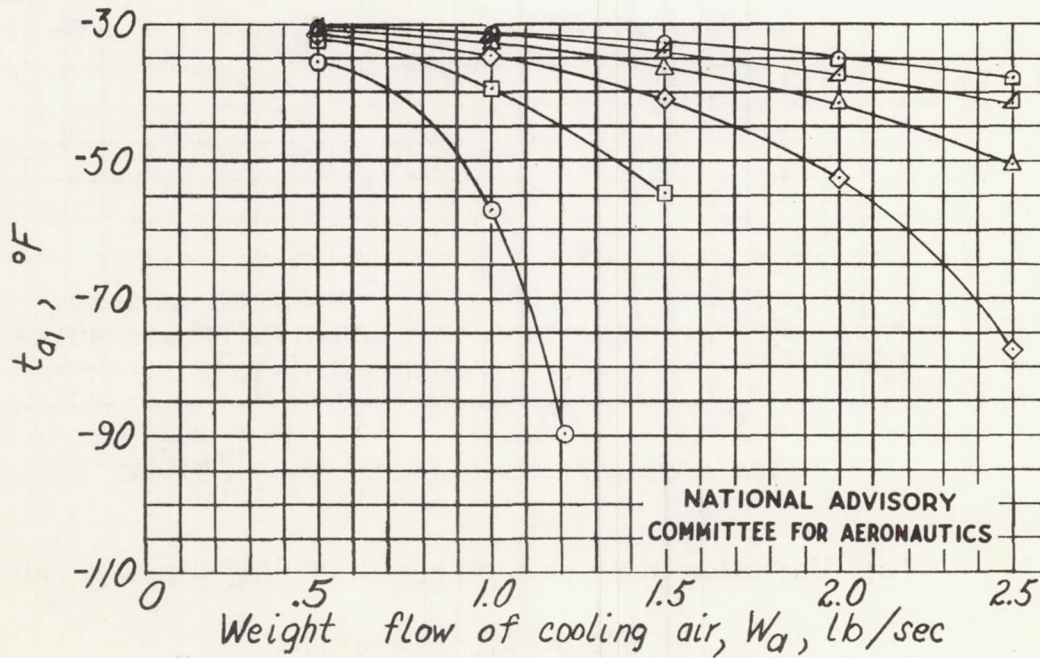
Figure 17.- Continued.
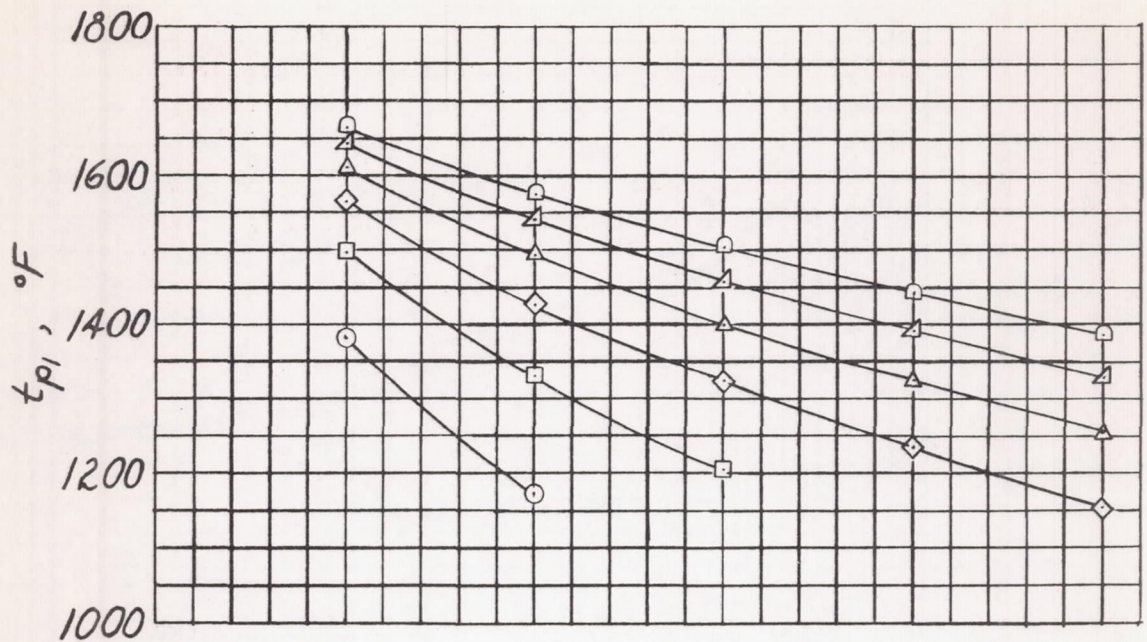
(e) Upstream exhaust-pipe temperature.

(f) Downstream exhaust-gas temperature.
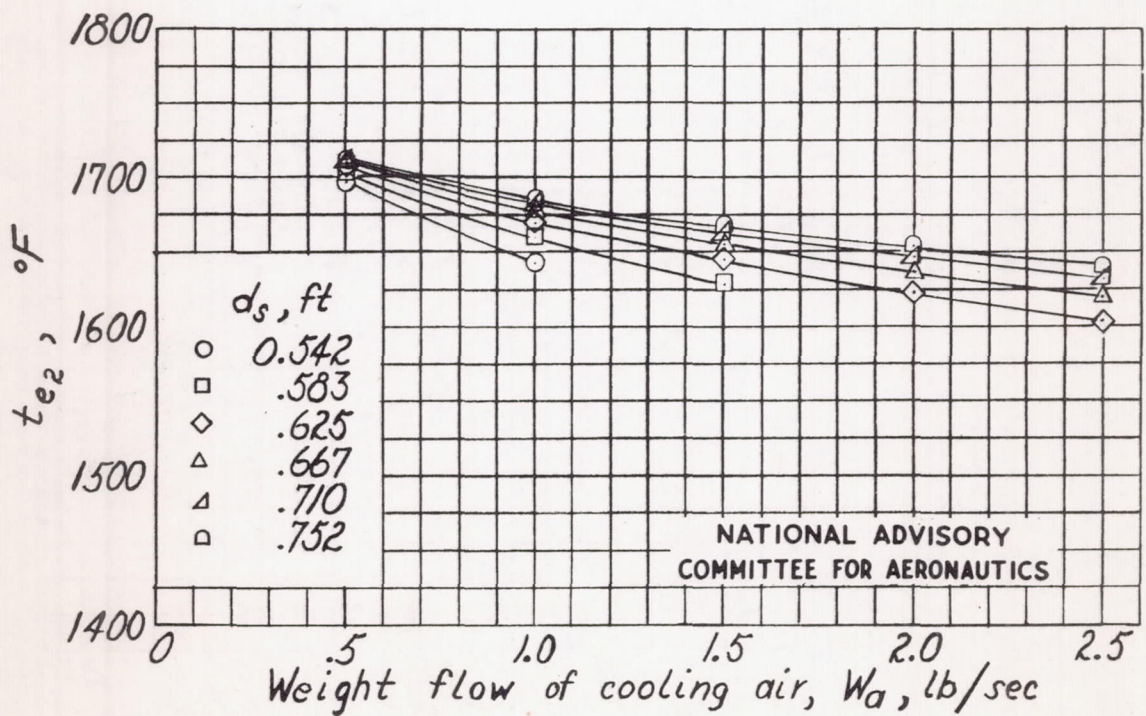
Figure 17.- Continued.
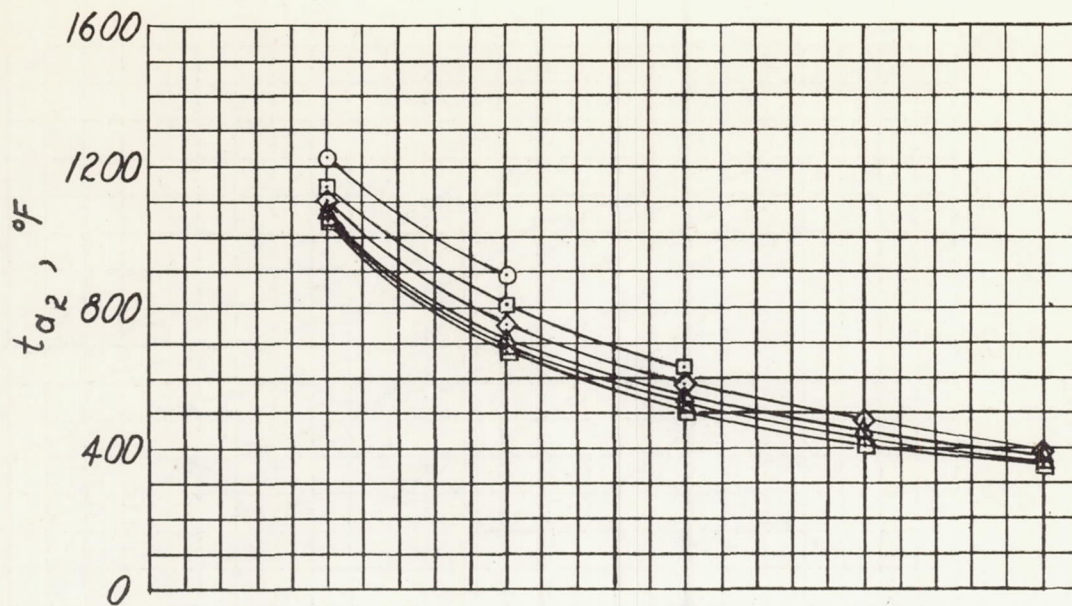
(g)   Downstream cooling-air temperature.
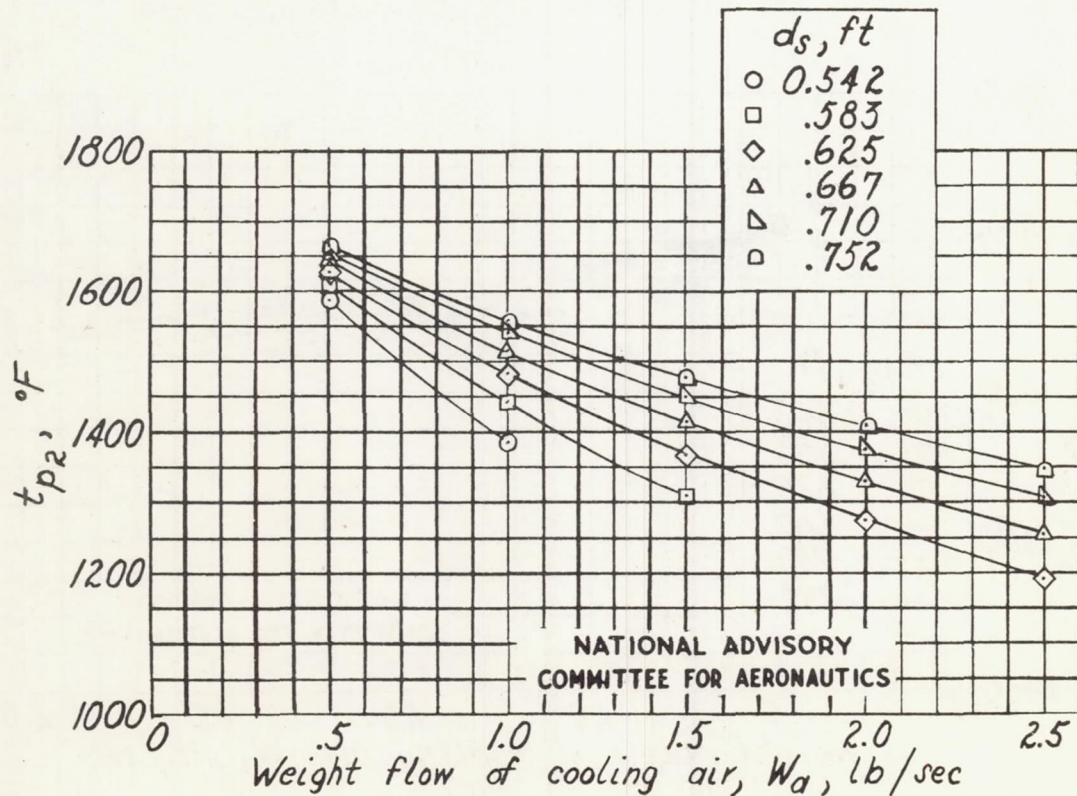
(h)   Downstream exhaust-pipe temperature.

Figure 17.-   Continued.
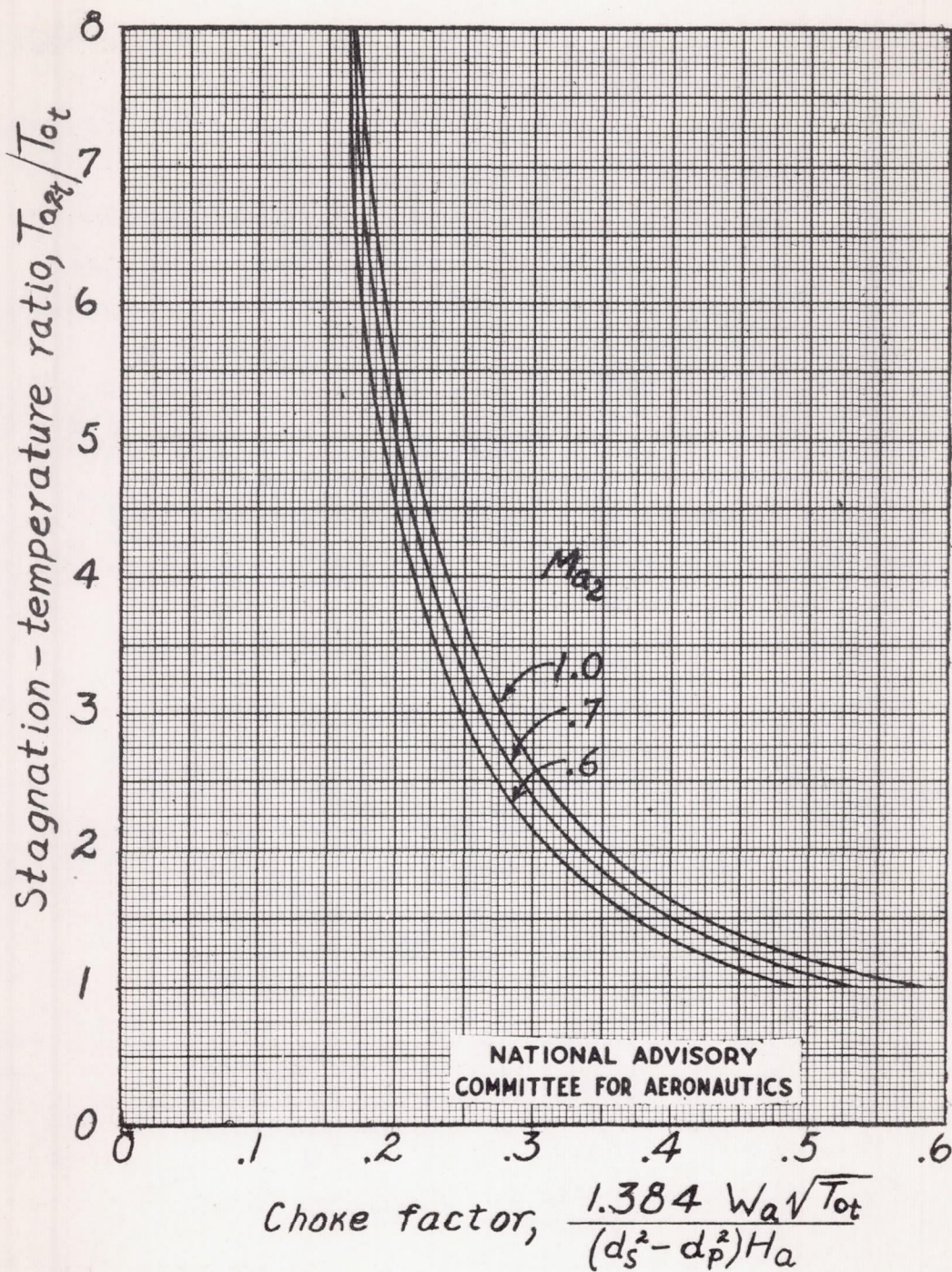
(i) Curve for determination of choke factor.

Figure 17.- Continued.
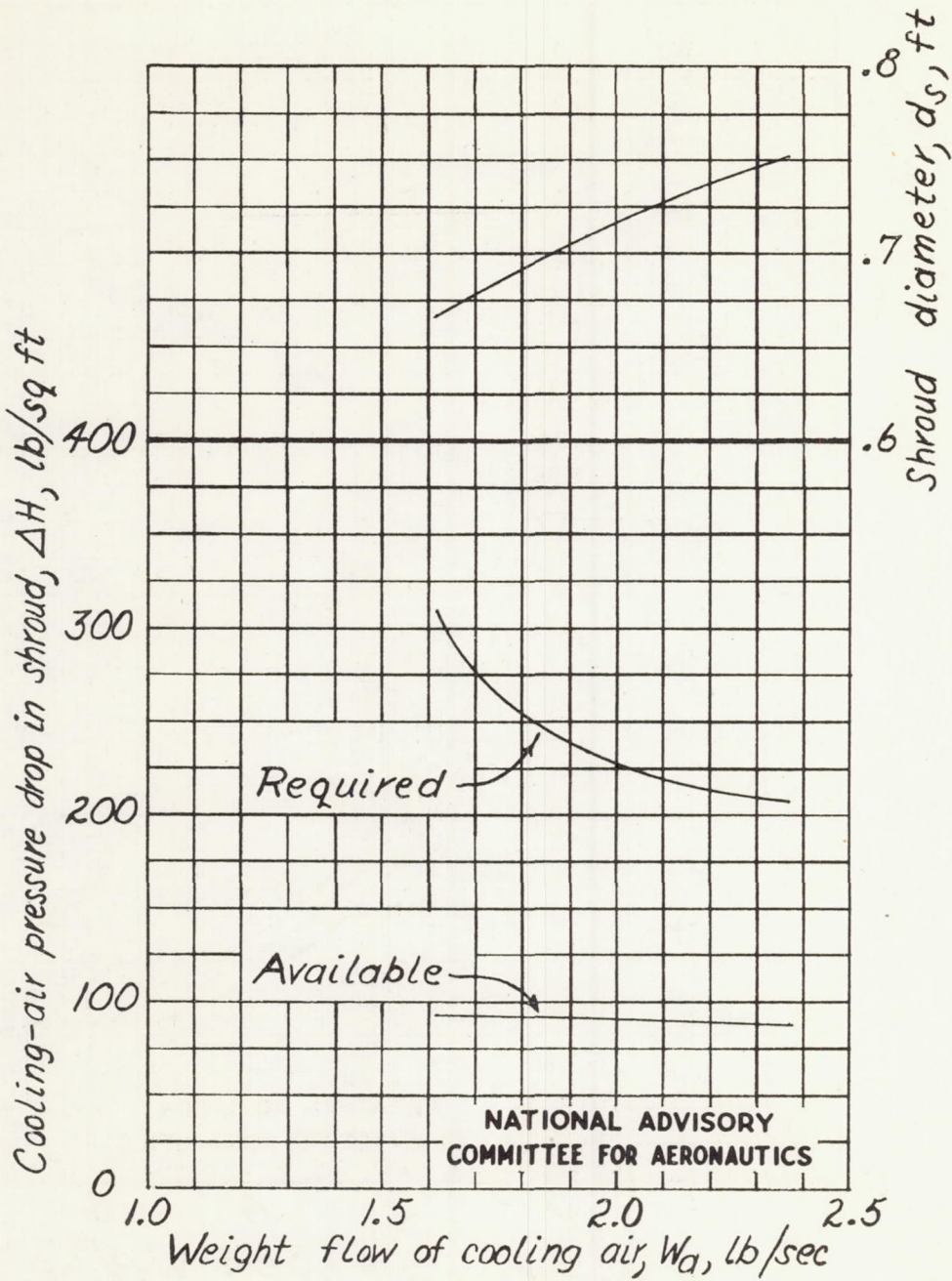
(j) Cooling-air pressure drop required and available in
shroud for required cooling.

Figure 17.- Concluded.
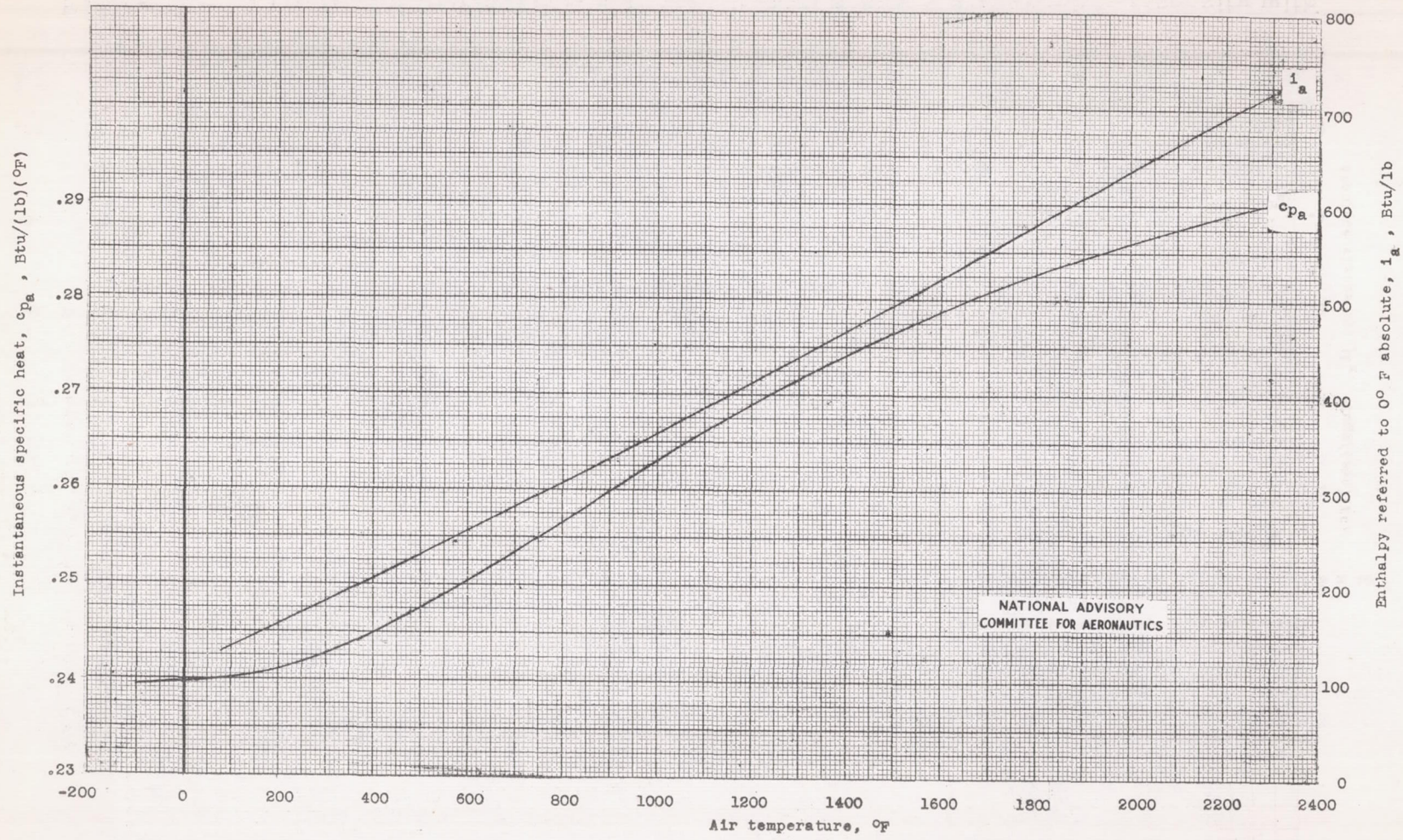
Figure 18.- Variation of instantaneous specific heat and enthalpy with air temperature.
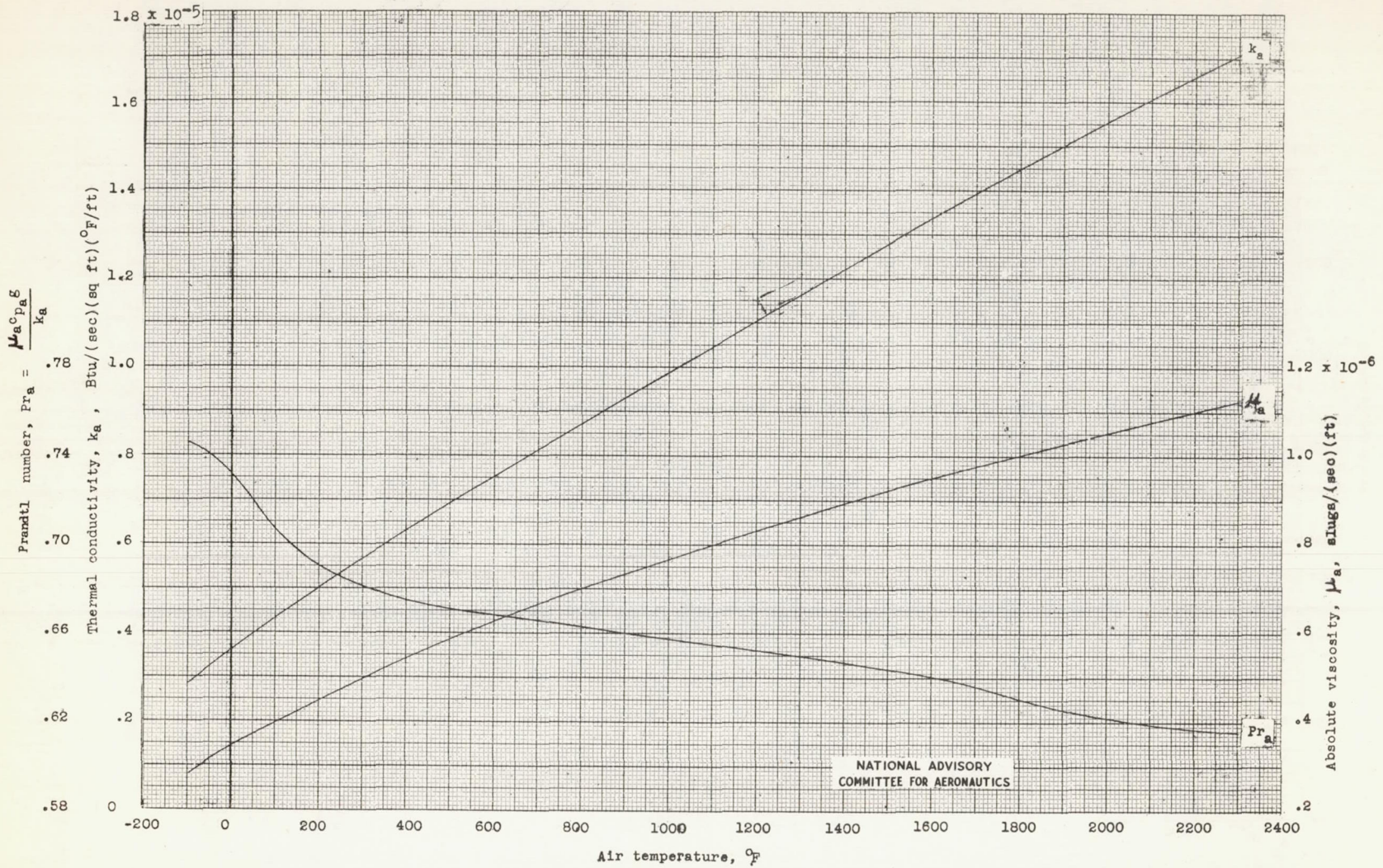
Figure 19.- Variation of thermal conductivity, Prandtl number, and absolute viscosity with air temperature.
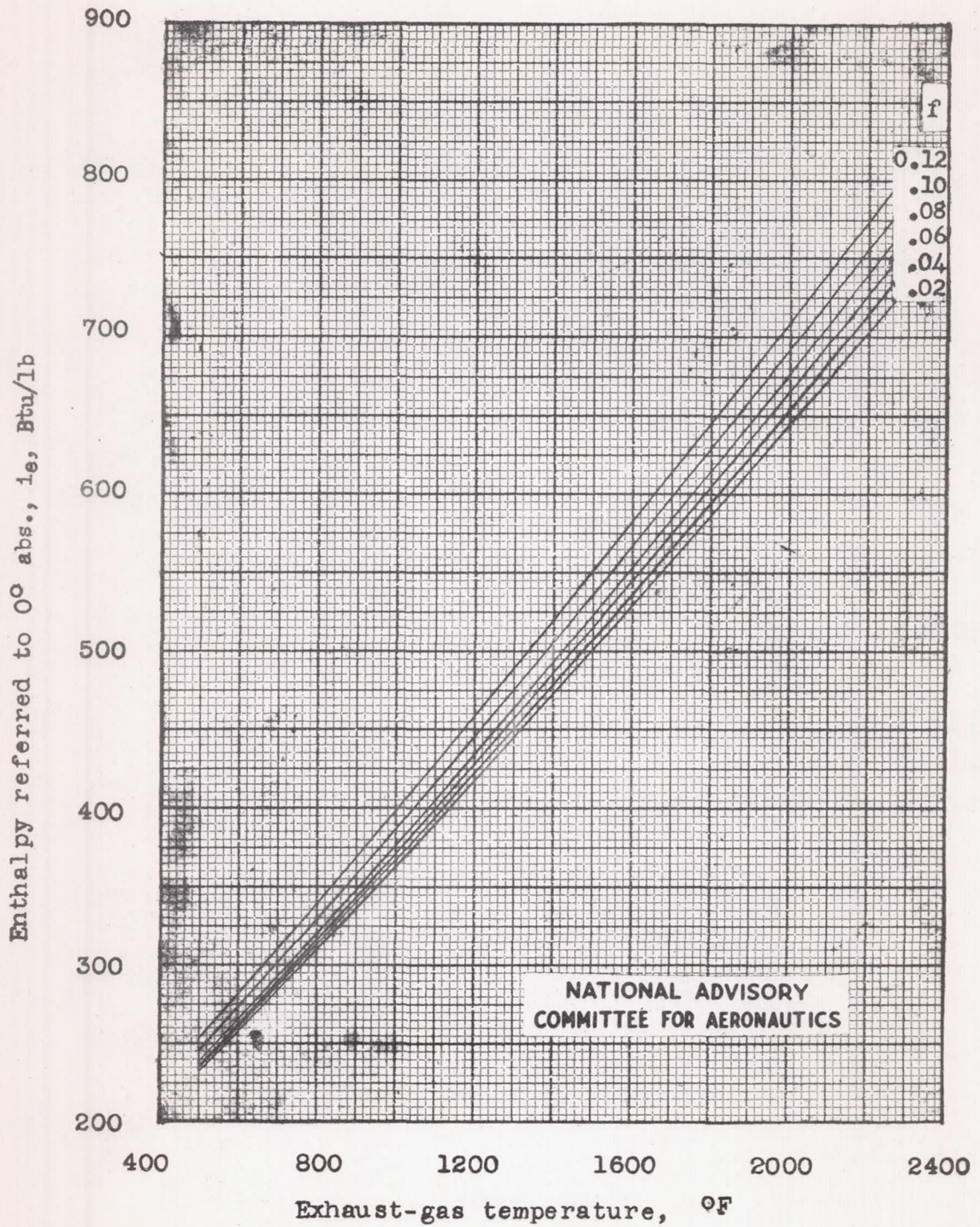
Figure 20.- Variation of enthalpy, referred to 0° absolute with exhaust-gas temperature for 0.10 hydrogen-carbon ratio.
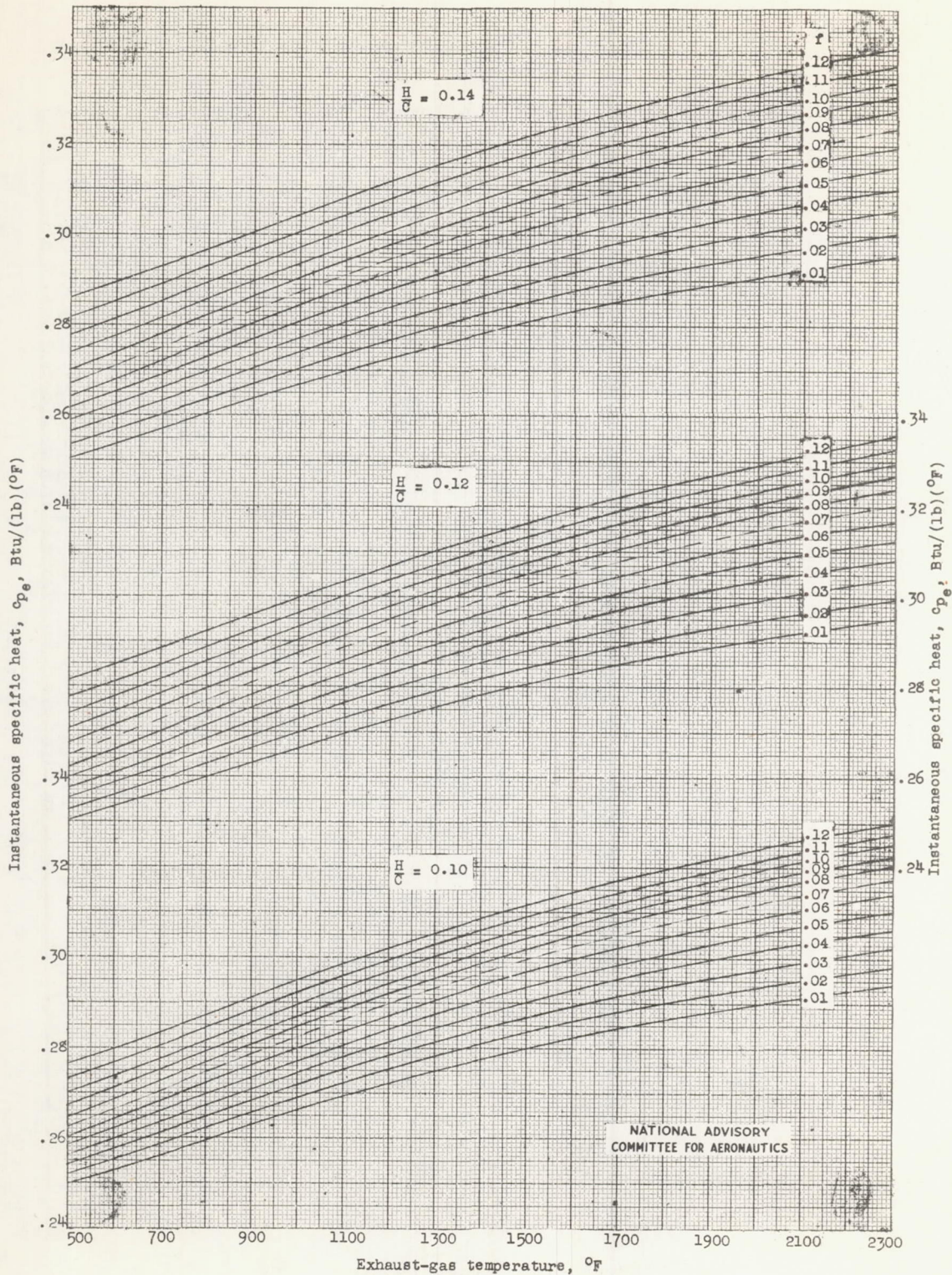
(a)   H/C : 0.10, 0.12, 0.14.

Figure 21.- Variation of instantaneous specific heat with exhaust-gas
temperature for practical fuel-air and hydrogen-carbon ratios.
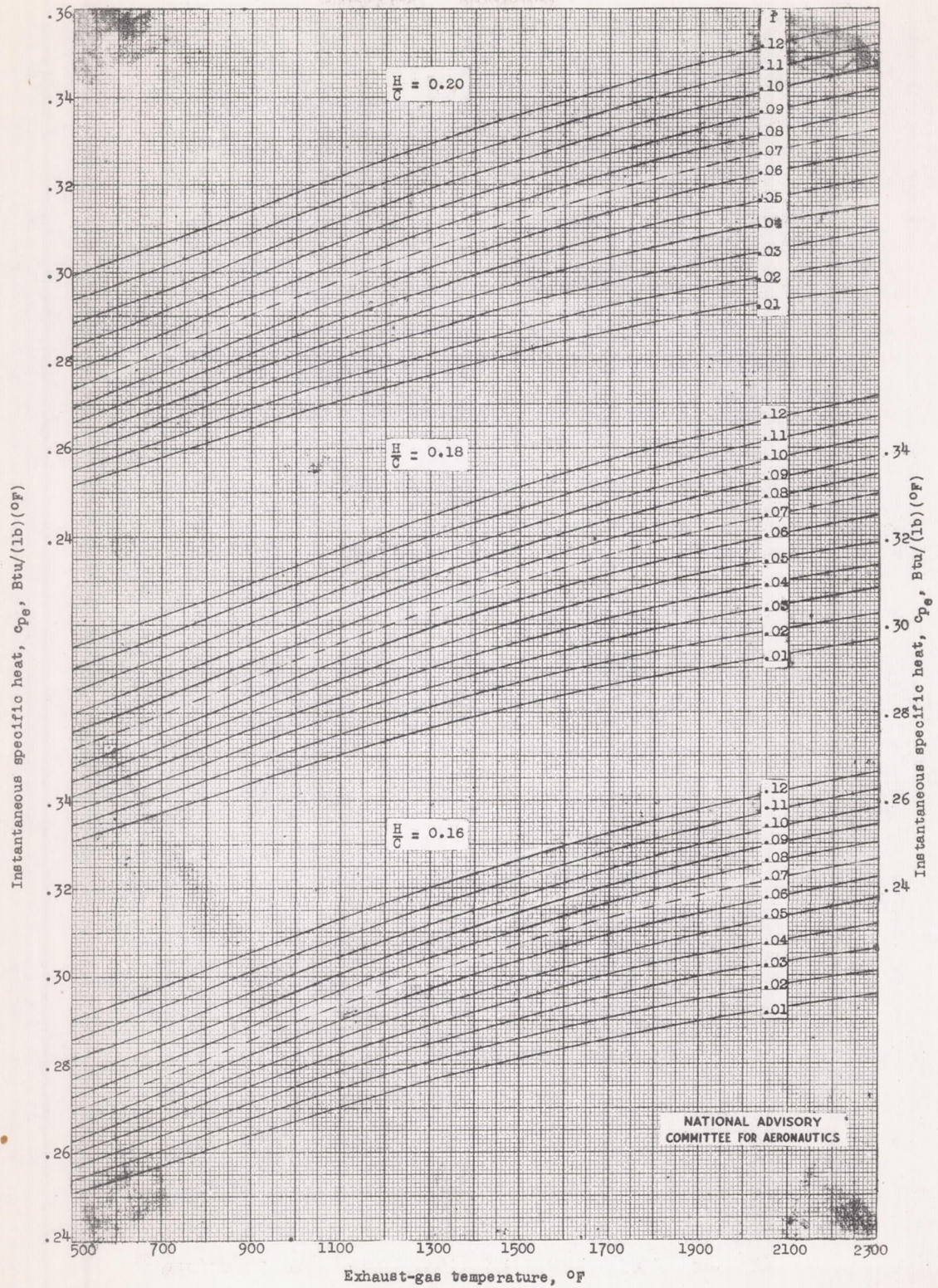
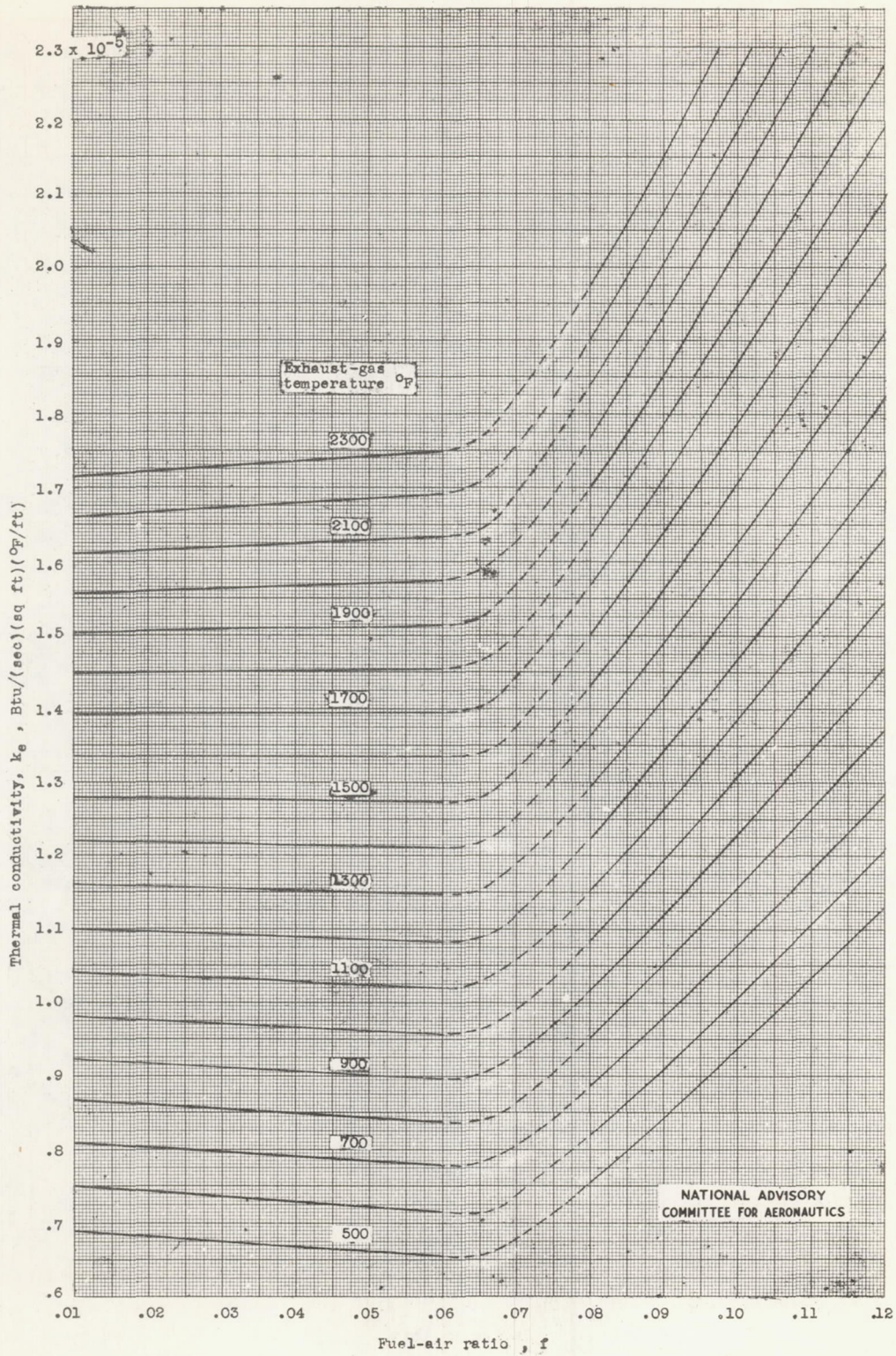(b) H/C : 0.16, 0.18, 0.20.

Figure 21.- Concluded.
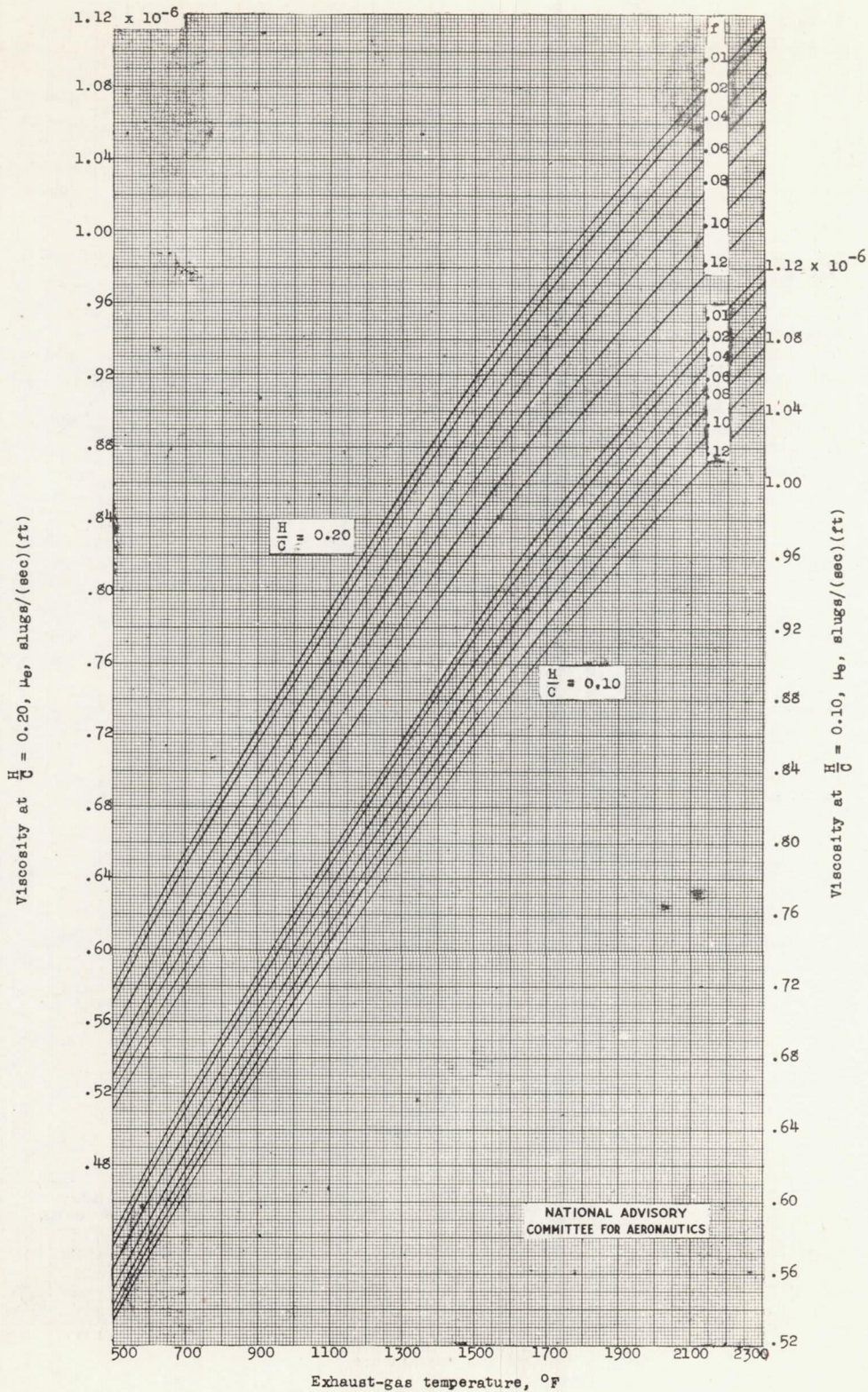
Figure 22.- Variation of exhaust-gas viscosity with temperature for 0.10 and 0.20 hydrogen-carbon ratios and various fuel-air ratios.
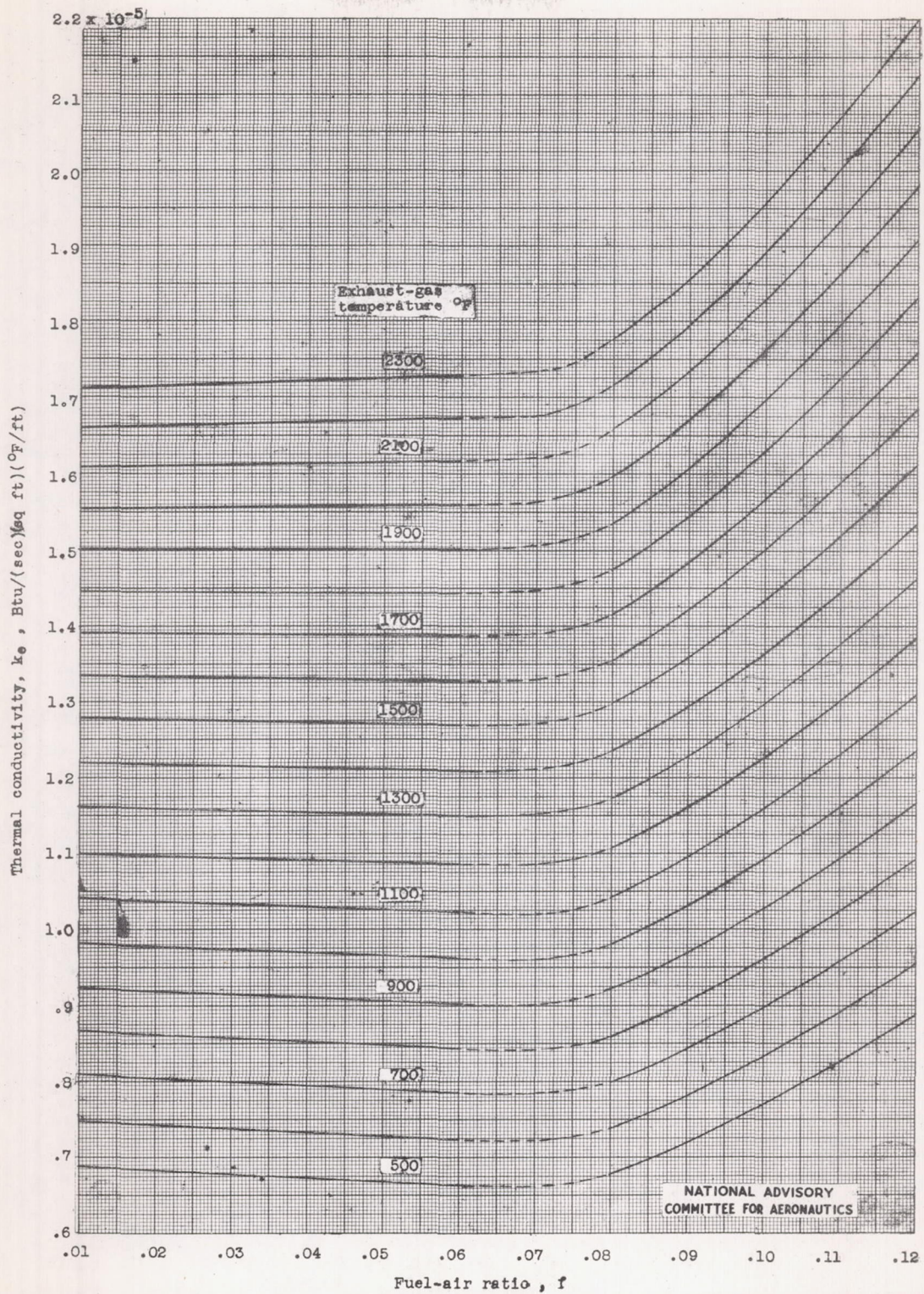
(a) H/C : 0.10.

Figure 23.-   Variation of thermal conductivity with fuel-air ratio for various exhaust-gas temperatures.

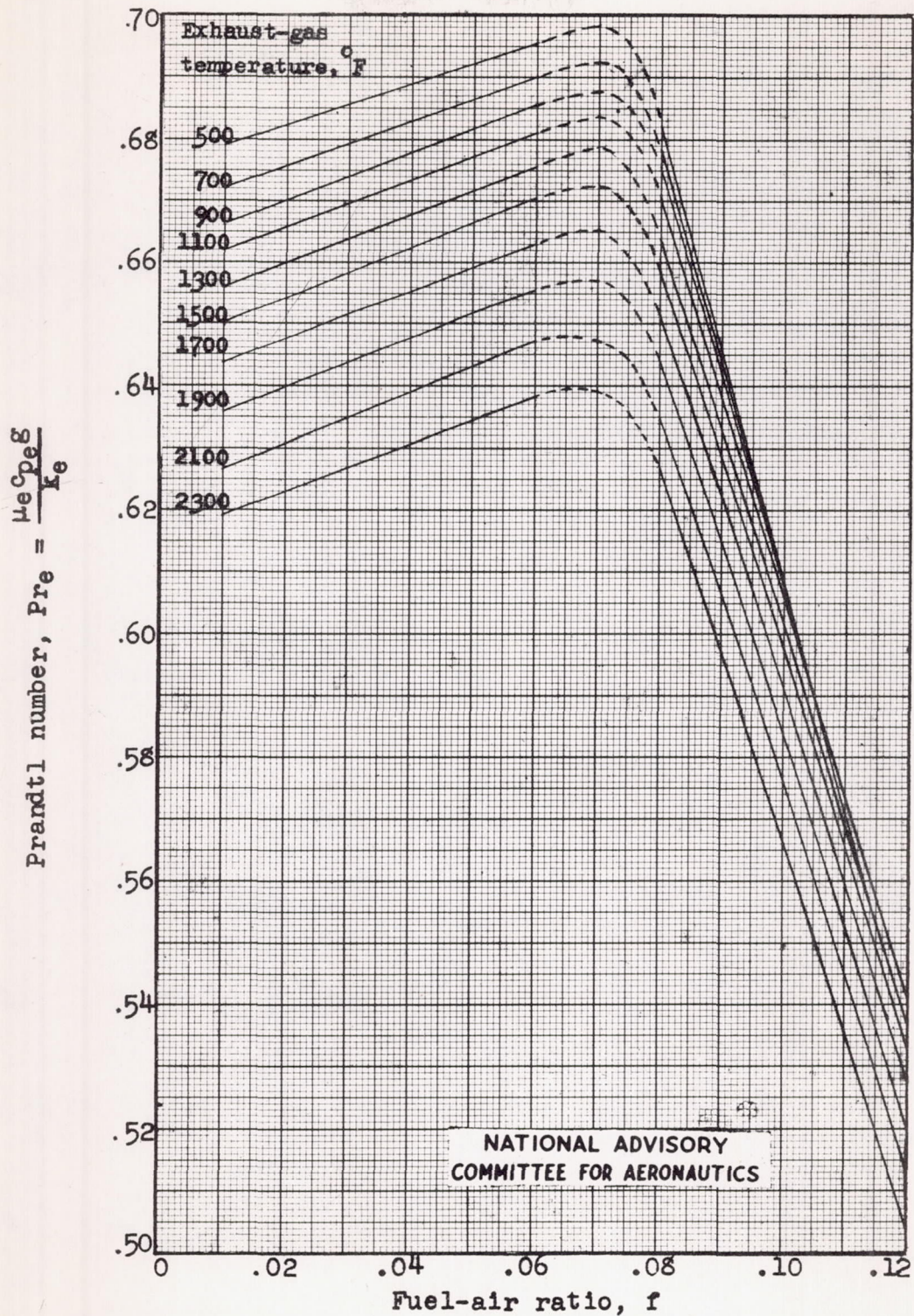(b) H/C : 0.20.

Figure 23.- Concluded.

Figure 24.- Variation of Prandtl number with fuel-air ratio for various exhaust-gas temperatures and hydrogen-carbon ratio of 0.10.